ARISTOTLE UNIVERSITY OF THESSALONIKI
SCHOOL OF GEOLOGY

IOANNA XANTHOPOULOU
Geologist

HYDROCARBON MIGRATION AND SEAL PROPERTIES SENSITIVITY ANALYSIS BY APPLYING 1D/2D/3D BASIN MODELING, PATRAIKOS GULF, WESTERN GREECE

MASTER THESIS

M.Sc. "HYDROCARBON EXPLORATION AND EXPLOITATION"

THESSALONIKI 2020

IOANNA XANTHOPOULOU
ΙΩΑΝΝΑ ΞΑΝΘΟΠΟΥΛΟΥ
Πτυχιούχος Γεωλόγος

HYDROCARBON MIGRATION AND SEAL PROPERTIES SENSITIVITY ANALYSIS BY APPLYING 1D/2D/3D BASIN MODELING, PATRAIKOS GULF, WESTERN GREECE
ΑΝΑΛΥΣΗ ΕΥΑΙΣΘΗΣΙΑΣ ΜΕΤΑΝΑΣΤΕΥΣΗΣ ΥΔΡΟΓΟΝΑΝΘΡΑΚΩΝ ΚΑΙ ΙΔΙΟΤΗΤΩΝ ΠΕΤΡΩΜΑΤΩΝ ΚΑΛΥΜΜΑΤΩΝ ΜΕ ΤΗΝ ΕΦΑΡΜΟΓΗ ΜΟΝΤΕΛΟΠΟΙΗΣΗΣ ΛΕΚΑΝΗΣ 1D/2D/3D, ΠΑΤΡΑΪΚΟΣ ΚΟΛΠΟΣ, ΔΥΤΙΚΗ ΕΛΛΑΔΑ

Υποβλήθηκε στο Τμήμα Γεωλογίας στα πλαίσια του Δι-Ιδρυματικού Προγράμματος Μεταπτυχιακών Σπουδών ´´Έρευνα και Εκμετάλλευση Υδρογονανθράκων´´

Ημερομηνία Προφορικής Εξέτασης: 15/07/2020
Oral Examination Date: 15/07/2020

<u>Three-member Examining Board</u>

Professor Andreas Georgakopoulos, Supervisor
Professor Kimon Christanis, Member
Professor Vasilios Karakitsios, Member

<u>Τριμελής Εξεταστική Επιτροπή</u>

Καθηγητής Ανδρέας Γεωργακόπουλος, Επιβλέπων
Καθηγητής Κίμων Χρηστάνης, Μέλος Τριμελούς Εξεταστικής Επιτροπής
Καθηγητής Βασίλειος Καρακίτσιος, Μέλος Τριμελούς Εξεταστικής Επιτροπής

HYDROCARBON MIGRATION AND SEAL PROPERTIES SENSITIVITY ANALYSIS BY APPLYING 1D/2D/3D BASIN MODELING, PATRAIKOS GULF, WESTERN GREECE
– *Master Thesis*

ΑΝΑΛΥΣΗ ΕΥΑΙΣΘΗΣΙΑΣ ΜΕΤΑΝΑΣΤΕΥΣΗΣ ΥΔΡΟΓΟΝΑΝΘΡΑΚΩΝ ΚΑΙ ΙΔΙΟΤΗΤΩΝ ΠΕΤΡΩΜΑΤΩΝ ΚΑΛΥΜΜΑΤΟΣ ΜΕ ΤΗΝ ΕΦΑΡΜΟΓΗ ΜΟΝΤΕΛΟΠΟΙΗΣΗΣ ΛΕΚΑΝΗΣ 1D/2D/3D, ΠΑΤΡΑΪΚΟΣ ΚΟΛΠΟΣ, ΔΥΤΙΚΗ ΕΛΛΑΔΑ
– *Μεταπτυχιακή Διπλωματική Εργασία*

Citation:
Xanthopoulou Ioanna, 2020. – Hydrocarbon migration and seal properties sensitivity analysis by applying 1D/2D/3D basin modeling, Patraikos Gulf, Western Greece. Master Thesis, School of Geology, Aristotle University of Thessaloniki, 87 pp.
Ξανθοπούλου Ιωάννα, 2020. –Ανάλυση ευαισθησίας μετανάστευσης υδρογονανθράκων και ιδιοτήτων πετρωμάτων καλύμματος με την εφαρμογή 1D/2D/3D μοντελοποίηση λεκάνης, Πατραϊκός Κόλπος, Δυτική Ελλάδα. Μεταπτυχιακή Διπλωματική Εργασία, Τμήμα Γεωλογίας Α.Π.Θ., 87 σελ.

Table of Contents

List of Figures

List of Tables

Abstract

This dissertation reviews the geological evolution of Western Greece by presenting the most external geotectonic zones, Gavrovo-Tripolis, Ionian, and Pre-Apulian (Paxos). Furthermore, there is a special emphasis on the internal Ionian Zone. The zone comprises Triassic evaporites to Jurassic-Upper Eocene carbonate sediments, and minor cherts, and shales. The Mesozoic sequence is overlain by the characteristic Oligocene turbidite sediments (flysch) of the area and the Miocene to present-day clastic sediments. Three organic-rich intervals of the Mesozoic sequence were used as potential source rocks for the present study. These are the Triassic shales which are dominated by kerogen type I organic matter, the Middle-Upper Jurassic shales, known as Posidonia beds, dominated by kerogen II organic matter and the Lower Cretaceous shales, known as Vigla shales, which are also dominated by kerogen type II organic matter.

A detailed basin modeling study is presented, considering the western Patraikos Gulf area. A variety of applied values were chosen based on data provided by Hellenic Petroleum S.A. and previous papers. Integrated analysis with 1D/2D/3D basin models is presented to better understand the petroleum system activity of the area. Burial history, thermal maturity, timing and extent of petroleum generation and expulsion, migration, and accumulations were modeled for the three source rocks. Based on the modeling results, the most conservative scenario suggests increasing maturity trend as following: Vigla shales < Posidonia beds < Triassic shales. Triassic shales are considered the most important source rock of the area with the capability to generate significant quantities of oil and gas, while Vigla shales, due to its limited expulsion generated low quantities of oil and often do not contribute to the trapped hydrocarbons as modeled. Posidonia beds generated and expelled low quantities of oil.

Sensitivity analysis, considering the thermal regime, rifting stage, seal properties, and source rock properties, was also conducted. The analysis was applied to 2D/3D modeling with outcomes of maturation modeling, migration, and hydrocarbon trapping possibilities. The analysis is also separated into two parts. In the first part, the models of various thermal regimes (increasing heat flow value) and rifting stage scenarios result in changes in the maturity level for all three source rocks thus, increasing the trapping hydrocarbons. In the second part, the models of various seal and source rock properties scenarios keep the maturity level constant. However, the increase in the applied values resulted in an increase in the trapped hydrocarbons. No change in the migration process is noticed for the different models.

Περίληψη

Η παρούσα διπλωματική εργασία αξιολογεί την γεωλογική εξέλιξη της Δυτικής Ελλάδας παρουσιάζοντας τις εξωτερικές ζώνες, Γαβρόβου-Τρίπολης, Ιονίου και Παξών (Προ-Απούλιας). Επιπλέον, έχει δοθεί μεγαλύτερη έμφαση στην εσωτερική Ιόνια ζώνη. Η ζώνη αυτή αποτελείται από Τριαδικούς εβαπορίτες και Ιουρασικά-Άνω Ηωκαινικά ανθρακικά ιζήματα με ελάχιστες ποσότητες πυριτικών και σχιστής αργίλου. Η Μεσοζωική ακολουθία υπόκειται των χαρακτηριστικών Ολιγοκαινικών τουρβιδιτικών ιζημάτων (φλύσχης) της περιοχής και τα Μειοκαινικά έως σημερινά κλαστικά ιζήματα. Τρία πλούσια σε οργανικό υλικό στρώματα της Μεσοζωικής ακολουθίας χρησιμοποιήθηκαν ως μητρικά πετρώματα για τον σκοπό αυτής της μελέτης. Αυτά είναι τα Triassic shales που περιέχουν οργανική ύλη κηρογόνου τύπου I, την Μέσο-Άνω Ιουρασική σχιστή άργιλο, γνωστή ως Posidonia beds που φιλοξενούν οργανική ύλη κηρογόνου τύπου II και την Κάτω Κρητιδική σχιστή άργιλο, γνωστούς ως Vigla shales, που επίσης περιέχουν οργανική ύλη κηρογόνου τύπου II.

Παρουσιάζεται μια λεπτομερής μοντελοποίηση λεκάνης, λαμβάνοντας υπόψη τον δυτικό Πατραϊκό Κόλπο. Πληθώρα εφαρμοσμένων τιμών επιλέχθηκαν βασισμένες σε δεδομένα που παραχωρήθηκαν από τα Ελληνικά Πετρέλαια Α.Ε. και από προηγούμενες εργασίες που μελετήθηκαν. Μία λεπτομερής ανάλυση με μοντέλα λεκάνης 1D/2D/3D παρουσιάζεται για την καλύτερη κατανόηση της δραστηριότητας του πετρελαϊκού συστήματος της περιοχής. Το ιστορικό ταφής, η θερμική ωρίμανση, το χρονοδιάγραμμα και η έκταση της γένεσης και αποβολής των υδρογονανθράκων, η μετανάστευση και οι συγκεντρώσεις μοντελοποιήθηκαν και για τα τρία μητρικά πετρώματα. Βάσει των αποτελεσμάτων, το πιο συντηρητικό σενάριο υποδηλώνει αύξηση της τάσης ωρίμανσης ως εξής: Vigla shales < Posidonia beds < Triassic shales. Έτσι τα Triassic shales θεωρούνται ως το πιο σημαντικό μητρικό πέτρωμα της περιοχής, ενώ τα Vigla shales, εξαιτίας περιορισμένης αποβολής υδρογονανθράκων, συχνά δεν συμμετέχει στους παγιδευμένους υδρογονάνθρακες. Τα Posidonia beds γεννούν και αποβάλλουν μικρές ποσότητες πετρελαίου.

Πραγματοποιήθηκε επίσης ανάλυση ευαισθησίας, λαμβάνοντας υπόψη το θερμικό καθεστώς, το στάδιο rifting και τις παραμέτρους των καλυμμάτων και των μητρικών πετρωμάτων. Η ανάλυση εφαρμόστηκε σε μοντελοποίηση 2D/3D με αποτελέσματα από μοντέλα ωρίμανσης, μετανάστευση και δυνατότητες παγίδευσης υδρογονανθράκων. Η ανάλυση χωρίζεται σε δύο μέρη. Στο πρώτο μέρος τα μοντέλα από ποικίλα σενάρια ως προς το θερμικό καθεστώς (αυξανόμενη τιμή θερμικής ροής) και το στάδιο rifting οδηγούν σε αλλαγές του επιπέδου ωρίμανσης και των τριών μητρικών πετρωμάτων, αυξάνοντας έτσι και τους παγιδευμένους υδρογονάνθρακες. Στο δεύτερο μέρος, τα μοντέλα διαφόρων σεναρίων για τις ιδιότητες των καλυμμάτων και των μητρικών πετρωμάτων διατηρούν σταθερό το επίπεδο ωρίμανσης. Ωστόσο, η αύξηση των εφαρμοσμένων τιμών έχει ως αποτέλεσμα την αύξηση των παγιδευμένων υδρογονανθράκων. Δεν παρατηρείται αλλαγή στην διαδικασία μετανάστευσης για τα διαφορετικά μοντέλα.

Foreword

The dissertation was carried out at Aristotle University of Thessaloniki (M.Sc. Hydrocarbons Exploration and Exploitation) in cooperation with Hellenic Petroleum S.A. (HELPE). I would like to express my sincere gratitude to Dr. Ioannis Oikonomopoulos, Senior Geochemist of HELPE, for the continuous support and his patience, motivation, and immense knowledge. His guidance helped me in all the time of research and writing of this thesis.

The dissertation focuses on the petroleum system activity at the broader area of Patraikos Gulf at western Greece. Past research provides information for the numerous oil seeps and the promising source rocks of the Ionian Zone. In particular, a basin modeling for western Patraikos Gulf is carried out, along with a sensitivity analysis to specify the parameters that mostly affect the results of the basin modeling.

The thesis summarizes the burial history, thermal maturity, timing of petroleum generation, expulsion and migration, and the accumulations trapped for a defined scenario which better reflects the conditions of the area. Afterward, full sensitivity analysis regarding hydrocarbon accumulations, migration paths, seal properties, source rock properties, and rifting stage will be quoted using 2D and 3D basin models. For all the above, the three possible source rocks, Triassic shales, Middle-Upper Jurassic shales known as Posidonia beds, and Lower Cretaceous shales known as Vigla shales were studied.

For the analysis and the creation of the geochemical models two software were used. Schlumberger's PetroMod software was used for 1D modelling as Schlumberger sponsorship with a full academic license to MSc Hydrocarbon Exploration and Exploitation. The Zetaware's Genesis and Trinity 3D software were used for the 1D/2D/3D modeling and were provided by HELPE.

Ioanna Xanthopoulou
July, 2020

1 Introduction

Previous hydrocarbon exploration in western Greece has shown that the region is characterized by the existence of organic-rich intervals classified as rich source rocks (*Karakitsios, 2013*). Former studies (*Karakitsios, 1995; Karakitsios, 2013, Rigakis et al., 2013, Mavromatidis, 2009, Karakitsios and Rigakis, 2003, Rigakis and Karakitsios 1998, Rigakis, 1999*) focus on the sedimentary rocks that establish their petroleum generation potential along with potential reservoir rocks and traps. Certainly, there is a need for systematic exploration activities and new data due to limited scientific knowledge and research in Greece.

2 Study Area

Taking into account the Alpine orogenic system, the paleogeography, and the evolution of formations in the region, Greece is distinguished into geotectonic zones (***Figure 1***). The geotectonic zones are grouped into two groups, namely the «Internal Hellenides», where the orogenetic activity took place during Upper Jurassic-Lower Cretaceous, and the «External Hellenides», which only suffered under the orogenetic action during Tertiary.

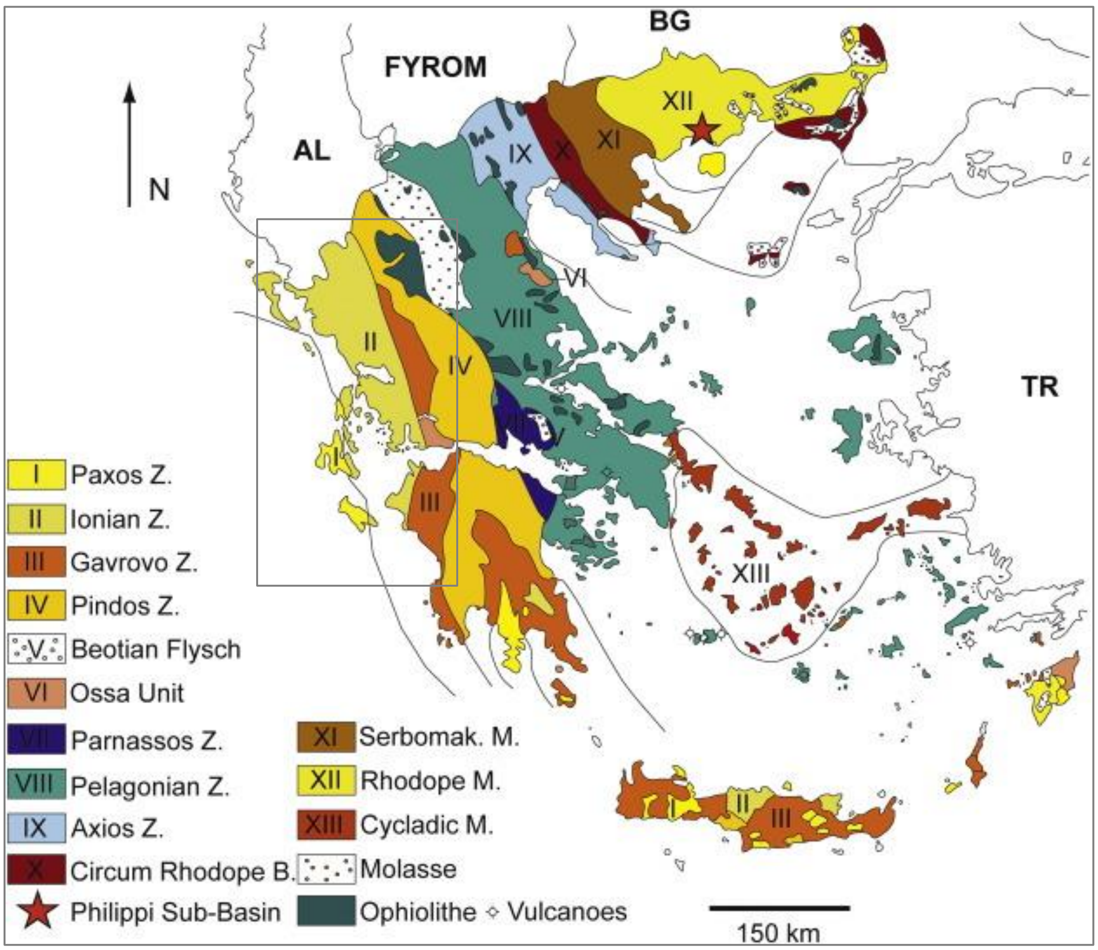

Figure 1*: The geotectonic zones of Greece (Source: http://users.uoa.gr/~hvasilat/files/maps/)*

Western Greece consists of three geotectonic zones, the Gavrovo-Tripolis Zone, the Ionian Zone, and the Pre-Apulian (Paxos) Zone. They are characterized as the most external geotectonic zones of Greece.

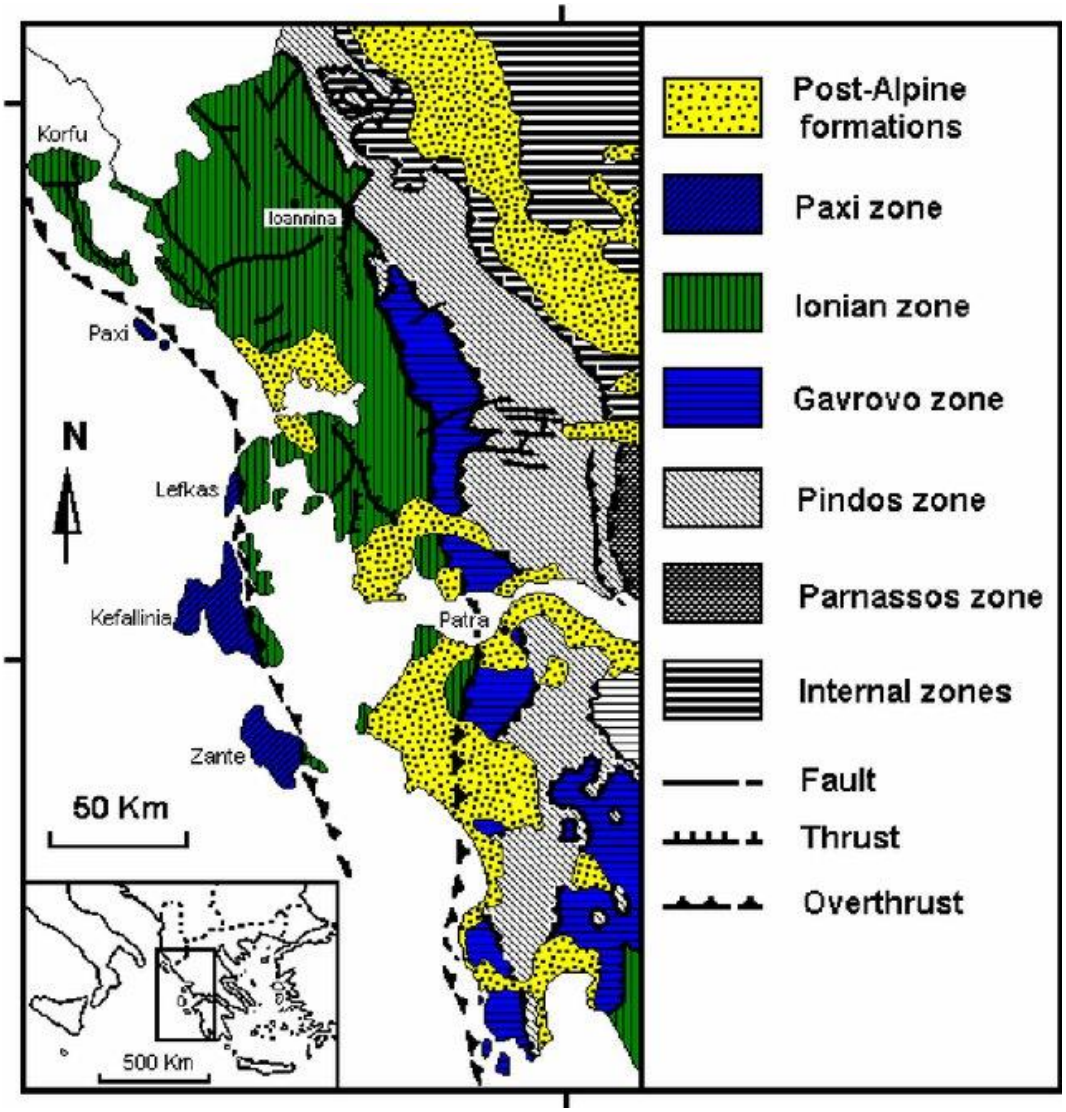

Figure 2*: Geological map of the external Hellenides in NW Greece (Source: Karakitsios, 1995, Karakitsios and Rigakis, 2007).*

The external geotectonic zones of Greece (***Figure 2***) with a NNW-SSE development have been described as indigenous and are characterized by the thrust and fold belt tectonics. The boundaries between them have been observed both in the field and in wells drilled in the region and found to be tectonic. The Pindos Zone is located thrusting towards the Gavrovo Zone and in many places, it has overlapped and has been thrusted over the Ionian Zone. The Gavrovo Zone, which was the margin of the Apulian platform, thrusted towards the Ionian Zone. Both of these boundaries have been studied in detail, while there is a clear lack of evidence about the boundary between the Ionian and the Pre-Apulian Zones because the latter displays only small outcrops in the region. It is considered that the Ionian Zone thrust towards the Pre-Apulian *(Mountrakis, 2010).*

The formations of the Gavrovo and Pre-Apulian Zones are considered rigid and easily fractured, whereas the Ionian Zone is composed of ductile sediments and thrust tectonic prevails in the region. The boundary between the Ionian and the Pre-Apulian Zones is characterized by the intrusive evaporites. The evaporites moved westwards due to pressures from the opposite direction. Many detachment levels were favored from the intrusive evaporites, resulting in the movement of blocks for long distances. Also, listric faults gave analogous movements *(Rigakis, 1999).*

The gradual emersion of the external zones occurred from east to west. Primarily, the Gavrovo Zone emerged during the Oligocene-Miocene boundary, followed by the compressional phase of NEE-SWW direction at Lower Miocene with the emersion of the Ionian Zone. Also, during this time the thrusting of Pindos and Gavrovo Zones along with the imbrications of the Ionian Zone took place in the region. The emersion of the Pre-Apulian Zone took place during the Lower-Middle Miocene. Finally, during the compressional phase and the diapiric movements during Upper Miocene-Pliocene times, the Ionian Zone thrusted towards the Pre-Apulian Zone *(Rigakis, 1999).*

From Triassic to the Late Cretaceous period, Western Greece was part of the Apulian continental block on the southern passive margin of Tethys *(Karakitsios and Rigakis, 2007).* Paleogeographically the Gavrovo Zone was a shallow submarine ridge that received platform carbonate sediments and separated Pindo's groove from that of the Ionian. The Pre-Apulian Zone was the slope of the Apulian platform to the Ionian basin *(Rigakis, 1999).*

Numerous oil seeps have been recorded during exploration in the three above mentioned geotectonic zones strengthening the possible down-deep hydrocarbon accumulations in the region. From detailed geological and geochemical oil-source correlation studies in the Ionian Zone (Western Greece), attribute the surface occurrences of hydrocarbons to the Mesozoic potential source rocks. Specifically, shales within the Lower Cretaceous (Vigla), Middle-Upper Jurassic (Posidonia), and Triassic Formations have been characterized (*Rigakis and Karakitsios 1998*) as good to excellent potential source rocks from which the oil seeps may have originated.

1.1 Gavrovo-Tripolis Zone

The Gavrovo-Tripolis lithostratigraphy is shown in ***Figure 3***. Generally, the zone consists of platform carbonates deposited in a high-energy intertidal environment. The sequence comprises Lower Cretaceous to Eocene limestone followed by the Oligocene flysch *(Rigakis et al 2013)*. No potential source rock intervals have been proved within the Mesozoic sediments of this particular geotectonic zone up to the present day.

<u>*Lithostratigraphic Evolution*</u>

Sedimentation started at Mesozoic with Upper Triassic dolomites and continued at Tertiary with Upper Eocene with dark-colored, shallow platform limestone intercalating with breccia. At Senonian-Campanian dissolving erosion took place and at Campanian-Maastrichtian deposition continued with internal platform sediments with a bioclastic interval at east, while reefal sedimentation took place at the western part of the region *(Rigakis, 1999)*.

Also, the discontinuation of the sedimentation in the region, in the Middle Eocene, is supported. Furthermore, the flysch deposition alternating with marly sandstones, siltstones, and carbonate conglomerates, took place from Upper Eocene to Oligocene as the final stage of the Alpine orogenesis where subsidence is observed for the area *(Rigakis, 1999)*.

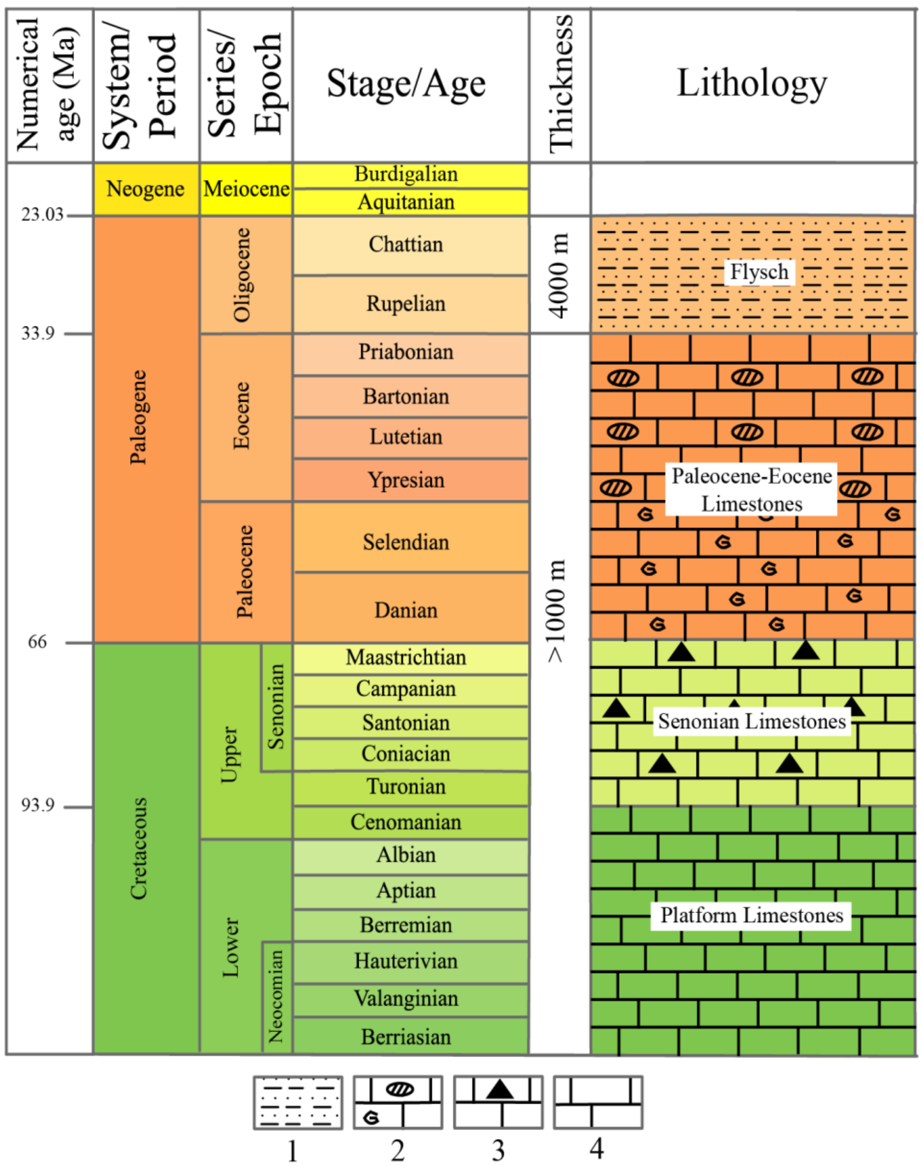

Figure 3*: Synthetic lithostratigraphic column of the Gavrovo Zone. 1) Flysch, 2) Platform carbonates with clastics, 3) Reefal-bioclastic carbonates, 4) Platform limestone (Source: Rigakis, 1999).*

Another emersion of the Gavrovo Zone is possible just before the flysch sedimentation at Upper Cretaceous, presented with an unconformity at the base of flysch. As a result, sedimentation conditions have changed. The Eastern part of the area constituted an external platform environment, while westward a high sea-bed environment existed. From Upper Eocene onwards, the sedimentation continued with marly limestone until the flysch deposition *(Mountrakis, 2010)*.

1.2 Ionian Zone

The Ionian lithostratigraphical column is shown in ***Figure 4***. The Ionian Zone, according to the latest theories, was characterized as a basin with hemipelagic-pelagic sedimentation formed during the Middle Lias between Apulian and Gavrovo platforms. It can be divided into Internal (eastern), Central and External (western) Ionian on the basis of thickness variation.

The zone comprises sedimentary rocks ranging from Triassic evaporites to Jurassic-Upper Eocene carbonates and minor cherts and shales, which are overlain by Oligocene flysch. Organic-rich intervals occur within Triassic evaporites and Jurassic-Cretaceous pelagic argillaceous-siliceous sediments *(Karakitsios and Rigakis, 2007)*.

Lithostratigraphic Evolution

The Ionian Zone consists of Alpine sedimentary rocks and is distinguished by three distinct stratigraphic sequences.

I) The *pre-rift sequence*, the first alpine sediments, is represented by Lower to Middle Triassic evaporites (>1500 m) dominated by anhydrite, gypsum, halite, and associated with dolomitic and carbonate breccia, high in clay content. The sedimentation took place in a shallow-platform environment. Triassic breccia formed by tectonic movements occurred during evaporitic substratum halokinesis. Further, at the stratigraphic sequence, Foustapidima limestone (50-150 m) of Ladinian-Rhaetian age, overlie the evaporites. They consist of black limestone with carbonate breccia and marls and are located in the External Ionian Zone. During Middle Lias the Ionian Zone undertook tensile forces resulting in its subsidence. The sequence is completed with the deposition of shallow water-platform limestone, known as Pantokrator limestone (>1000 m), of Lower Jurassic age. In many regions, Pantokrator limestone has been subjected to dolomitization *(Karakitsios, 1995; Rigakis, 1999; Karakitsios, 2013)*.

II) The *syn-rift sequence* starts with the deposition of Louros Limestone and their lateral equivalent Siniais Limestone (20-150 m). Locating fossils like foraminifera, brachiopods and ammonites declare Pliensbachian age and hemipelagic sedimentation. The Ionian Basin was divided into smaller basins which were characterized by different accommodation spaces. The Siniais Limestone occupy the Central Ionian Zone, while the Louros Limestone occupy the External and Internal Ionian Zone. Subsequently, the half-graben geometry of the Ionian Zone during the Jurassic/Cretaceous rifting stage, gave differentiation of formations' thicknesses for the syn-rift sequence. The deeper parts of synclines consist primarily of the formations Ammonitico Rosso and their lateral equivalent Lower Posidonia beds of Toarcian-Bajocian age. In regions of complete development Filamentous Limestone, of Bajocian-Callovian age, are identified shortly after at the stratigraphic sequence. The sedimentation proceeds with the Upper

Posidonia beds and their lateral equivalent Tokas Limestone, of Callovian-Tithonian age. The thickness of the syn-rift sequences varies from 20 to 200 m *(Karakitsios, 1995; Rigakis, 1999; Karakitsios, 2013)*.

Regarding lithology of the formations, Ammonitico Rosso consists of limestone and marls, red in color, with an oversupply of ammonites. At the base of the formation grey marly layers have been identified. Lower Posidonia beds consist of marly limestone layers of limited thickness and cyan to grey color and laminated marls with high silica and bitumen content. Filamentous Limestone consists of limestone of grey-beige color, high in actinozoan and filament fossils. Upper Posidonia beds consist of alternating cherty and shale beds and Toka Limestone consist of pelagic limestone with cherty nodules and marls. The succession of the syn-rift sequence is interrupted by hiatuses and unconformities. Occasionally, Filamentous Limestone is absent, so the Upper Posidonia beds lie directly on the Lower ones *(Karakitsios, 1995; Rigakis, 1999; Karakitsios, 2013)*.

III) The <u>*post-rift sequence*</u> begins with the deposition of the Vigla Limestone, of Berriasian-Turonian age. It is about pelagic limestone with cherts. Two important zones are also presented, consisting of cherty layers with shale and marl intercalations. From Tithonian time, extended subsidence took place at the Ionian Basin, and thus, the sedimentation conditions were homogenized throughout the region. It is important to point out that sometimes the Vigla Limestone lies directly on the pre-rift sequence, so its base represents the breakup unconformity of the post-rift sequence *(Karakitsios and Rigakis, 2007)*. Different thicknesses are observed for the Vigla Limestone and are attributed to continuous halokinesis of the evaporites in the region. Afterward, the Ionian Zone was separated as a topographically higher area. As a result, the sedimentation suffered a reduction.

Furthermore, the Carbonate platforms of Gavrovo and Apulian gave the feed of clastic material. So, the sequence continues with the Senonian Limestone (100-300 m). Two facies are identified in the formation, which consist of calciturbidite limestone with intervals of globotruncardis, rudist and microbreccia, and limestone with rudist fragments and calcareous cement with a high content of pelagic fauna *(Karakitsios and Rigakis, 2007)*.

The Gavrovo and Apulian platforms suffered an erosional phase during Cretaceous, more intense during Paleocene, which provides Ionian Zone's brecciated material. In the Ionian Zone, during Paleocene-Eocene time, sedimentation was homogenous and proceed with the deposition of limestone with rare cherty intercalations and clastic material (200-400 m). There is also a zone with marly limestone, which indicates the transition from the Senonian Limestone to the flysch deposition *(Karakitsios, 1995; Rigakis, 1999)*.

During Oligocene, flysch deposition took place in the Ionian Zone, namely siltstone and sandstone overlying a basal conglomerate. The thickness largely varies, but in some regions, it exceeds 1400 m. The flysch represents deep marine environments of a developing orogen. Its deposition took place during the early stage of the orogenesis and is characterized as syn-orogenic sediment. At the end of Burdigalian, the inversion of the Ionian Zone took place with major orogenic movements. The uplift of the zone took place during Aquitanian with the formation of shallow basins, so the zone accepted clastic sediments at Burdigalian *(Karakitsios and Rigakis, 2007)*.

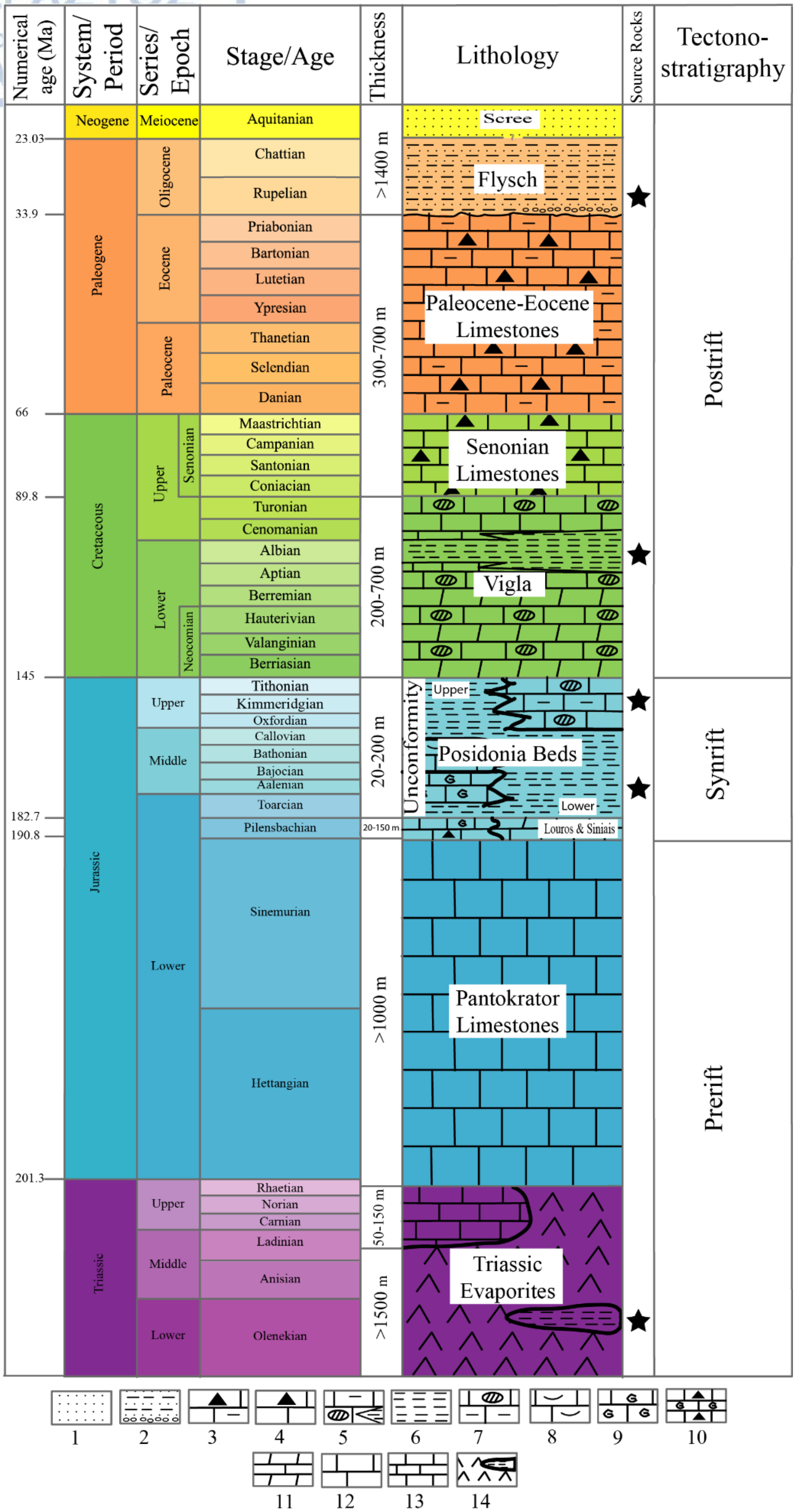
Numerical age (Ma)
System/ Period
Series/ Epoch
Stage/Age
Thickness
Lithology
Source Rocks
Tectono-stratigraphy
Neogene
Meiocene
Aquitanian
23.03
Paleogene
Oligocene
Chattian
Rupelian
33.9
Eocene
Priabonian
Bartonian
Lutetian
Ypresian
Paleocene
Thanetian
Selendian
Danian
66
Cretaceous
Upper
Senonian
Maastrichtian
Campanian
Santonian
Coniacian
89.8
Turonian
Cenomanian
Lower
Albian
Aptian
Berremian
Neocomian
Hauterivian
Valanginian
Berriasian
145
Jurassic
Upper
Tithonian
Kimmeridgian
Middle
Oxfordian
Callovian
Bathonian
Bajocian
Aalenian
Toarcian
182.7
190.8
Lower
Pilensbachian
Sinemurian
Hettangian
201.3
Triassic
Upper
Rhaetian
Norian
Carnian
Middle
Ladinian
Anisian
Lower
Olenekian
>1400 m
300-700 m
200-700 m
20-200 m
20-150 m
>1000 m
50-150 m
>1500 m
Scree
Flysch
Paleocene-Eocene
Limestones
Senonian
Limestones
Vigla
Unconformity
Upper
Posidonia Beds
Lower
Louros & Siniais
Pantokrator
Limestones
Triassic
Evaporites
Postrift
Synrift
Prerift
1
2
3
4
5
6
7
8
9
10
11
12
13
14

Figure 4*: Synthetic lithostratigraphic column of the Ionian Zone. 1) Scree, 2) Pelites, sandstone and congomerates, 3) Limestone with rare cherty intercalations, brecciated, 4) Pelagic limestone with calciturbidite intercalation, 5) Pelagic limestone with cherts and shale intercalations, 6) Upper: Alternating cherty and shale beds, Lower: Marly limestone and laminated marls, 7) Pelagic limestone with cherty nodules and marls, 8) Pelagic limestone with lamellibranches, 9) Pelagic, nodular red limestone with ammonites, 10) External platform limestone with brachiopods and small ammonites, 11) Pelagic Limestone with rare cherty intercalations, 12) Platform limestone, 13) Thin-bedded black limestone, 14) Evaporites with shale horizons (Source: Karakitsios, 1995; Rigakis, 1999).*

Tectonics

Structural analysis of the Ionian zone shows that orogenesis essentially took place during the major phase of deformation at the end of early Miocene. It was the result of the compression of Tertiary age, with intense imbrications favored by the evaporitic halokinesis. The folding of the zone is accompanied by rifting which created continuous thrust and imbrications. The Ionian zone was considered to be the assemblage of anticlines and synclines pushed against each other by a system of moderate westward overthrusts, which were accompanied by a transcurrent fault system that made the thrust mechanism easier (*Karakitsios, 1995*).

The structures of the zone present divergence whereas the western and central zone is displaced towards the west and the eastern zone towards the east. Generally, extensional faults were reactivated with either reverse or transcurrent displacement, consistent with classical inversion tectonics. In some cases, during the compressional phase, extensional faults were not reactivated as simple thrusts, but the elevated extensional footwalls were thrusts over pre-existing hanging walls due to movements of the basal evaporitic units. This was facilitated by diapiric movements involving the basal evaporitic interval. Field and available seismic data suggest that at least moderate décollement took place along the evaporites *(Karakitsios and Rigakis, 2007)*.

1.3 Pre-Apulian Zone (Paxos)

The Pre-Apulian Zone (***Figure 5***) is the most external domain of the Hellenic fold and thrust belt and is characterized by continuous neritic sedimentation and the absence of flysch. However, it is believed that an informal flysch formation shows up at Pre-Apulian platform, due to the gradual transition from the typical flysch of the Ionian Zone to the calcareous facies of Pre-Apulian. Part of the zone is detected in the Ionian islands. The zone, during Mesozoic-Cenozoic period, constituted the internal Apulian Platform that extended towards the Ionian Basin *(Karakitsios and Rigakis, 2007)*.

Lithostratigraphic Evolution

The Pre-Apulian sedimentation begins, at shallow platforms, with the Triassic Evaporites (>1700 m), containing dolomites with shale intercalations and anhydrite. Their age has been attributed to Upper Triassic, due to the identification of Glomospirella sp. and Trochamina Almalensis microfossils. The sedimentation continues with limestone and dolomitic limestone, anhydrite, and shale intercalations of Lower Jurassic age (1650 m). Further, marly limestone and basal anhydrite with cherts and shale layers, rich in organic carbon, were deposited during Middle Jurassic (150 m), which are covered with limestone, marly limestone and marls of Upper Jurassic age (500-730 m). Occasionally, the Upper Jurassic succession represents a possible hiatus and the total thickness of the Jurassic sequence is much more developed than the corresponding Ionian succession due to transition towards the Apulian well *(Rigakis, 1999; Karakitsios, 2013)*.

In some cases, at the base of the Cretaceous succession, a conglomerate formation is detected with calcareous and magmatic elements which afterward continues with pelagic limestone and chert nodules. At the upper parts of the sequence, the limestone become more brecciated, high in rudist fragment, and sometimes are represented by a hiatus. The thickness of the sequence varies from 700 to 1550 m *(Rigakis, 1999; Karakitsios, 2013)*.

The sedimentation continued at Paleocene with the deposition of pelagic limestone with brecciated intercalations which in the upper parts contain marly layers. During this time, intense tectonic activity and erosional facies at Oligocene had a result of a differentiation of the Pre-Apulian Zone with the inversion of some parts of the zone and the presence of unconformities. Subsequently, the deepening of the zone at Early Miocene gave the deposition of marly limestone at the lower parts, and marls at the upper parts of the sequence. The Pre-Apulian succession is completed with the presence of marine marls and sands with lignite intercalations of the Plio-Pleistocene age. Besides, the bound between the Miocene and Pliocene successions is characterized by an unconformity and the presence of evaporites *(Rigakis, 1999; Karakitsios, 2013)*.

Figure 5*: Synthetic lithostratigraphic column of the Pre-Apulian Zone. 1) Marine marls and sand, 2) Limestone commonly marly, 3) Pelagic limestone or marly limestone and brecciated intercalations, 4) Mixed pelagic-neritic limestone sometimes with breccias, 5) Pelagic limestone, 6) Mixed pelagic-neritic calcareous and magmatic elements, 7) Pelagic limestone with nodules and rare cherty intercalations, 8) Conglomerates, 9) Pelagic limestone commonly marly, 10) Limestone, shales and basal anhydrite, 11) Limestone and dolomitic Limestone, anhydrite and shale intercalations, 12) Evaporites, 13) Shale layers (Source: Karakitsios, 1995; Rigakis, 1999).*

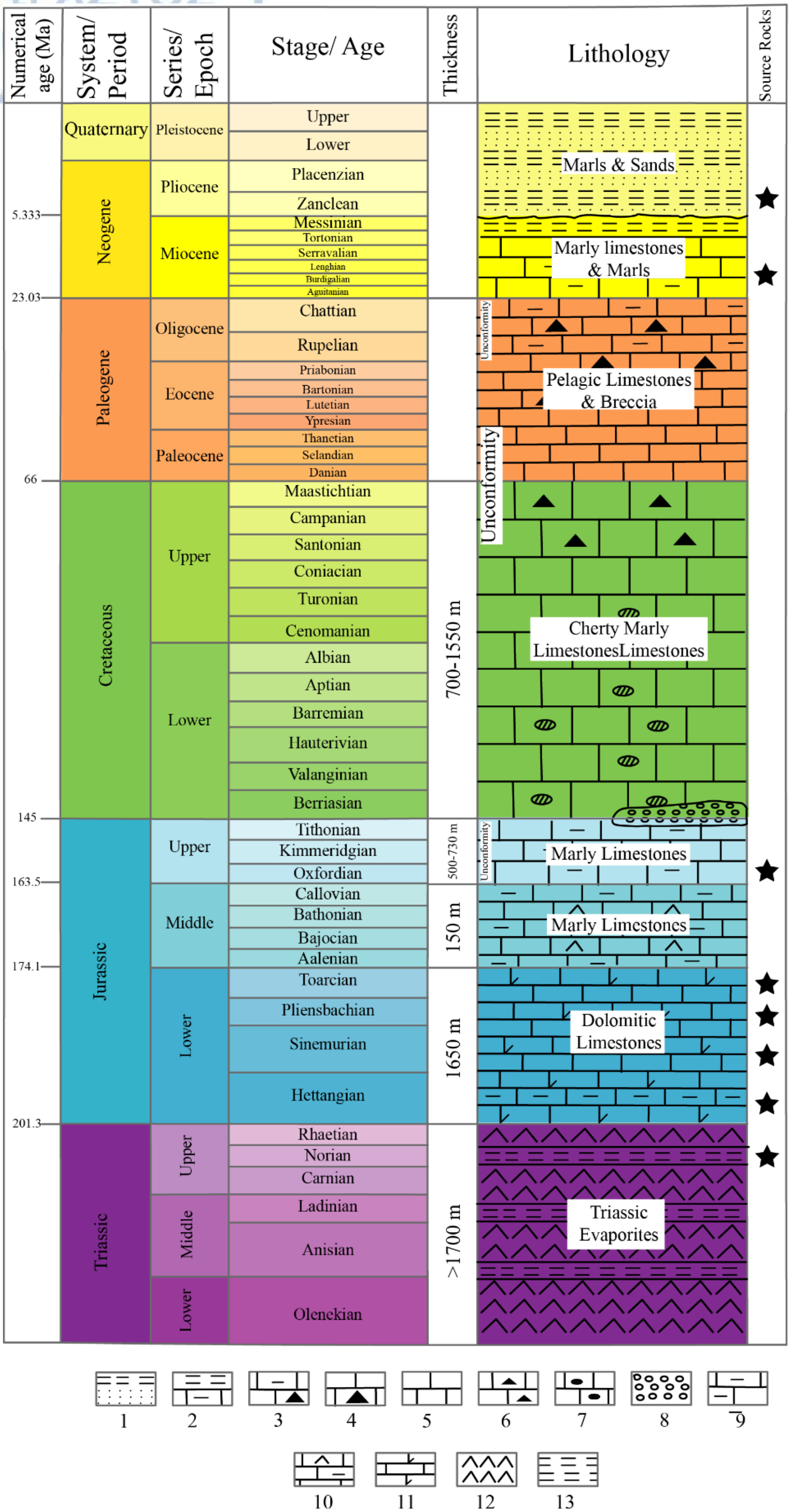
Numerical age (Ma)
System/ Period
Series/ Epoch
Stage/ Age
Thickness
Lithology
Source Rocks
5.333
23.03
66
145
163.5
174.1
201.3
Quaternary
Neogene
Paleogene
Cretaceous
Jurassic
Triassic
Pleistocene
Pliocene
Miocene
Oligocene
Eocene
Paleocene
Upper
Lower
Middle
Upper
Lower
Placenzian
Zanclean
Messinian
Tortonian
Serravalian
Lenghian
Burdigalian
Aquitanian
Chattian
Rupelian
Priabonian
Bartonian
Lutetian
Ypresian
Thanetian
Selandian
Danian
Maastichtian
Campanian
Santonian
Coniacian
Turonian
Cenomanian
Albian
Aptian
Barremian
Hauterivian
Valanginian
Berriasian
Tithonian
Kimmeridgian
Oxfordian
Callovian
Bathonian
Bajocian
Aalenian
Toarcian
Pliensbachian
Sinemurian
Hettangian
Rhaetian
Norian
Carnian
Ladinian
Anisian
Olenekian
700-1550 m
500-730 m
150 m
1650 m
>1700 m
Marls & Sands
Marly limestones & Marls
Unconformity
Pelagic Limestones & Breccia
Unconformity
Cherty Marly LimestonesLimestones
Unconformity
Marly Limestones
Marly Limestones
Dolomitic Limestones
Triassic Evaporites
1
2
3
4
5
6
7
8
9
10
11
12
13

2 Petroleum system elements

The geological conditions of Western Greece have been assumed to be favored for the development of petroleum accumulations. Many researchers have already studied the area and found possible traps, source rocks, reservoir rocks and cap rocks. In thrust and fold belt areas, like in Western Greece, where the geological setting is quite complex, the areas with favorable or unfavorable conditions vary drastically within a few kilometers. Therefore, the petroleum system elements along with the generation, expulsion, migration, and accumulation of hydrocarbons should be determined by detail in each area separately. The petroleum system elements will be discussed in the next chapters.

2.1 Source rocks

Six possible source rocks have been discovered in the Ionian Zone.

- Triassic shale fragments
- Ammonitico Rosso marls
- Lower Posidonia beds
- Upper Posidonia beds
- Vigla shales

From east towards the west, in the Gavrovo Zone, no possible source rock has been discovered yet. In the Internal Ionian Zone, the most promising source rock, in terms of TOC (Total Organic Carbon) and HI (Hydrogen Index), is the Vigla shales of Albian-Cenomanian age which are interbedded within the Lower Cretaceous Vigla Limestone. In the Central and External Ionian Zone, the Middle-Upper Jurassic, Posidonia shales, and the Lower Triassic shales are considered as the most important source rock intervals in terms of TOC and HI. In the Pre-Apulian Zone, the Upper Jurassic shales, the Lower Jurassic thin shaly intervals, and the Upper Triassic shales are of the greatest interest *(Rigakis and Karakitsios, 1998)*.

2.2 Reservoir rocks

The reservoir rocks, one of each petroleum system elements, must be characterized by good porosity and permeability to have the ability to store and accumulate fluids inside the pores. The research for reservoir rock in Western Greece has focused on the carbonate formations and clastic sediments. The most promising reservoir rocks of Western Greece are primarily the Senonian Limestone and the Paleocene-Eocene Limestone. Hydrocarbon accumulations within such rocks have been proved in many cases in Albania through discoveries. However, the following potential reservoir rocks could be considered, and are currently under investigation:

- Pantokrator Limestone
- Vigla Limestone (Partially the case of Katakolo)
- Neogene sands

It is important to mention the extensive dolomitization that occurred at the Internal Ionian Zone, which is more intense towards deep. The layers that suffered dolomitization have a better ability as reservoir rocks. Also, areas with intense tectonic activity have given formations with high secondary porosity and highest permeability and therefore, better reservoir characteristics *(Rigakis et al., 2013).*

2.3 Seal/Cap rocks

Cap rock is an impermeable rock, usually shale, which is an obstacle preventing the leakage of hydrocarbons to the surface. Cap rock is characterized by low porosity and permeability. Oligocene flysch and the Upper Pliocene-Miocene marls (as is the case of Katakolo) are considered as the primary seal formations in Western Greece. However, formations that potentially can act as seals in Western Greece are the following:

- Triassic Evaporites
- Jurassic shales and limestone

It is worthy to mention that the seal formations should not have been affected by the tectonic activity of the area and have not acquired secondary porosity *(Rigakis, 1999).*

2.4 Trapping

In the Ionian Zone, due to intense erosion, most topographic highs, anticlines, were eliminated together with the hydrocarbon accumulations that came along. However, topographic lows, synclines, and their corresponding minor anticlines, of the area have been preserved, avoiding erosion, along with their flysch cover and are considered good potential traps *(Rigakis, 1999).*

Important hydrocarbon traps may be found at the tectonic boundaries of the Ionian, Pre-Apulian, and Gavrovo Zones. Also, at the Pre-Apulian Zone, major anticlines are assumed to form good hydrocarbon traps.

Major traps are considered between the evaporitic succession and their basement. The Jurassic extensional phase triggered halokinesis of the basement evaporites. This affected the syn-rift mechanism by enhancing the extensional fault throws, resulting in the formation of small, structurally controlled subbasins with half-graben geometry. During the compressional orogenetic phase, pre-existing extensional structures were reactivated. The precise geometric characteristics of inverted basins depend on the intensity of evaporitic halokinesis and on the lithological properties of the evaporites, as well as on diapiric intrusions in the Ionian tectonic Zone and on the detachment of the individual thrust sheets along the Triassic evaporites. The result is the tectonic duplication of the Ionian series which favors hydrocarbon trapping within the lower carbonate series *(Karakitsios, 2013).*

3 Basin Analysis

3.1 Introduction

The overall goal of the current basin modelling scenario is to simulate the thermal and maturity evolution of the western Patraikos Gulf area. Basin analysis was conducted, with a special emphasis on a specified charging model, with multiple input data, such as crustal thickness, beta-factor, rifting time, radioactive heat, source rock parameters, and seal properties. Consequently, basin analysis is to estimate and reconstruct the burial and the hydrocarbon charge history. More specifically, it estimates the hydrocarbon generation, expulsion, migration, accumulation, and respective timing.

3.2 Modeling method and parameters

The modeling processes for the Patraikos Gulf area were performed using the PetroMod 1D Modeling software by Schlumberger and the Genesis and Trinity 3D petroleum modeling software by Zetaware.

Hellenic Petroleum S.A. (HELPE) provided 32 selected points, known as “Pseudowells” derived from the combination of onshore equivalents and seismic interpretation. For each pseudowell, a model was simulated. For this dissertation, pseudowell-A (PW-A) was selected for 1D modeling. ***Figure 6*** shows a detailed location map for the western Patraikos Gulf block area. In the 3D modeling, pseudowell-B (PW-B) was also used for better optimization of the results. All created images for PW-B are presented in the ***Appendix (Figures A-I)***. The location of both wells is under confidentiality and is not included in this study.

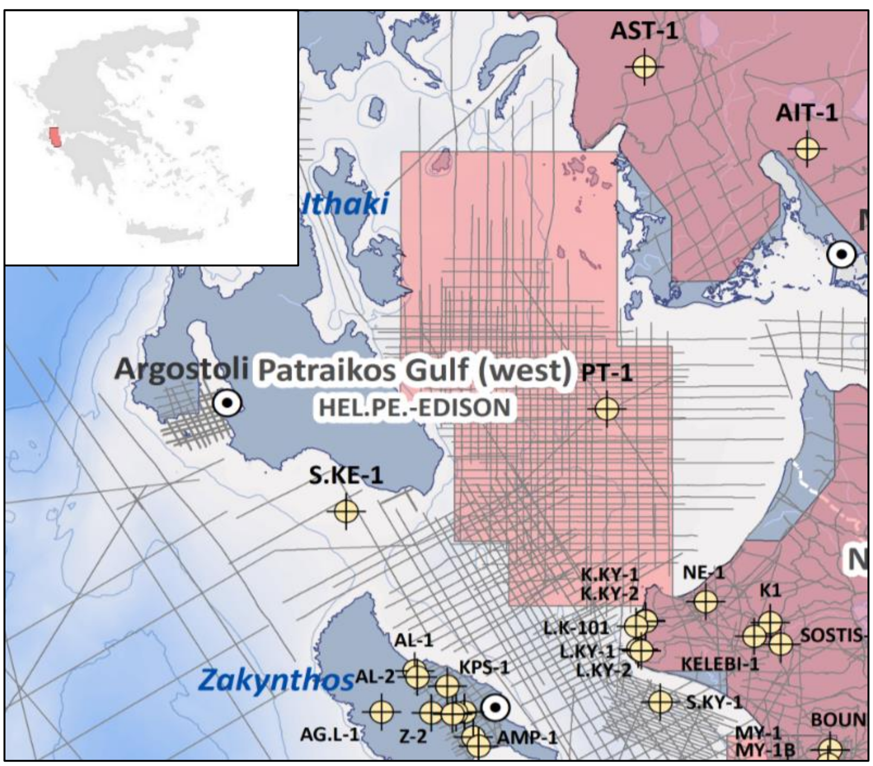

***Figure 6**: Detailed location map for the Patraikos Gulf block (https://www.greekhydrocarbons.gr/)*

The input data that was used for the modelling, issued from published literature and HELPE. The input parameters include:

- Formation tops derived from the seismic interpretation (seismic depth grids).
- Thicknesses were interpreted and calibrated by onshore equivalents, well data, and published data.
- Lithologies based on onshore equivalents and according to the published work (*Getsos et al., 2007; Rigakis, 1999; Rigakis and Karakitsios, 1998; Rigakis et al., 2013*).
- Tectono-stratigraphic history of the area (ages and additional tectonic events such as thrusting, non-preserved deposition, and equivalent erosion).
- Source rock parameters (Kerogen types, initial TOC, HI values, etc.) based on geochemical analyses data.
- Paleo-bathymetry was estimated based on paleo-depositional environments and known lithologies from onshore equivalents.
- Sediment surface interface temperature based on equations of *Beardsmore and Cull (2001).*

For the better understanding of the results, some key parameters for the predicted sequence of PW-A, concerning two erosional and one thrusting events, are pointed out. Those were considered critical and would affect the thermal maturity of the underlying source rocks.

The first erosional event applied in the Oligocene (30-28 Ma) age, represents a missing section of 700-m-thick sediments. The second erosional event applied during Miocene (7-5 Ma) and corresponds to the removal of 1600 m of previously deposited sediments. Furthermore, a thrusted sheet, known as Echinades thrust, was added on the section at Oligocene-Miocene (23.7-16.6 Ma) age, between the two previous erosional events. The thrust caused the addition of 1312 m of sediments in the area.

The following tables list information about the applied values considering the heat flow parameters (***Table 1***), the seal capacity parameters (***Table 2***) and the source rock properties (***Table 3***). The values considering the thermal regime of the area were sorted after thorough research of published maps (***Appendix, Figures J-L***). An average composition of the crust was selected. In addition, values for the stretching factor and the radioactive heat were used based on analogues (geological settings) of nearby areas.

Table 1*: Parameters used to constrain the different thermal and maturity models considering the thermal regime of the area.*

Parameters		**Scenario 1**		**Scenario 2**		**Scenario 3**		**Scenario 4**	
Crust (km)		35		35		25		35	
Lithosphere (km)		90		85		95		85	
Radioactive Heat Production (mW/m^3)		2.5		2.8		3		2.8	
b-Factor	**Rifting (Ma)**	2.5	190-145	1.3	190-145	1.1	190-145	1.3	247-242
								1.3	190-180
								1.4	180-170
								1.8	170-160
Heat Flow (mW/m^2)		36		44		49		-	

Table 2*: Parameters used to constrain the different basin models considering the seal capacity of the formations for the area. Seal capacity values are in meters.*

Formation	Scenario I	Scenario II	Scenario III	Scenario IV
Plio-Pleistocene	1	50	100	800
Late Miocene	1	50	100	800
Middle Miocene	1	50	100	800
Early Miocene	1	50	100	800
Late Oligocene	1	50	100	800
Early Oligocene	1	50	100	800
Eocene	1	50	100	800
Senonian		1	1	1
Vigla Shales	1	1	1	1
Early Cretaceous	1	1	1	1
Posidonia Beds	1	1	1	1
Early Jurassic	1	1	1	1
Triassic Shales	1	1	1	1

Table 3*: Parameters used to constrain the basin models considering the source rock properties of the area (Sc: Scenario).*

Parameters	Triassic Shales			Posidonia Beds			Vigla Shales		
	Sc. A	Sc. B	Sc. C	Sc. A	Sc. B	Sc. C	Sc. A	Sc. B	Sc. C
Age	Tithonian-Norian			Callovian-Tithonian			Albian-Cenomanian		
Kerogen Type	I			IIS			II		
Organo-facies	C			A			A		
Average TOC (%)	1.5	3	6	1	2	4	1	1.8	3.6
Average HI	600	650	700	550	600	650	450	500	550
Average Thickness (m)	25	30	60	40	60	100	40	60	100

The results of the 1D modeling were used for the estimation of the thermal maturity level of the organic matter and the timing of hydrocarbons' generation and expulsion. On the other hand, 3D modeling provides information about the petroleum generation and accumulation processes, the calculation of the expelled hydrocarbons and the vertical and lateral migration process.

Figure 7 illustrates the workflow for the Patraikos Gulf thermal maturity model simulation.

It is advisable to firstly present a model in order to understand the general status of the area. For the simulation of this model the following parameters were used: Scenario 2 from thermal regime parameters (***Table 1***), Scenario III from seal properties (***Table 2***), and Scenario B from source rock properties (***Table 3***). Furthermore, the 1D modeling charts for Scenario 1 issued from the dissertation of ***Styliani Bragou*** with the title *"Hydrocarbon generation and expulsion sensitivity analysis by applying 1D/2D/3D basing modeling, Patraikos Gulf, Western Greece", 2020*. It also represents a detailed sensitivity analysis for the timing window of the hydrocarbons' generation and expulsion.

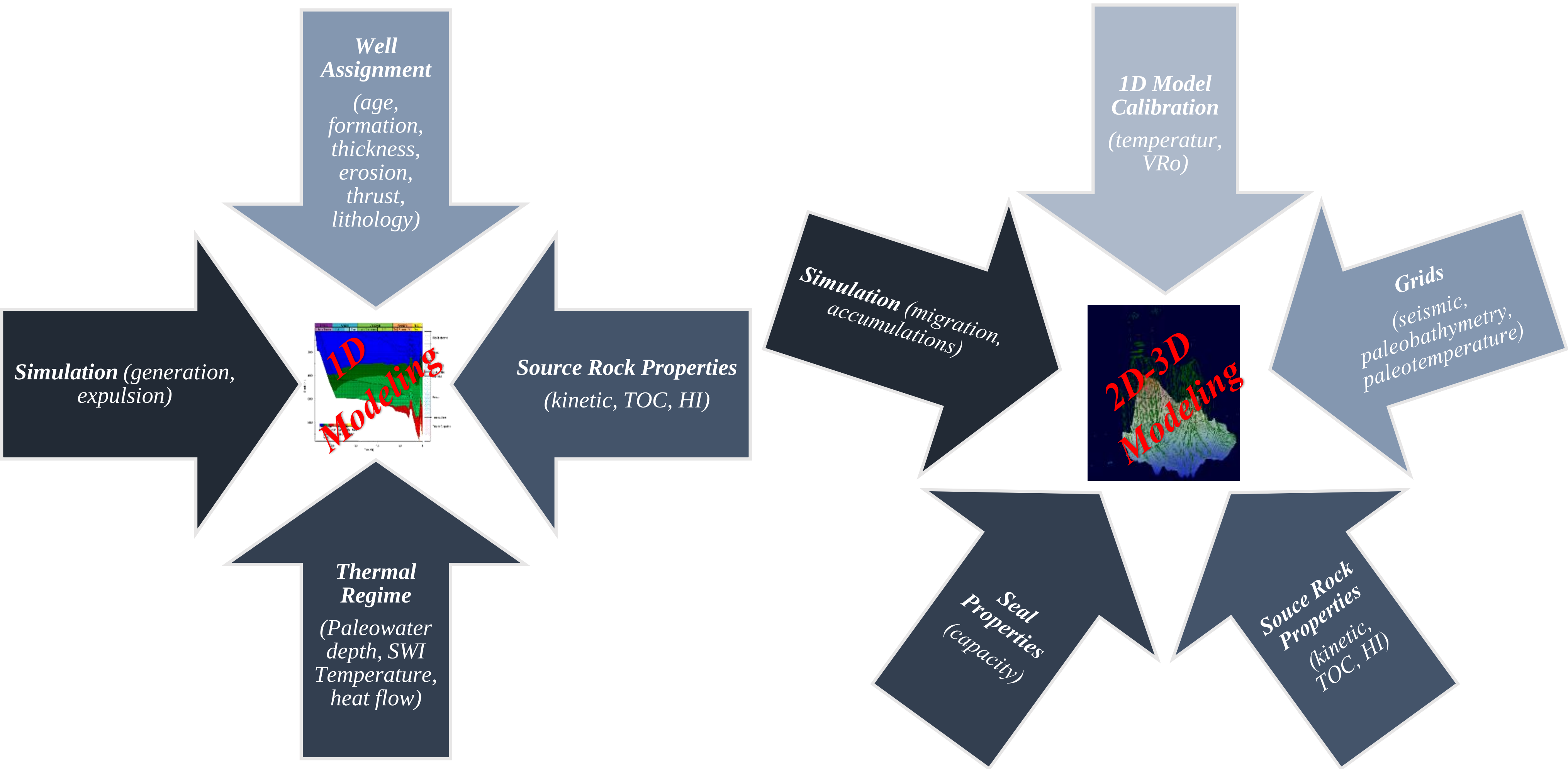

Figure 7: *Workflow during the reconstruction of the Patraikos Gulf thermal maturity model.*

3.2.1 Burial History

Figure 9 and ***Figure 10*** show the burial history curves of the representative PW-A. Information on the current depth and calculated maximum depth of the burial for the three source rocks of the area are listed in ***Table 4***.

***Table 4**: Current depth, calculated maximum depth of burial.*

Burial history location	Source rock		
Pseudo-well #A	**Vigla Shales**	**Posidonia Beds**	**Triassic Shales**
Current depth	3570 m	3930 m	7454 m
Maximum depth	4100 m	4550 m	8100 m

The thermal regime through time is shown in ***Figure 8***. For heat flow measurements PetroMod 1D Modeling Software utilizes the McKenzie Heat Flow Model. According to this model, the rifting event is instantaneous. An explanation of this event is based on the "instantaneous" finite extension (stretching) of a double-layer lithosphere (*Sheplev and Reverdatto, 1998*). In the pre-rift period, the model's function is linear, capturing the rapid increase of crustal heat. In the syn-rift and post-rift period McKenzie's model function becomes exponential, capturing the smooth decrease of the crustal heat.

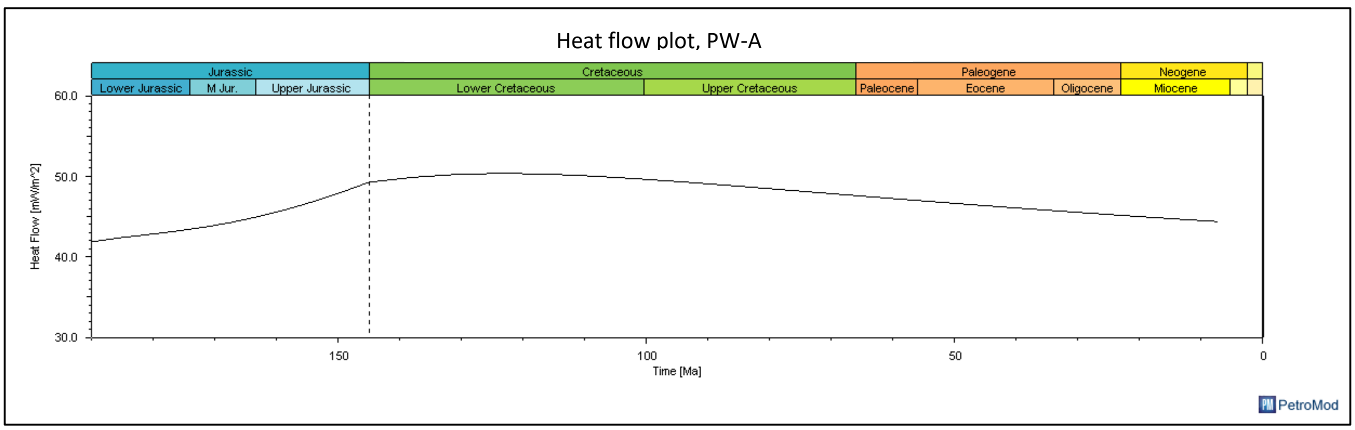

***Figure 8**: Heat Flow curve for Scenario 2. Heat flow values are in mW/m^2.*

The burial history curves suggest that during Middle Triassic to Upper Triassic (240-230 Ma), Triassic Evaporites and the first (deepest in the normal stratigraphic sequence) potential source rock of the area known as Triassic shales, were deposited. The sediment accumulation thickness, according to published research, is more than 3000 m, although at PW-B appears with almost 1550-m thick sediments. Later, from Upper Triassic to Lower Jurassic (230-193 Ma) the deposition of Pantokrator platform carbonates took place. The formation appears with 3464 m thickness. During the Syn-Rift period from Lower Jurassic to Upper Jurassic (190-145 Ma), and more specifically from 193 to 146 Ma the sedimentation rate looks fairly constant and relatively slow. During this period, the second potential source rock of the area, known as Posidonia beds, was deposited, with 60 m thickness. Between, Lower to Upper Cretaceous (146-89 Ma) the deposition rate remains slow, with the deposition of the Vigla Carbonates and the third potential source rock

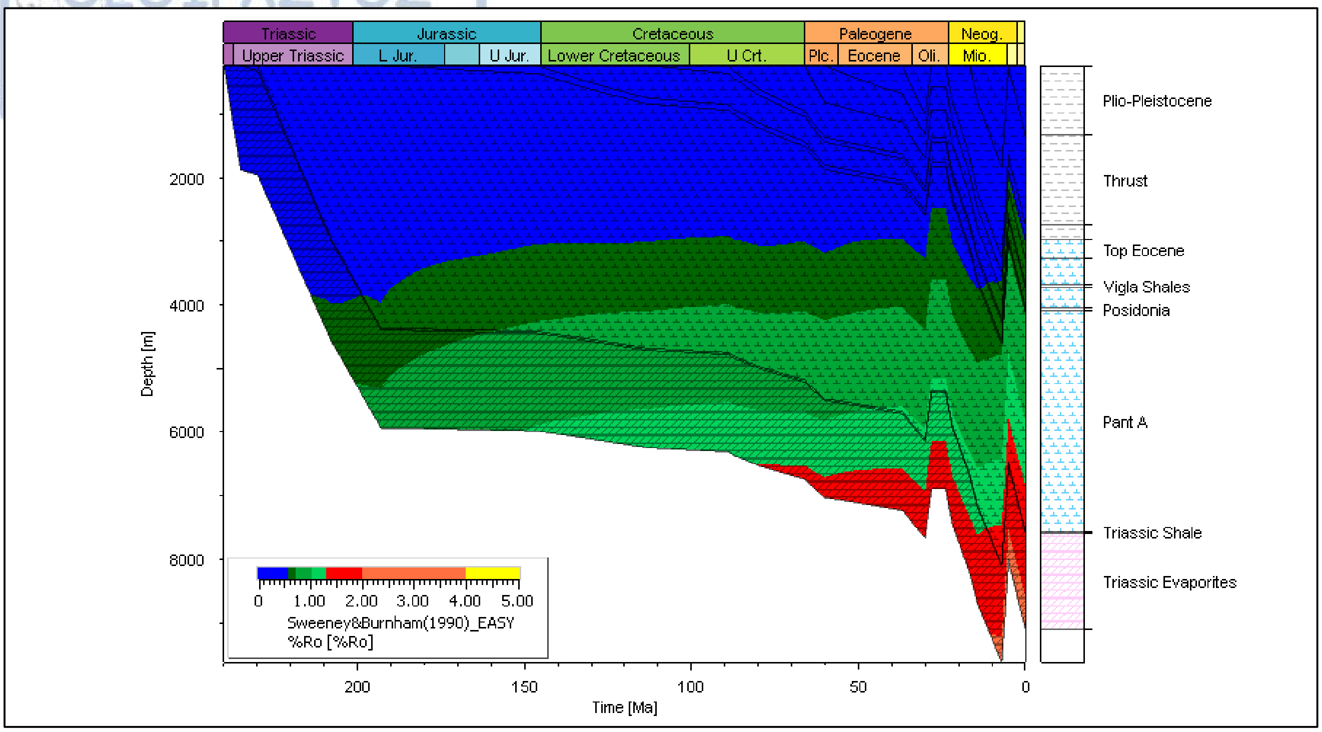

Figure 9: Burial history plot (240 Ma to Present) of the PW-A at Patraikos Gulf.

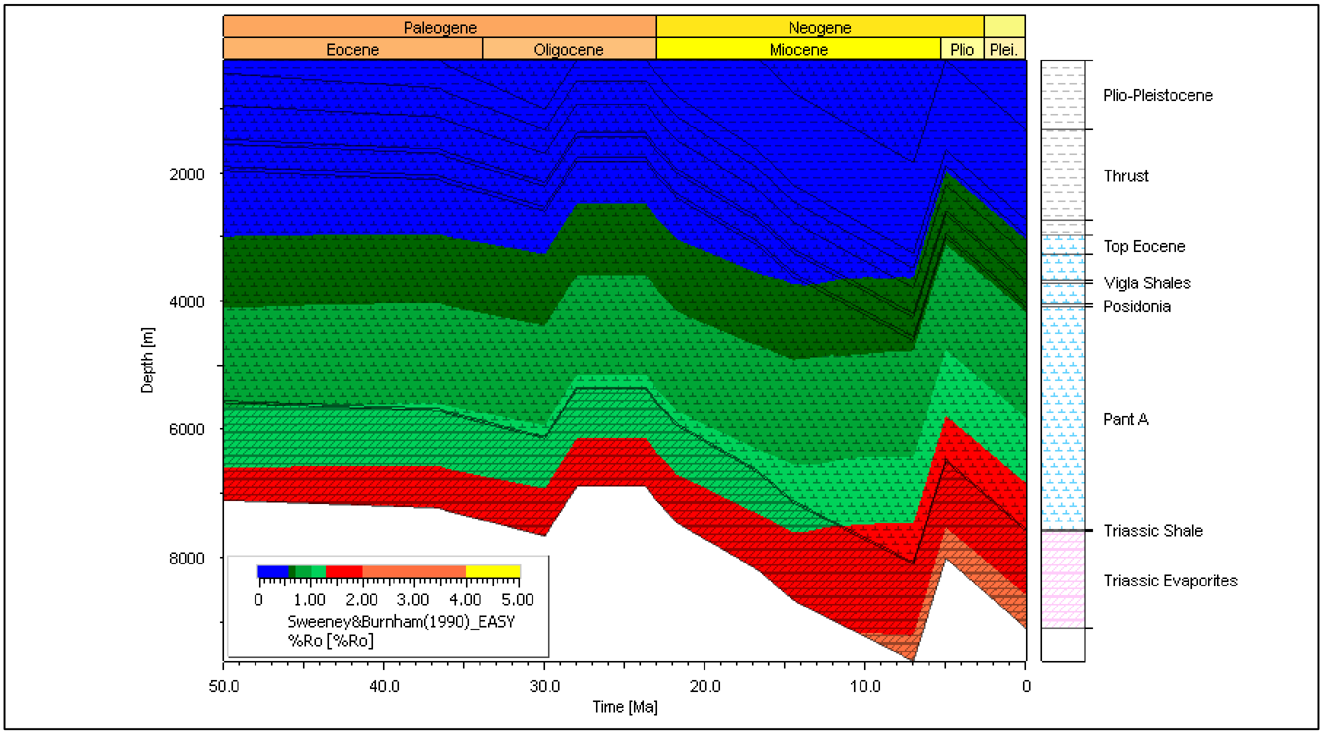

***Figure 10**: Burial history plot (50 Ma to Present) of the PW-A at Patraikos Gulf.*

of the area, known as Vigla shales. The formations appear 300 m and 60 m thick, respectively. During Upper Cretaceous to Oligocene (89-36.6 Ma) Senonian Carbonates, Paleocene-Eocene Limestone, and the Ionian Flysch were deposited with approximately 940 m of thickness. The first erosional event lasted about 2 Ma and ended with the beginning of thrusting. There is a removal of about 700 m of the section. After that, the burial history curve drops steeply, representing the rapid increase in sediment accumulation rate during thrusting between 23.7 to 16.6 Ma. Maximum burial occurred around 7 Ma when the second erosional event lasted about 2 Ma. The erosional event started with the end of thrusting and ended with the deposition of the Plio-Pleistocene sediments. Removal of 1600 m of sediment was observed. In the last 5 Ma almost 1100 m of sediment have been deposited in the area of western Patraikos Gulf.

A comparison between the two applied pseudowells is necessary to better understand their differences. The results of PW-A are, in detail, in the previous sections, while all resulted diagrams for PW-B are shown in the ***Appendix (Figures A-I)***. The thermal regime for both models remains the same.

At first, only Triassic shales and Posidonia beds appear at PW-B as the potential source rocks of the area. Triassic shales at PW-A show earlier generation and expulsion compared to PW-B, considering that the source rock remains at the late oil window and the wet gas window, for a longer period. On the other hand, Posidonia beds generated and expelled hydrocarbons at an earlier time and to greater extent in PW-B than in PW-A, due to its higher maturation level. The above variations may be due to different erosion and thrusted thickness. As modeled, the thickness for the applied erosional and thrusted events are doubled in PW-B, illustrating deeper burial and higher temperature and pressure conditions. Besides, the effect of the thrusted sheet appears more intense in PW-B.

3.2.2 Maturation History

The maturation history performed for PW-A, is based on calculated vitrinite reflectance (%Ro). As illustrated for VRo in ***Figures 11 and 12***, the blue-colored area represents the immature to marginally mature organic matter (< 0.55 %Ro). The light green-colored area represents the early window of oil generation (0.55 – 0.7 %Ro). The green-colored area represents the main window of oil generation (0.7- 1.0 %Ro). The dark-green colored area represents the late oil window (1.0- 1.3 %Ro). The orange-colored area represents the wet gas window (1.3- 1.5 %Ro). The red-colored area represents the dry gas window (2.0- 2.4 %Ro).

The three source rocks of the area are considered oil-prone. Triassic shales are composed of Type I Kerogen and at present (0 Ma) are partially in the oil and partially in the gas window depending on the location as ***Figure 12*** shows. Posidonia beds and Vigla shales are mostly composed of Type II Kerogen. Both source rocks at present are either immature or within the early oil window depending on the location as ***Figure 12*** illustrates. An increase in maturation for all three source rocks is noticed due to the thrusting event in Miocene. In particular, Triassic shales VRo vs. Time chart suggests that the thrusting event affected the maturation process of the source rock, thus, entering the gas window.

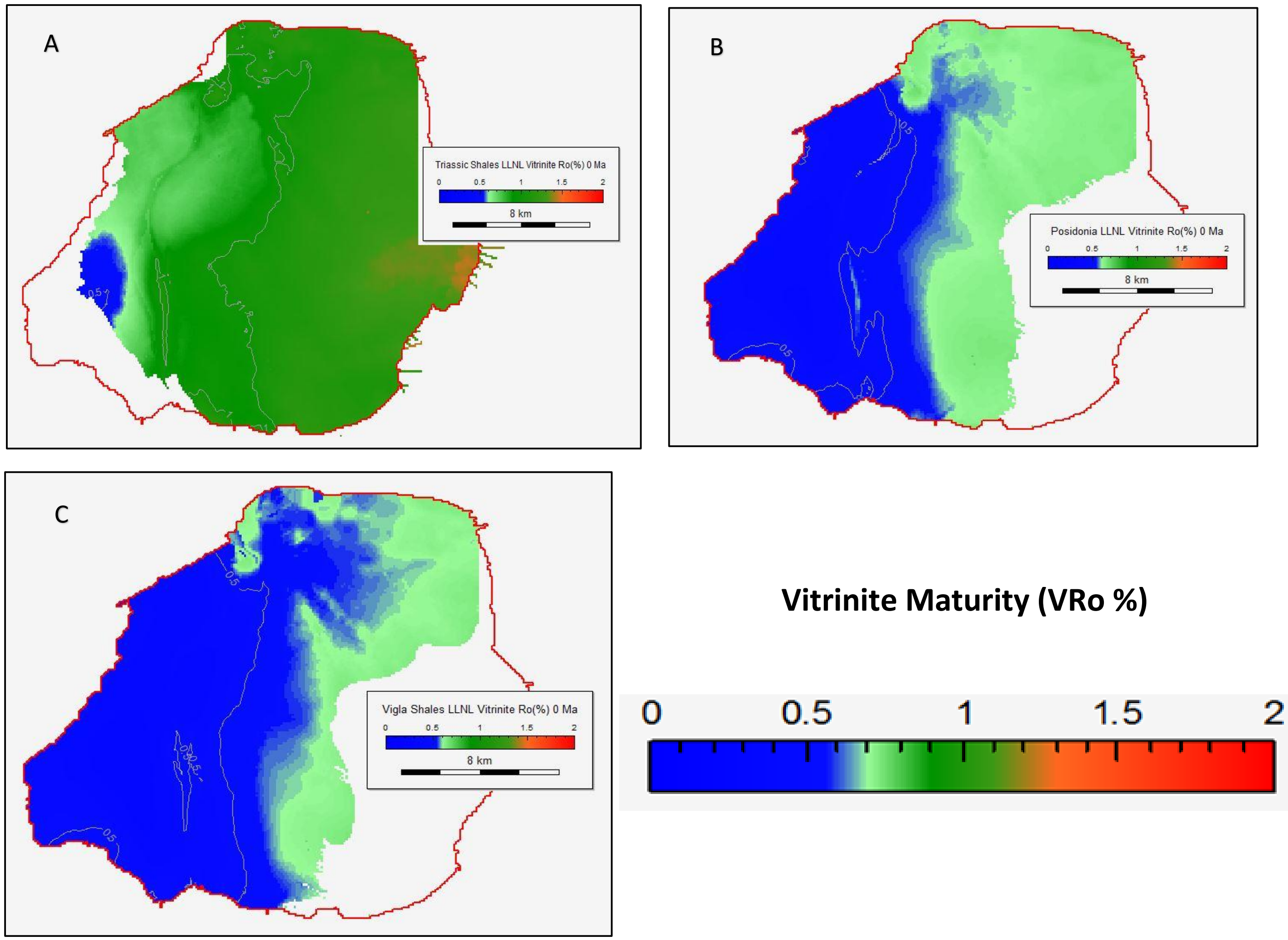

Figure 11*: Vitrinite reflectance equivalent present-day maturity maps for A) Triassic shales, B) Posidonia beds and C) Vigla shales source rocks.*

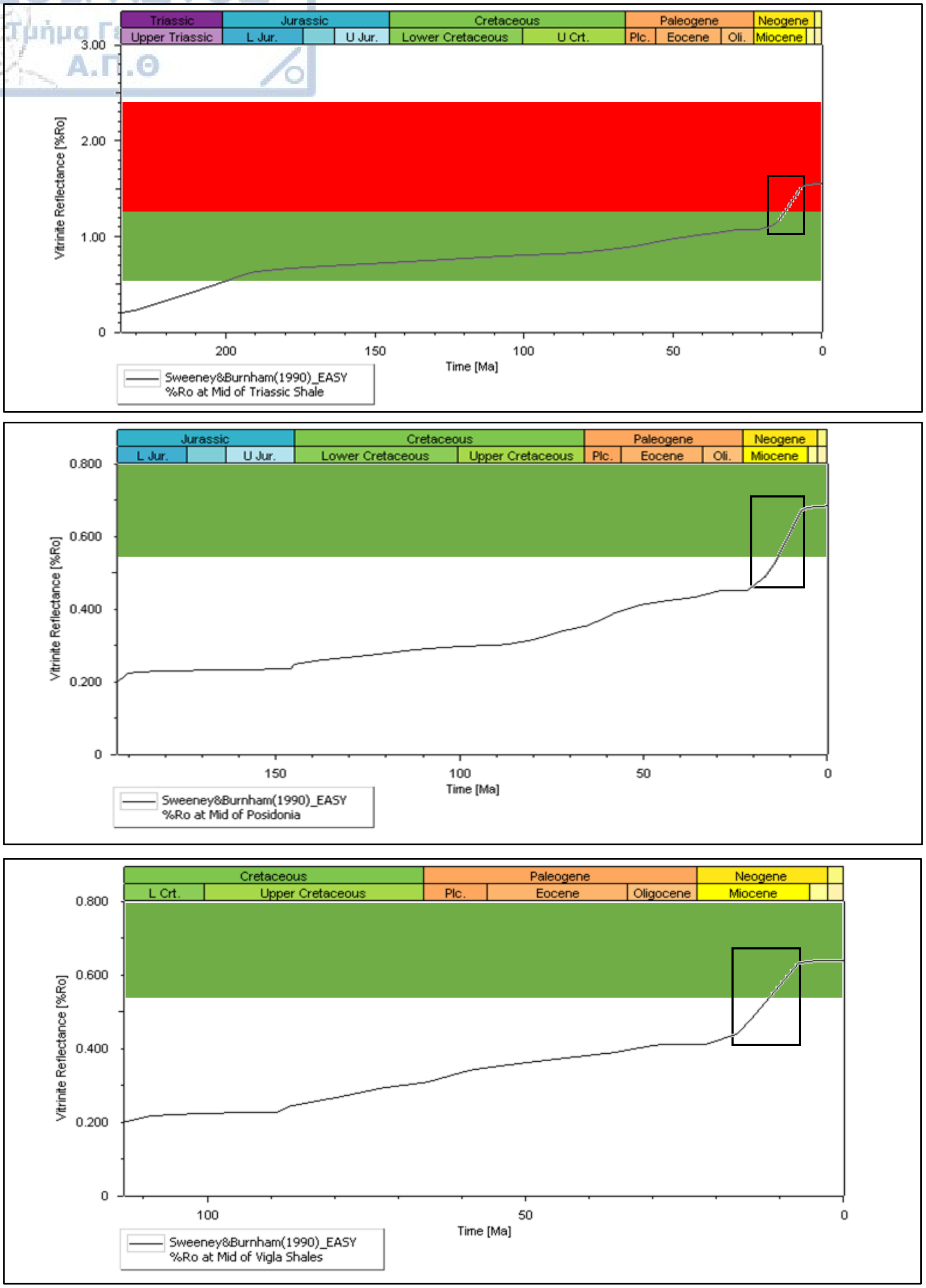

Figure 12*: Vitrinite reflectance curve- Time based on Burnham and Sweeney (1990). The black frame highlights the thrusting effect. The green-colored area corresponds to 0.55 – 1.3% Ro and the red-colored area corresponds to 1.3 – 2.4% Ro.*

Table 5*: Timing of oil and gas generation for modeled source rock horizons and the burial history location. Age values are in Ma. Depth values are calculated at depth at which %Ro value is reached (in meters).*

Burial History Location	**Source Rock**					
	Vigla Shales		**Posidonia Beds**		**Triassic Shales**	
PW-A	**Age**	**Depth**	**Age**	**Depth**	**Age**	**Depth**
0.55 %Ro – Start Oil	11	3750	14	3850	190	3850
1.0 %Ro – Peak Oil	-	-	-	-	48	5500
1.30 %Ro – Start Gas	-	-	-	-	12	7500

Table 5 lists information about the time (Ma) that each of the potential source rock attained the %Ro values of 0.55, 1.0 and 1.3% and the depths of the source rock at the specific %Ro maturity level. In addition, ***Figure 11*** illustrates the Vitrinite reflectance equivalent maturity maps for the source rocks described in ***Table 3***. The maturity maps for each source rock show increased maturation to the east, towards the kitchen area. Therefore, the effect of the thrusting event of the area on the maturation of the organic material is critical.

3.2.3 Petroleum Generation History

The generated volume, has a positive relation with the transformation ratio. Thus, based on the transformation ratio data, the main timing and extent of hydrocarbon generation of the three potential source rocks at the burial history location of the PW-A, were calculated. The results are listed in ***Table 6*** and summarized in ***Figures 13 and 14***.

The transformation ratio derives from Rock-Eval Pyrolysis. It represents the ratio of the petroleum formed by the kerogen to the total amount of petroleum that the kerogen is capable of generating (*Aguilera*, *2018*). It takes values from 0 to 1 and is represented as a percentage. It is at the discretion of the modeler to choose the percentage that represents the starting time of an effective generation. For this dissertation, the applied value is 20%.

Table 6*: Timing of oil generation for the three modeled source rocks based on transformation ratio curves. Age values are in Ma. Depth values are in meters. Transformation ratio percentages are in %.*

Source Rock	**Generation**		**Effective Generation**	
	Age (Ma)	**Transformation ratio (%)**	**Age (Ma)**	**Transformation ratio (%)**
Triassic Shales	190	1.75	138	20
Posidonia Beds	14	3.71	7	20
Vigla Shales	11	6.13	0	14.19

As expected, earlier and most extensive petroleum generation occurs for Triassic shales, which are characterized by most deeply buried history. Also, the thrusted sheet affected the Triassic source rock, thus cracking the oil to gas. In addition, for the Jurassic and Cretaceous source rocks, the most extensive petroleum generation occurs at Posidonia beds which experienced deeper burial depths comparing to the Vigla shale source rock horizons.

Triassic shales represent the earliest timing and greatest extent of petroleum generation, following a normal process and starting at about 190 Ma. The timing of oil cracking to gas is observed at the end of the late oil window at about 12 Ma and is controlled by the thrusting event, due to the deeper burial depths. Oil generation in the Posidonia beds and Vigla shales began at about 14 Ma and 11 Ma, respectively. Both source rocks generate hydrocarbon to a limited extent for the first years. The

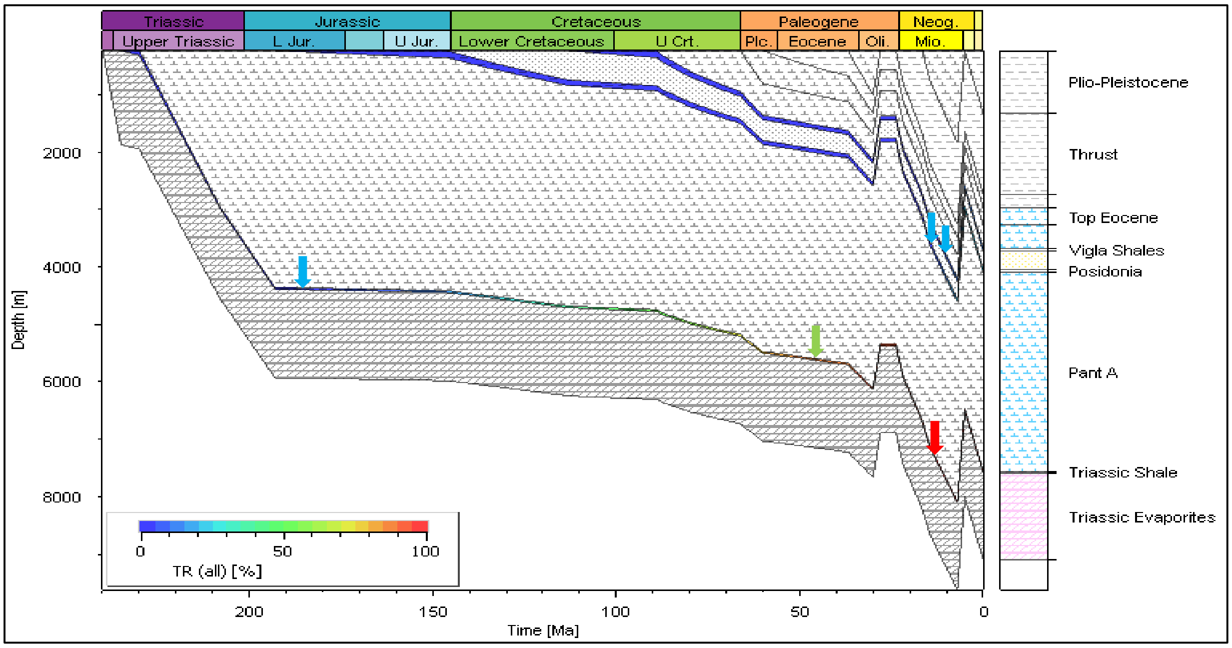

Figure 13: *Transformation ratio of organic matter (240 Ma to present) including the three modeled source rocks (Triassic shales, Posidonia beds, and Vigla shales) through geological time. Blue, green and red arrows illustrate the start, peak, and end of oil generation for all three modeled source rock intervals.*

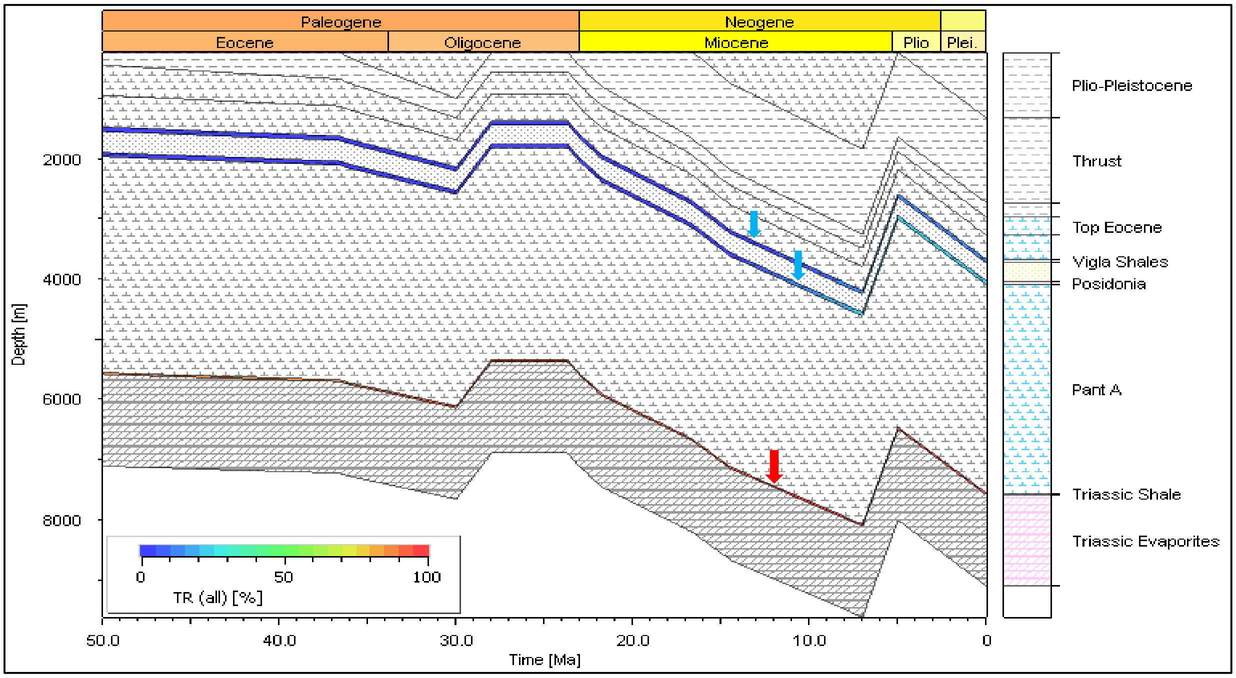

Figure 14: *Transformation ratio of organic matter (50 Ma to present) including the three modeled source rocks (Triassic shales, Posidonia beds, and Vigla shales) through geological time.*

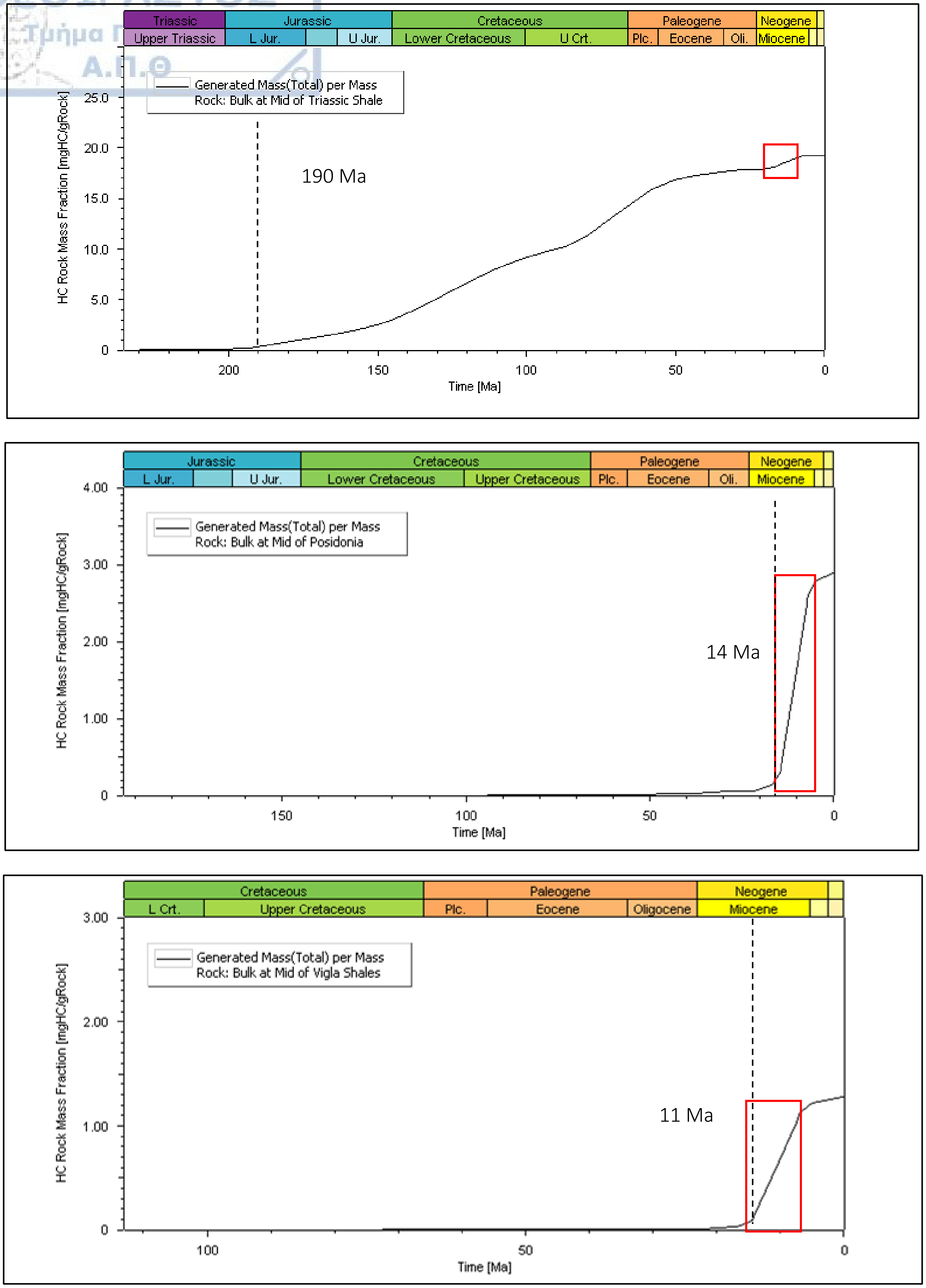

***Figure 15**: Generation Mass curves through geological time for the three modeled source rocks, namely Triassic shales, Posidonia beds, and Vigla shales, respectively. Generation mass values are in mg HC/g rock and time values are in Ma. The red frame highlights the thrusting effect.*

ages suggest that the thrust emplacement significantly affected the generation process for all three source rocks due to the increasing rate during Miocene. The above is more intense for Posidonia beds and Vigla shales since both generated oil after the thrusting event. Considering the effective generation, Triassic shales and Posidonia beds reach 20% TR at 138 Ma and 7 Ma, correspondingly. On the contrary, Vigla shales, at the present time, have reached only 14.19% TR. The values confirm the previous conclusions.

Figure 15 illustrates the Generation vs. Time curves for each of the potential source rock. The timing and extent of petroleum generation from the prescribed source rocks are summarized in ***Table 7***.

3.2.4 Petroleum Expulsion and Migration History

Efficient petroleum expulsion occurs after a minimum hydrocarbon saturation reached in the source rock. The amount is around 4%. The above interprets the existing lag between the petroleum generation and expulsion timing. The main expulsion for the Triassic shales occurred at 140 Ma

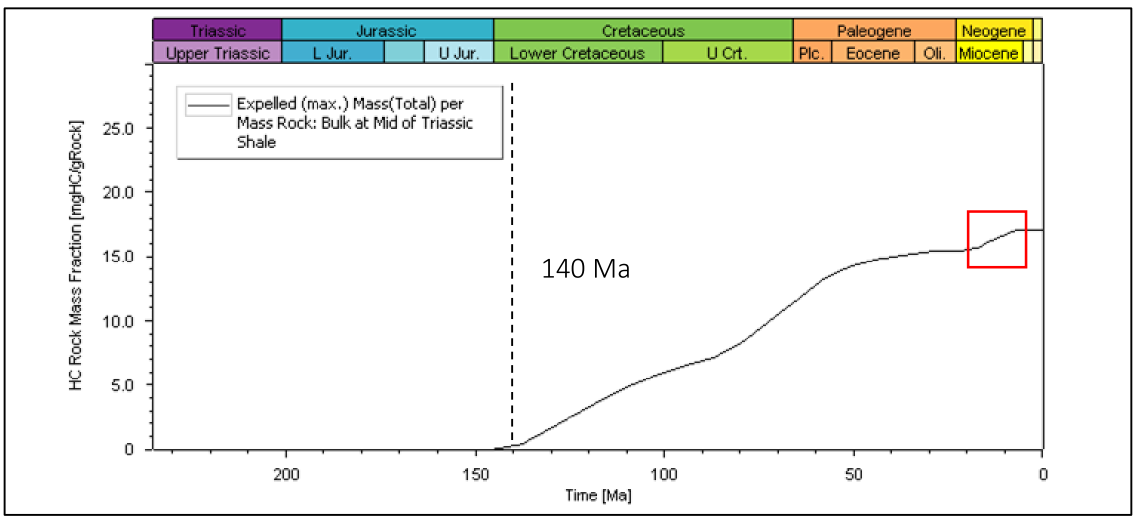

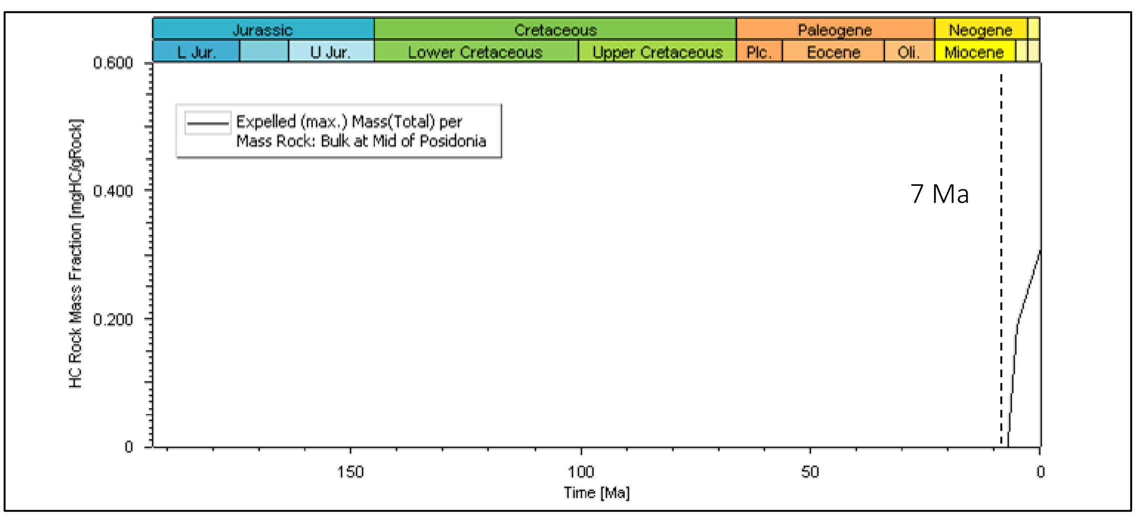

Figure 16*: Expulsion Mass curves through geological time for two modeled source rocks, namely the Triassic shales and the Posidonia beds. Expulsion mass values are in mg HC/g Rock and time values are in Ma.*

following the normal process. Expulsion for Posidonia comes after thrust emplacement at about 7 Ma. No expulsion is observed for Vigla shales. There is a possibility that the petroleum mass which has generated from Vigla shales to be not competent to expel hydrocarbons, according to the standards of PetroMod 1D modeling. ***Figure 16*** illustrates the Expulsion vs. Time curves for each of the potential source rocks. The expulsion timing mass values are summarized in ***Table 7***.

Table 7*: Generation and Expulsion critical times, generation and expulsion mass values, and generation mass value at expulsion starting time. Time values are in Ma. Mass values are in mg HC/ g Rock.*

Source Rock	Generation (Start Ma)	Generation End Value (mg HC/g Rock)	Expulsion (Start Ma)	Generation Value at Expulsion Starting Time (mg HC/g Rock)	Expulsion End Value (mg HC/g Rock)
Triassic Shales	190	19.43	140	3	17.08
Posidonia Beds	14	2.9	7.00	2.36	0.31
Vigla Shales	11	1.28	-	-	-

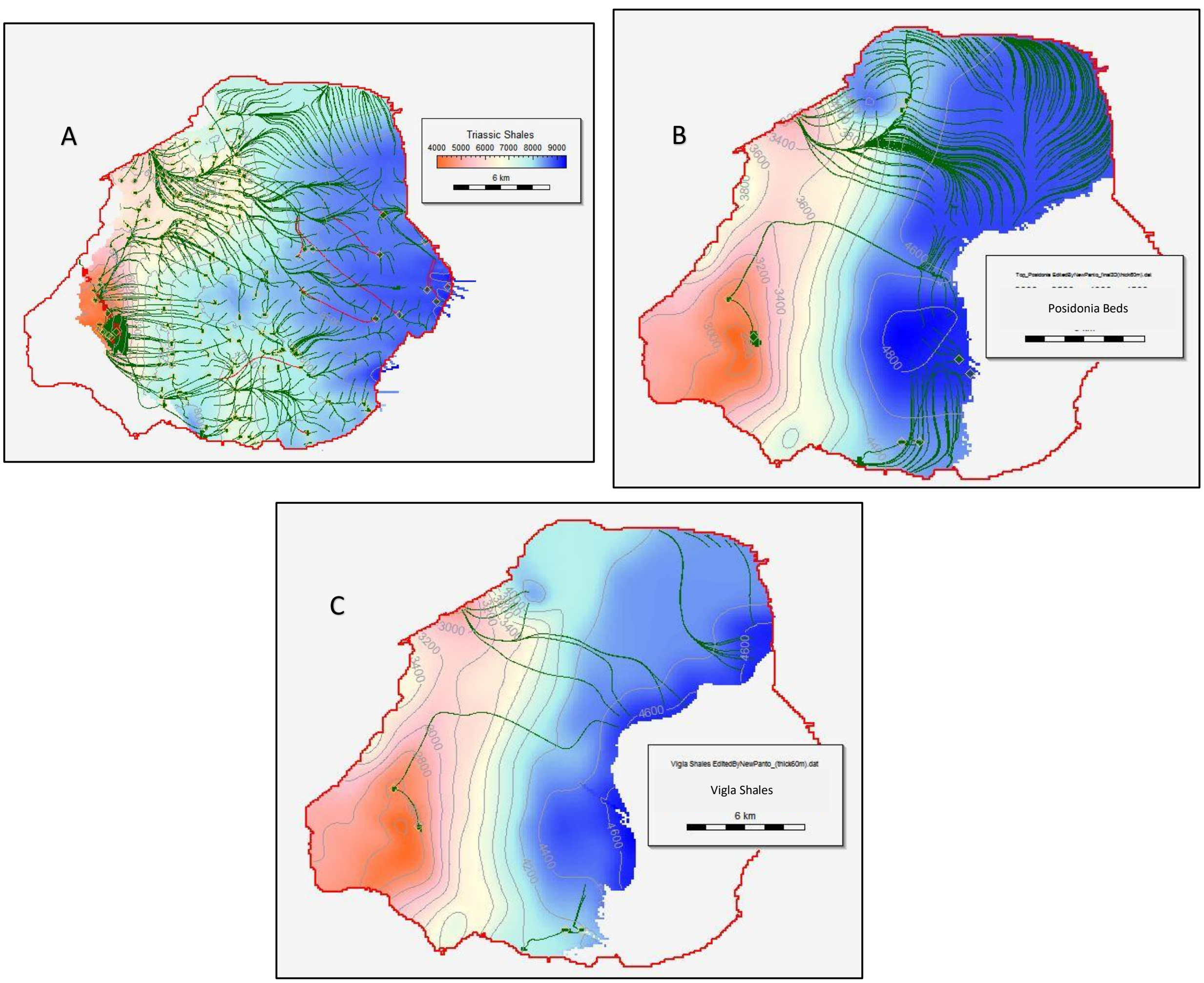

Figure 17*: Migration and accumulation maps for: A) Triassic shales, B) Posidonia beds, C) Vigla shales.*

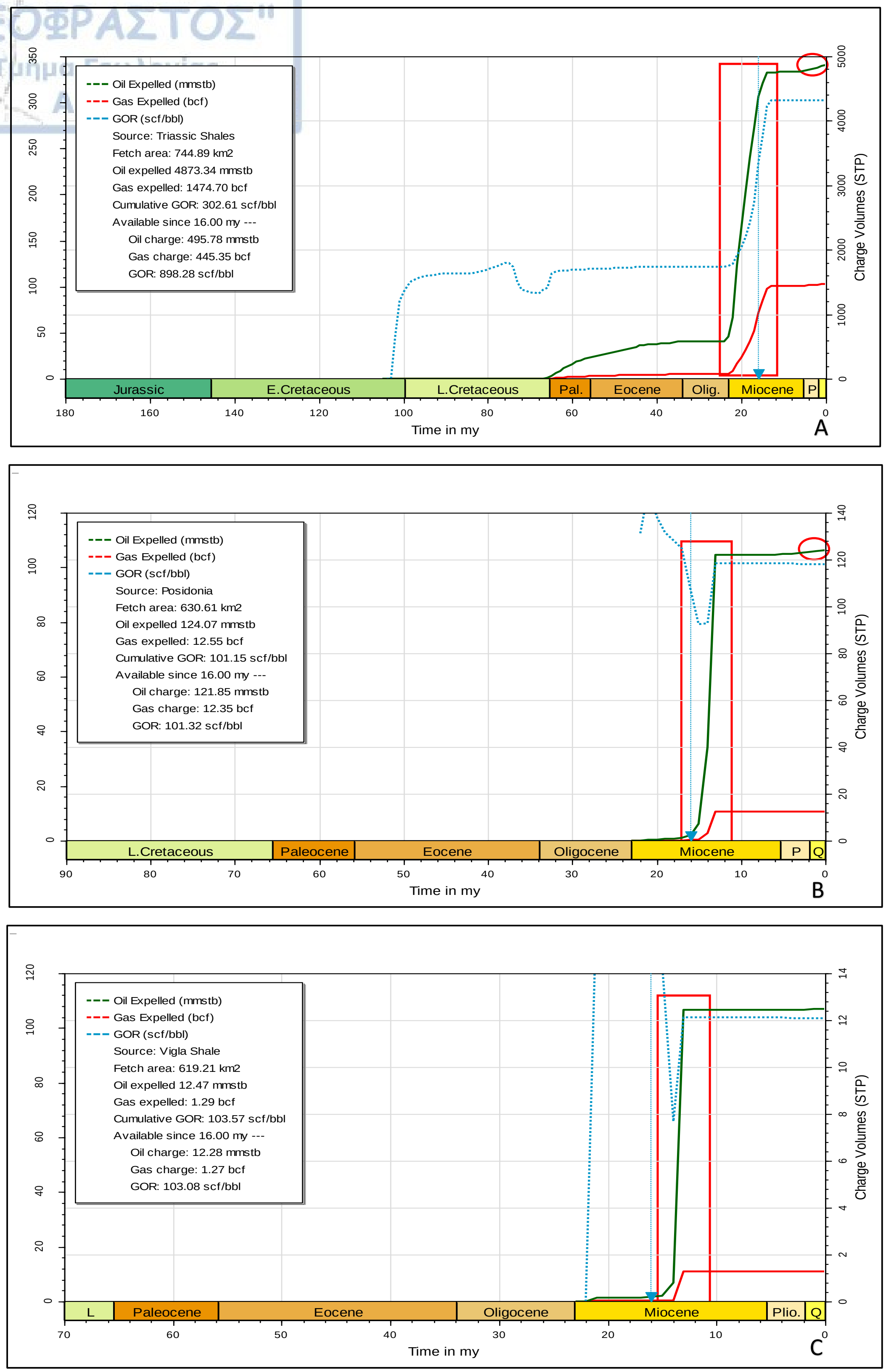

***Figure 18**: Predicted volumes of oil and gas expelled from A) Triassic shales, B) Posidonia beds, C) Vigla shales. The red frame and circle highlight the thrusting and high sedimentation rate effect, respectively.*

Figure 18 shows that charging from Triassic shales started at Paleogene, whereas for Posidonia beds and Vigla shales began at Miocene. In more detail, in the pre-thrusting period, a minimum expulsion of hydrocarbons is noticed. In contrast, in the post-thrusting period, two stages can be pointed out. A period of intense increase in hydrocarbon volumes due to the thrusting emplacement in Miocene, and a static period after the thrusting effect. The static period may occur due to the erosional event that negatively affects the expulsion process. Besides, a slight increase in hydrocarbon volume is detected in the last 5 Ma due to the high sedimentation rate.

As previously described, Triassic shales followed a normal process of petroleum generation and the deepest burial history. From the specific simulated model, it was observed that 4.8 MMstb of oil and 1.8 Tcf of gas were expelled totally from the source rock. Considering that the potential trap we study was created with the thrusting event at 16 Ma the available volumes will be 477 MMstb of oil and 672 Bcf of gas. Expulsion for Posidonia beds comes after thrust emplacement and results in 103 MMstb of oil and 10.3 Bcf of gas, however at 16 Ma the available volumes at the possible prospect nearby the kitchen area will be 102 MMstb and 10.2 Bcf. For Vigla shales the expulsion was observed at the 3D simulated model only, suggesting post-thrust expulsion of 8.4 MMstb of oil as well as 0.83 Bcf of gas. More specifically, at 16 Ma the available volumes will be 8.2 MMstb oil and 0.8 Bcf of gas. All the above are illustrated in ***Figure 18***, and summarized in ***Table 8***.

Losses for Posidonia beds and Vigla shales are limited, as modeled. Triassic shales appear with an extent of petroleum loss, due to early generation/expulsion when compared with the formation of the potential trap.

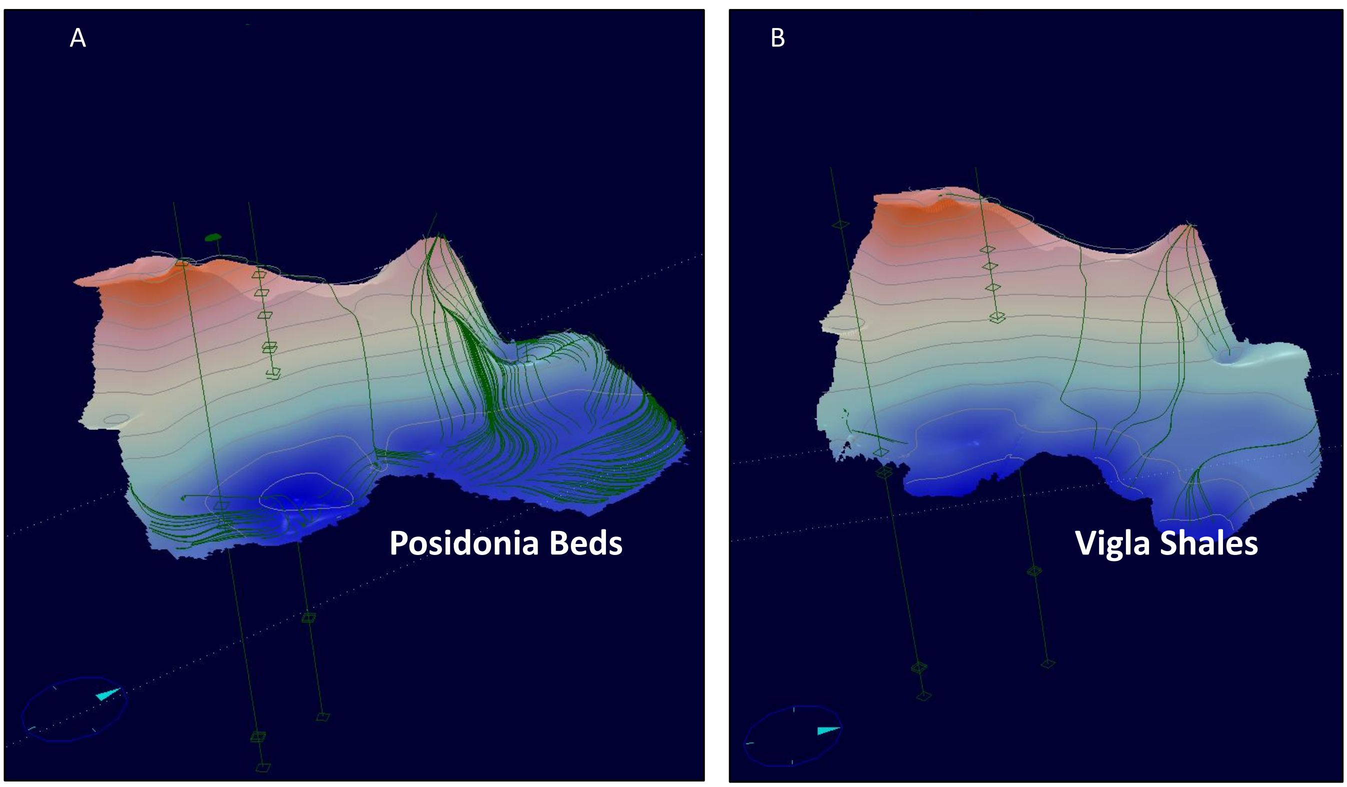

Figure 19*: 3D Perspective View of Migration for*
A) Posidonia beds, B) Vigla shales.

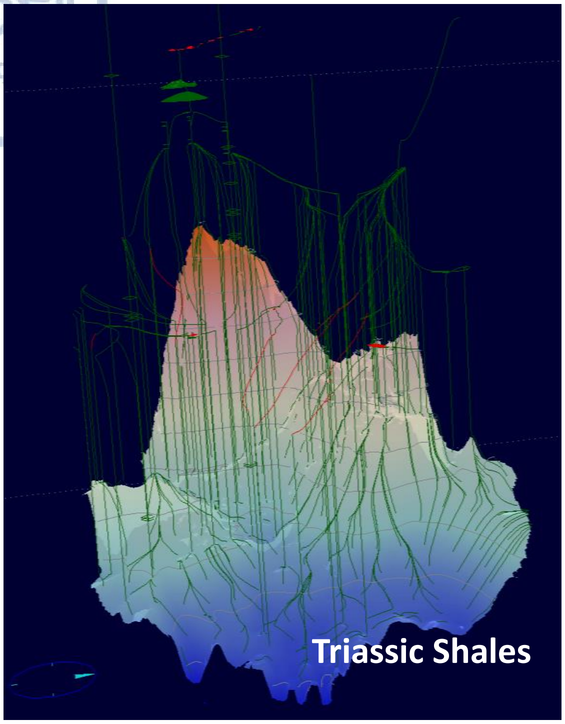

Figure 20*: 3D Perspective View of Migration for Triassic shales.*

Migration and accumulation graphs for the three potential source rocks are shown in ***Figures 19*** and ***20***. The 3D migration graphs are modeled for the prediction of possible migration pathways, according to the geometry and the lithology of the area. Besides, they aim to acknowledge traps with access to charge, and movements between them until hydrocarbon accumulation.

The migration is observed westwards. More specifically, Triassic shales are distinguished by both lateral and vertical migration. Closer to the kitchen area to the east, the migration is combinatorial. This terminates at the base of the Pantokrator limestone where hydrocarbons migrated vertically, throughout, due to fracturing. At the base of Posidonia beds, migration continues combined, due to restricted fracturing, until the petroleum gets trapped. Some gas flow-paths are identified, which are joined with those of oil due to solubility. Furthermore, Posidonia beds and Vigla shales are characterized by a combination of vertical and lateral migration. It is noteworthy that in all three potential source rocks northwest flowpaths occur. Therefore, further research is needed. All the above are illustrated in ***Figures 20 & 21***. The accumulations in ***Figure 21*** are analyzed in ***Chapter 5.3.***

For Scenario 2 of the area, a multilayer reservoir system (***Figures 20 & 22***) is identified with accumulations at Vigla shales, Vigla Carbonates, Senonian, Eocene, and Oligocene formations. The representative cross-section shows accumulation at the latest three formations. This indicates that enough charge volumes are available to fill more than one formation. The inclined OWC shown with the red circle is due to limitations.

According to the initial GOR (Gas to Oil Ratio), for each source rock, the generated oil can be characterized as heavy oil (<300 scf/bbl) or light oil (300-10000 scf/bbl). For Triassic shales, GOR is slightly above 300 scf/bbl, specifically 384.84 scf/bbl, and can be characterized as light oil. For both Posidonia beds and Vigla shales, with GOR at about 100 scf/bbl, it is characterized as heavy oil.

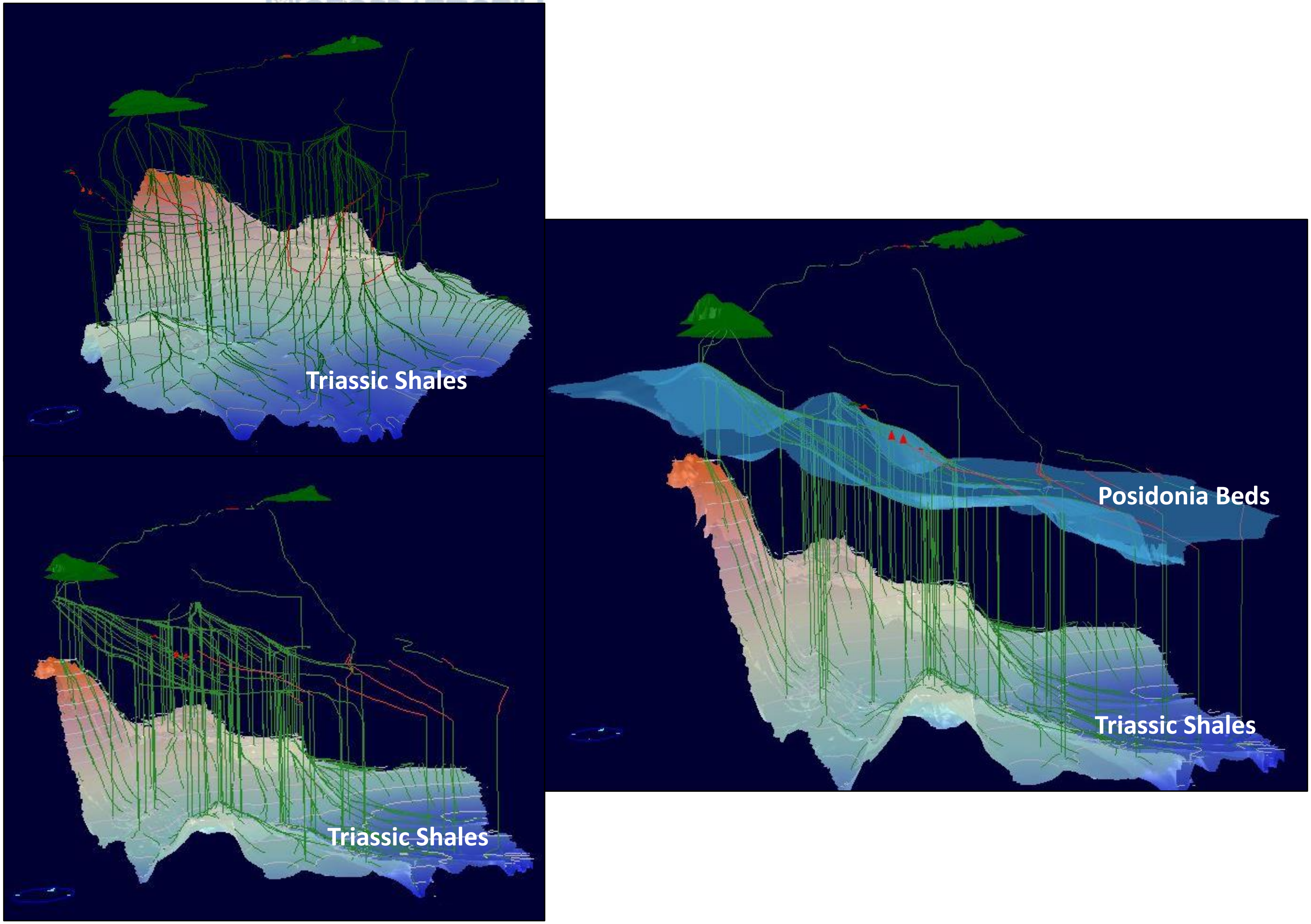

Figure 21: *3D Perspective View of Migration for Triassic shales.*

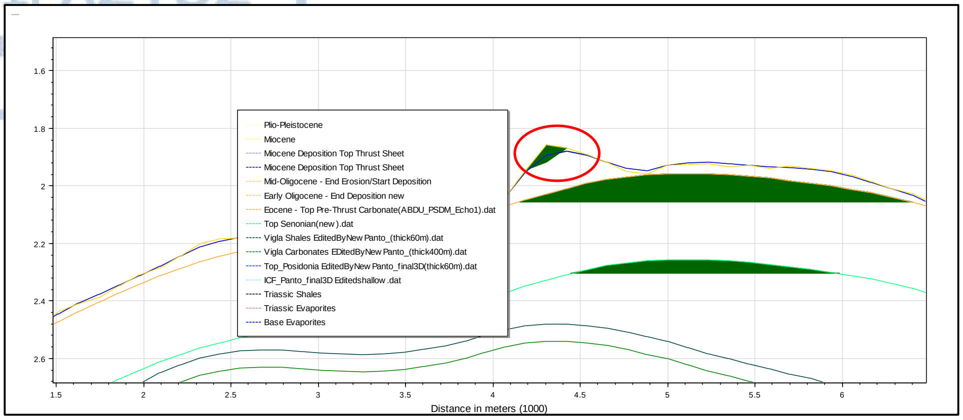

Figure 22: *Representative cross-section of multilayer reservoir of Triassic shales hydrocarbon system.*

Table 8: *Information of initial and available volumes and GOR for the three potential source rocks.*

Source Rock	Oil (MMstb)		Gas (bcf)		GOR (scf/bbl)	
	Initial	**16 Ma**	**Initial**	**16 Ma**	**Initial**	**16 Ma**
Triassic Shales	4808.42	477.29	1850.48	671.79	384.84	1407.51
Posidonia Beds	103.31	102.35	10.32	10.21	99.89	99.77
Vigla Shales	8.38	8.20	0.83	0.80	99.33	97.76

3.2.5 Accumulations

Further analysis was attempted with a special focus on the potential trap and the Eocene horizon, taking into consideration minimum migration losses. The calculation of the predicted volumes for each accumulation observed was based on the geometry, reservoir properties, and seal effectiveness. In ***Table 2***, information about the applied values of Scenario III of seal capacity properties, for each horizon, is listed.

From the available 3D graphs (***Figures 23 & 24***), a closure perspective of the multilayer reservoir system above the Eocene horizon is noticed. Numerous restricted quantities of gas accumulations are discerned further up from the oil accumulations. In the presented model of Scenario 2, the third source rock of the area, Vigla shales, does not contribute to the trapped petroleum accumulations. The above deduced from the limited expulsion of the source rock.

Tables 9 and ***10*** list information about the possible trapped hydrocarbons observed, applying the Triassic shales and Posidonia beds source rocks, respectively. It is highlighted that for the following sensitivity analysis the gas concentrations, 3 to 10, will be treated in total.

Table 9: *Information of possible trapped hydrocarbons, Triassic shales.*

Parameters \ Accumulations	1	2	3	4	5	6	7	8	9	10
Column high (m)	100	100	18.42	12.07	22.52	3.48	11.91	12.01	4.48	13.94
Oil (mmbls)	21.8	7.5	0.0	0.0	0.0	0.0	0.0	0.0	0.0	0.0
Gas (bcf)	11.1	4.2	0.4	0.3	1.0	0.0	0.3	0.3	0.1	0.5
GOR	507.7	551.3								

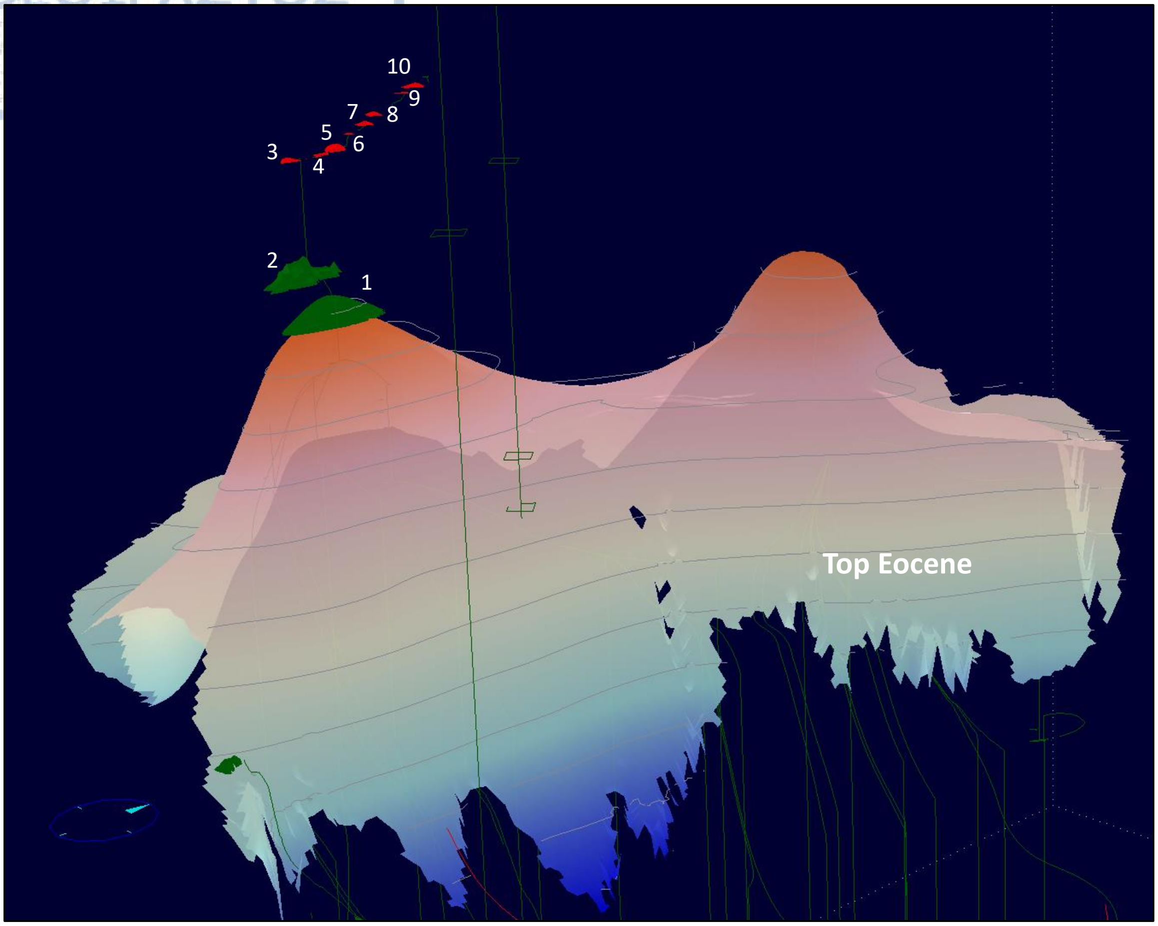

Figure 23: *3D Perspective View of Migration and Trapped Accumulations, based on Triassic shales source rock.*

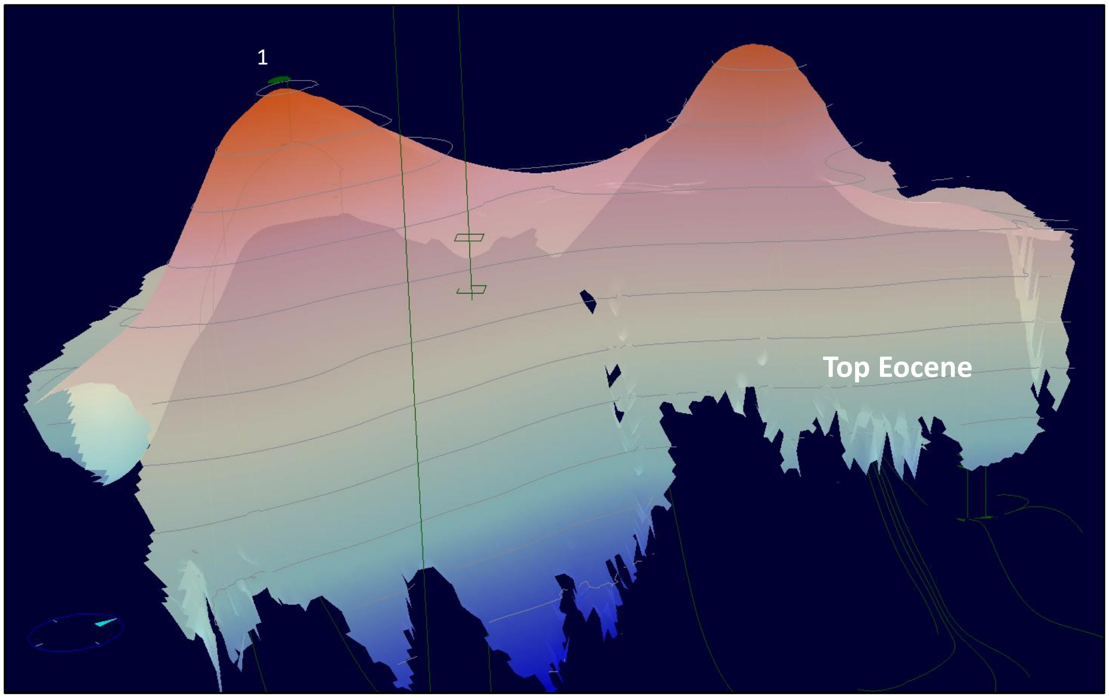

Figure 24: *3D Perspective View of Migration and Trapped Accumulations, based on Posidonia beds source rock.*

Table 10: *Information of possible trapped hydrocarbons, Posidonia beds.*

Accumulations / Parameters	1
Column high (m)	9.65
Oil (mmbls)	0.20
Sol Gas (Bcf)	0.0
GOR	50.7

4 Sensitivity Analysis

4.1 Introduction

The objective of the sensitivity analysis is to understand the impact of the variant input data on the timing and the volume of the generated hydrocarbons concerning the migration mechanism. The sensitivity analysis focuses on the thermal regime of the area and the quality parameters such as the seal capacity of the overlying horizons and the source rock properties. For the evaluation of the resultant effects, outcomes were taken for the available charging history and the hydrocarbons filling the prospect geometry.

For the sensitivity analysis, the results focused on three potential targets. The primary target concerns the Eocene Limestone whereas the two-secondary targets refer to Oligocene and Miocene formations. It should be noted that there is no change in the migration process, concerning the flow-paths, and in the effect of the thrusting event.

4.2 Thermal regime

Three representative scenarios, using the minimum, intermediate and maximum values of present-day heat flow, were simulated. The scenarios are presented in ***Table 1***. The models were created using Scenario III of seal capacity parameters (***Table 2***) and Scenario B of source rock properties (***Table 3***).

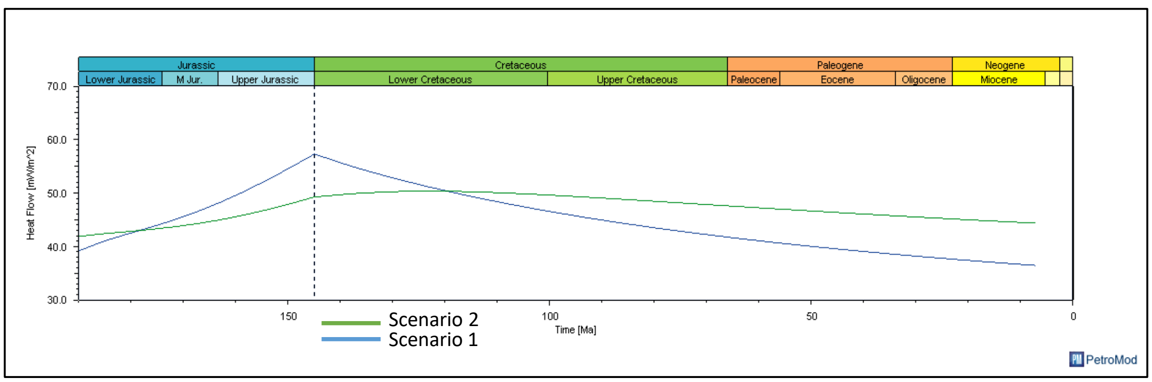

Figure 25*: Comparison of the heat flow curves for Scenario 1 and Scenario 2 of Table 1. Heat flow values are in mW/m^2.*

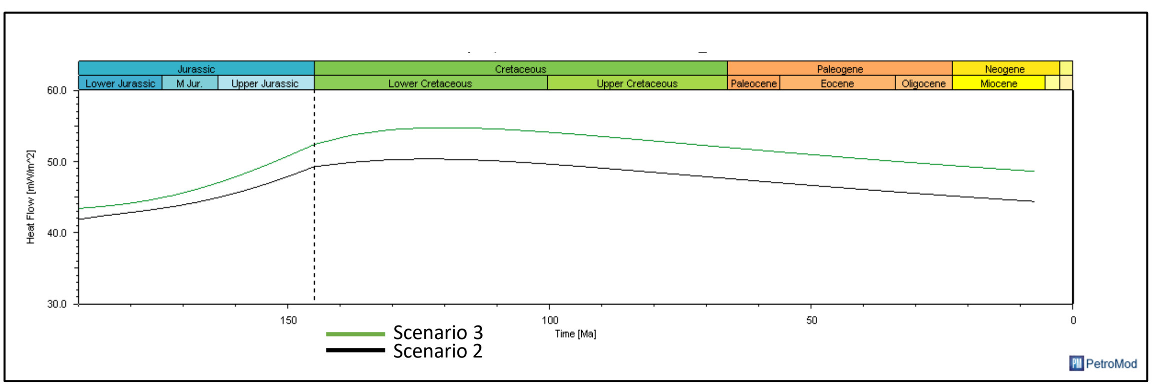

Figure 26*: Comparison of the heat flow curves for Scenario 2 and Scenario 3 of Table 1. Heat flow values are in mW/m^2.*

Figures 25 and ***26*** show the comparison between the three simulated scenarios of ***Table 1***. As ***Table 11*** lists, the present-day heat flow increases from the first to the third scenario. On the other hand, Scenario 1 has the highest peak heat flow and then follows Scenario 3 and Scenario 2. As a conclusion, the three potential source rocks of the area reach the highest temperature with Scenario 1 at 145 Ma. Besides, they experience slower temperature reduction with Scenario 3. Thus, it is interesting to see the different effects of the peak and present-day heat flow.

Table 11*:Values of Present-day and Peak heat flow for the three simulated scenarios of Table 1.*

Heat Flow (mW/m^2)	Scenario 1	Scenario 2	Scenario 3
Present Day	36	45	49
Peak	57	51	55

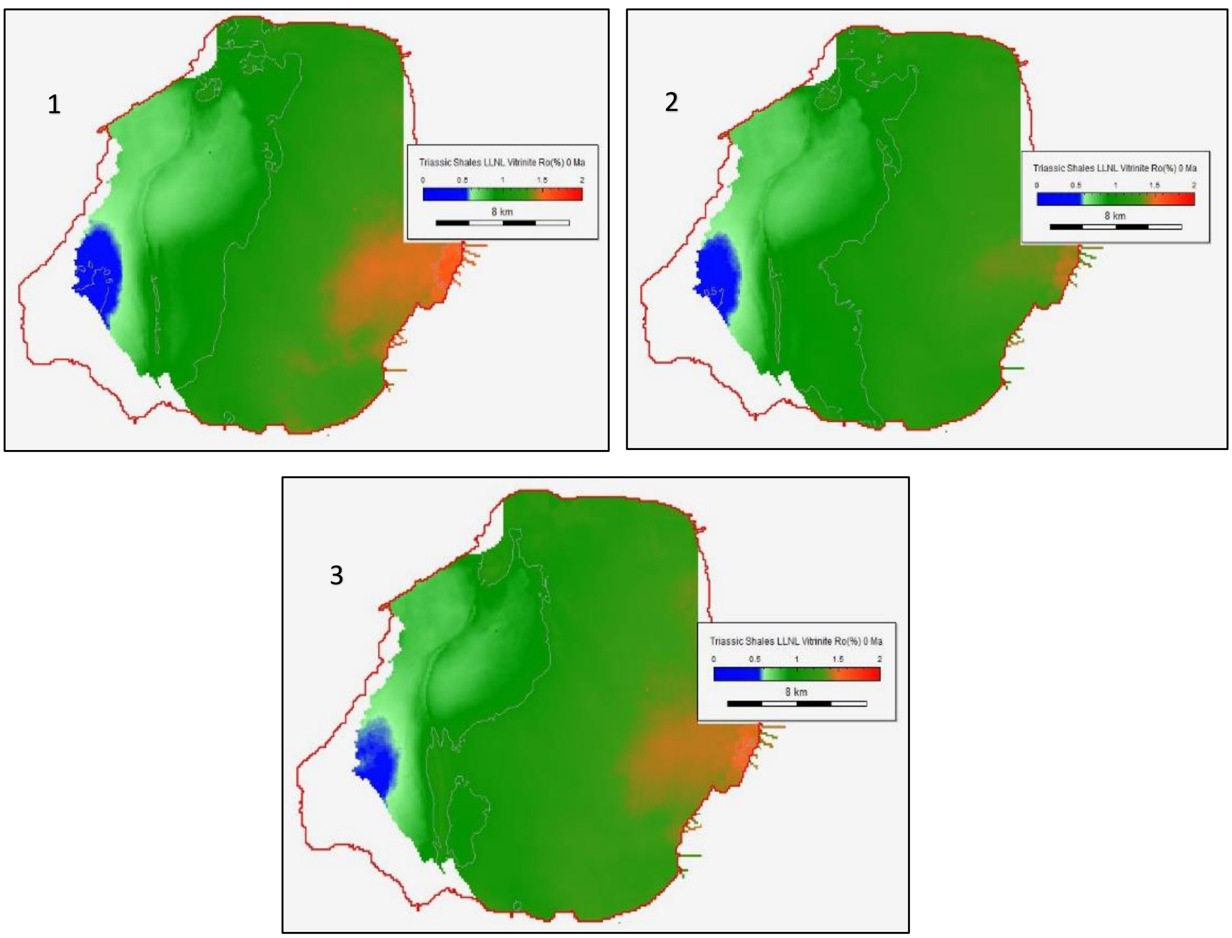

Figure 27*: Vitrinite reflectance equivalent present-day maturity maps for Triassic shales, for Scenario 1, Scenario 2, and Scenario 3 respectively.*

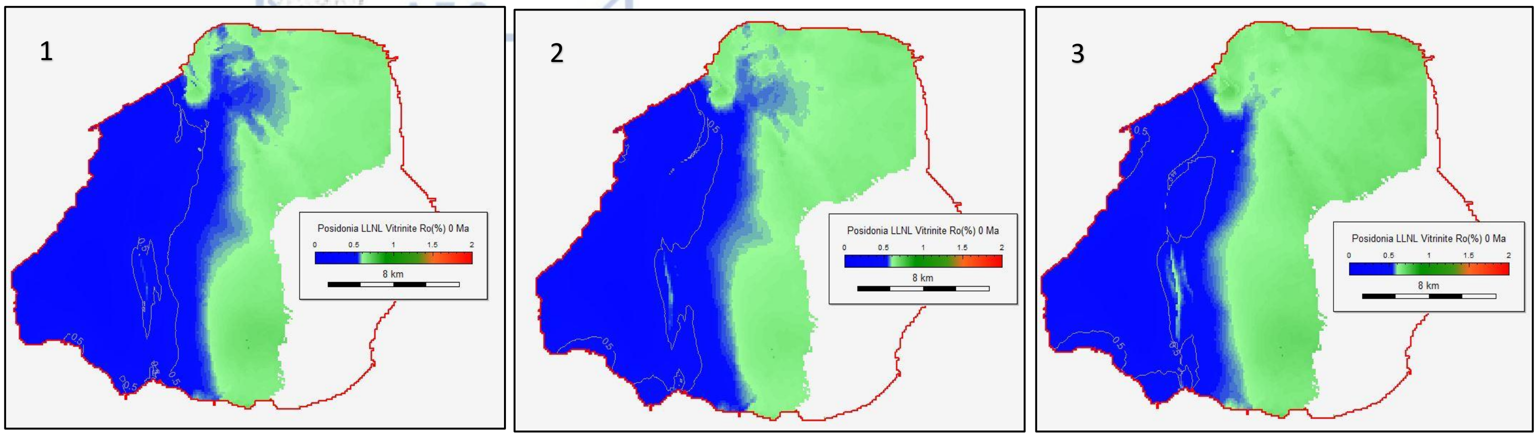

Figure 28*: Vitrinite reflectance equivalent present-day maturity maps for Posidonia beds, for Scenario 1, Scenario 2, and Scenario 3 respectively.*

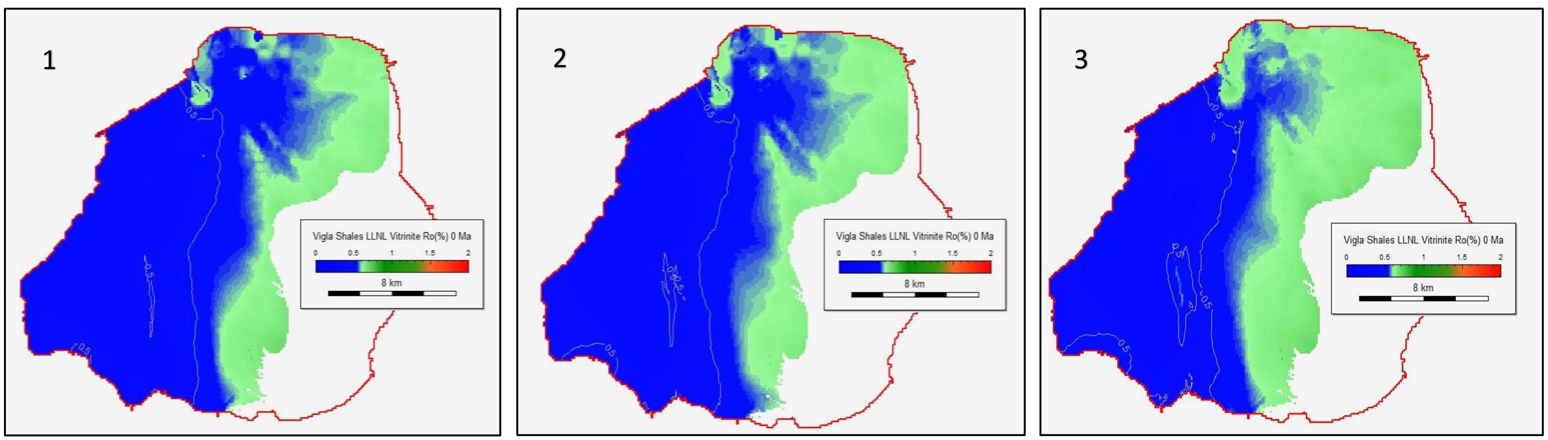

Figure 29*: Vitrinite reflectance equivalent present-day maturity maps for Vigla shales, for Scenario 1, Scenario 2, and Scenario 3 respectively.*

The comparison of the Vitrinite reflectance equivalent present-day maturity maps for the three potential source rocks is shown in ***Figures 27-29***. They suggest that an increase in present-day heat flow results in increased maturity. For Triassic shales, although Scenario 2 illustrates a larger area in the oil window the level of maturity is increased. It is noteworthy, that the increase in the thermal regime for the third scenario gives, for Posidonia beds and Vigla shales, a slight increase in the maturation of the organic matter but to a greater extent. The maturity increases eastwards, where the kitchen area exists. A limited change is noticed in the other simulated models.

Due to the important impact of the increased maturity, a following increase of the generated hydrocarbons is expected. The increase in maturation also leads to an augmentation of the initial charging volume of hydrocarbons. The above is illustrated in ***Figures 31-33*** and summarized in ***Tables M-O*** in the ***Appendix***. Certainly, the trapped quantities depend on the geometry, the lithologies, and the seal capacity of the overlying horizons, and will be discussed in the next section.

The results of the Triassic shales are more complex compared to those of the other two source rocks. The gas quantities and the GOR factor display a decrease from Scenario 1 to Scenario 2, following the corresponding decrease of the peak heat flow. Afterward, an increase is noticed in Scenario 2 to Scenario 3. On the contrary, the initial oil expelled volume shows a continuous increase from Scenario 1 to Scenario 3, while the oil volume available at 16 Ma displays an increase from Scenario 1 to Scenario 2 and afterward a decrease to Scenario 3. The different temperature distribution in the area results in different maturation of the organic matter both in level and time. The difference in the level of maturity, and consequently the transformation ratio, affects the initial quantity with the rising oil production. Thus, Scenario 3 provides the highest initial oil expulsion (***Figure 30***). The difference in time affects the point where the transformation ratio reaches its maximum value. Thus, the second scenario has a higher TR (%) value at 16Ma compared to the other two scenarios, resulting in a higher generation and expulsion volumes. Furthermore, the higher GOR factor results from Scenario 1, with 484 scf/bbl. This value indicates a light oil type of hydrocarbon. The same conclusion derives from the other two scenarios.

In addition, Posidonia beds and Vigla shales show similar behavior. They illustrate a decrease in all quantities from Scenario 1 to Scenario 2 and then an increase from Scenario 2 to Scenario 3, following the peak heat flow rate. As expected, the greatest values, for the oil and gas volumes and GOR factor, result in Scenario 3. Also, the GOR factor for all three Scenarios indicates a heavy oil type of hydrocarbon.

Table 12*: Timing of oil and gas expulsion for the different simulated thermal regime scenarios.*

Source Rocks	Scenario 1	Scenarios 2 & 3
Triassic Shales	L. Cretaceous	Paleogene
Posidonia Beds	Miocene	Miocene
Vigla Shales	Miocene	Miocene

Comparing the heat flow and charging history, the increased initial volumes for Scenario 3 are due to its greater time where the source rocks experienced increased temperature conditions, taking into account that more quantities had been generated. On the other hand, Scenario 1 shows an earlier expulsion for Triassic shales (***Table 12***).

Further information on the trapped volumes is listed in ***Table 13***. It is observed that the oil quantity, for the three thermal regime scenarios, remains constant for the three potential traps, while the amount of gas presents slight differentiation. Also, the increase in present-day heat flow gives a decrease in the GOR factor.

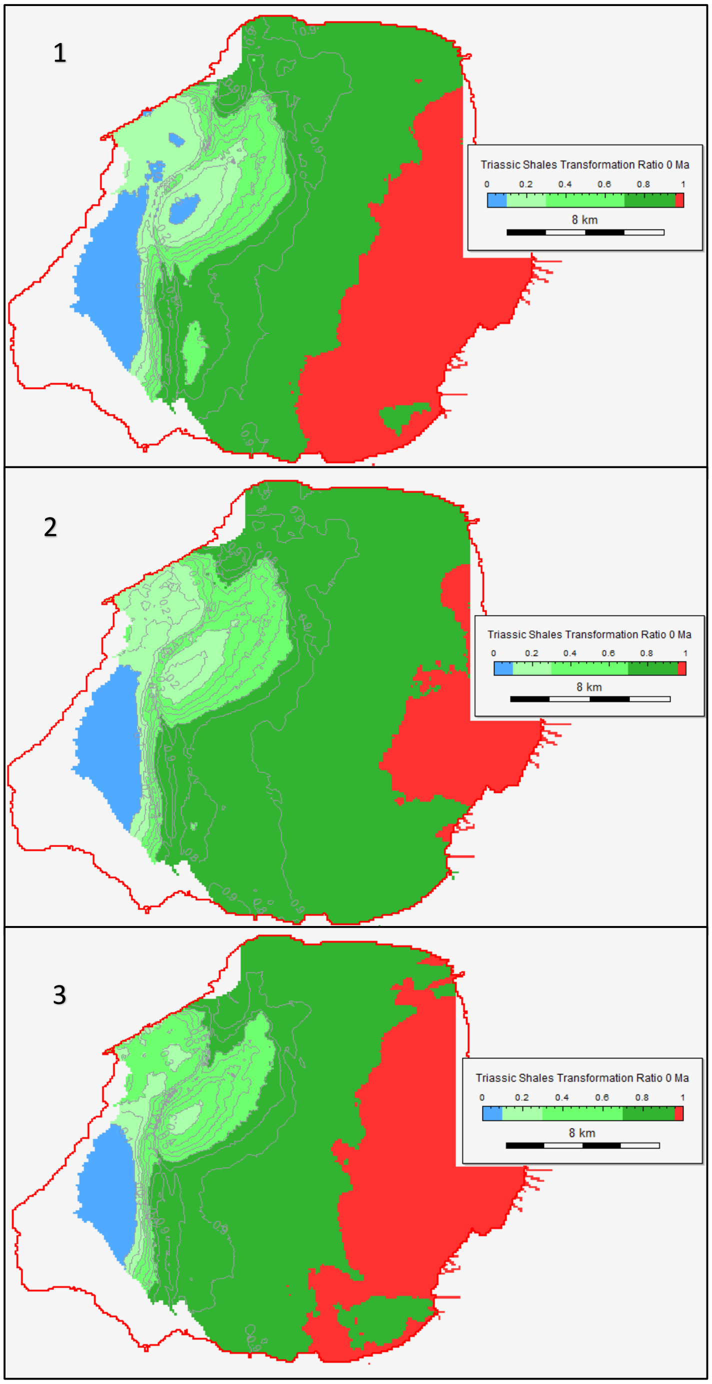

Figure 30*: Transformation Ratio of Triassic shales for the three thermal regime simulated scenarios.*

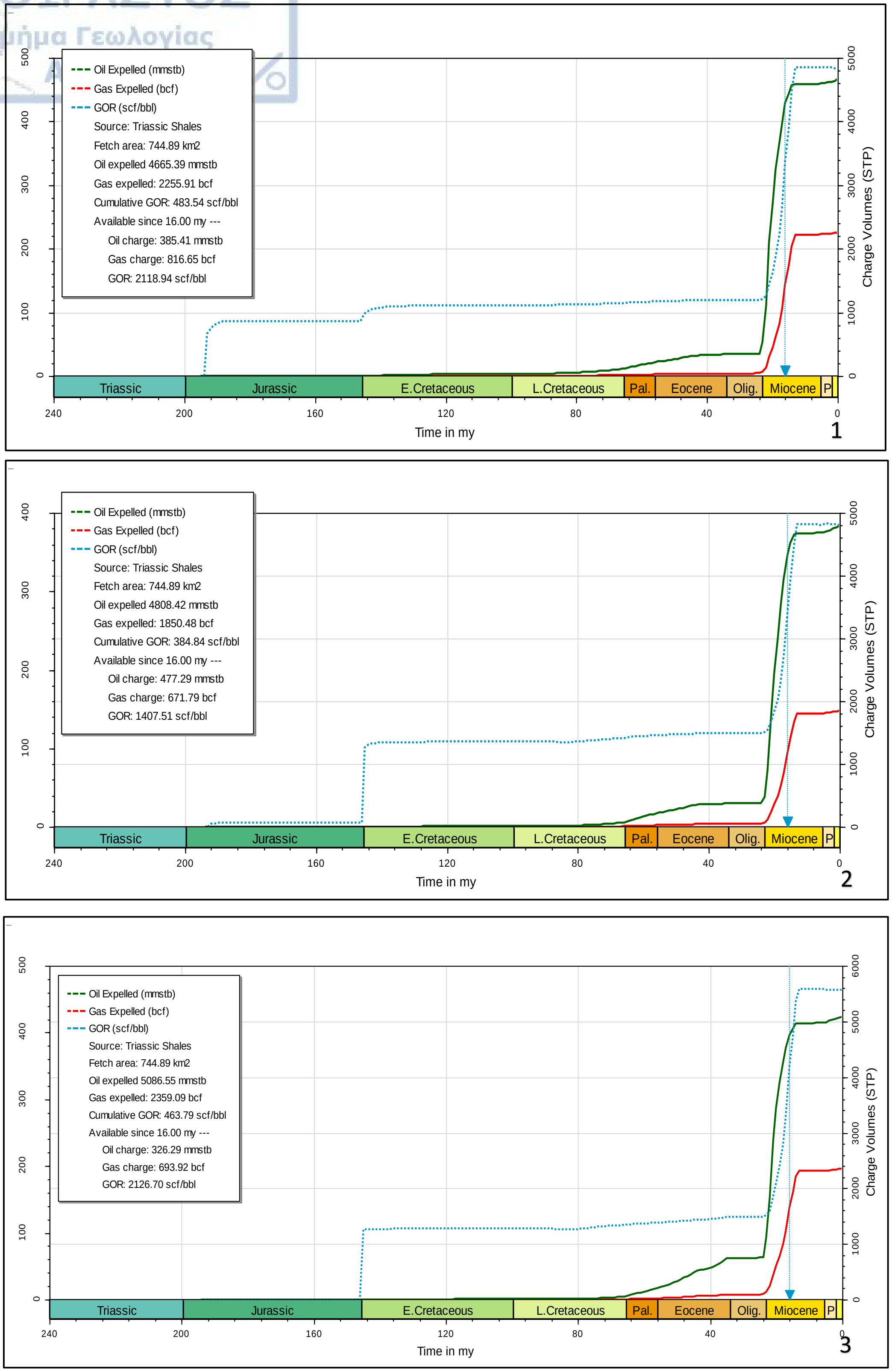

Figure 31: *Predicted volumes of oil and gas expelled from Triassic shales for the three thermal regime scenarios 1,2 and 3, respectively.*

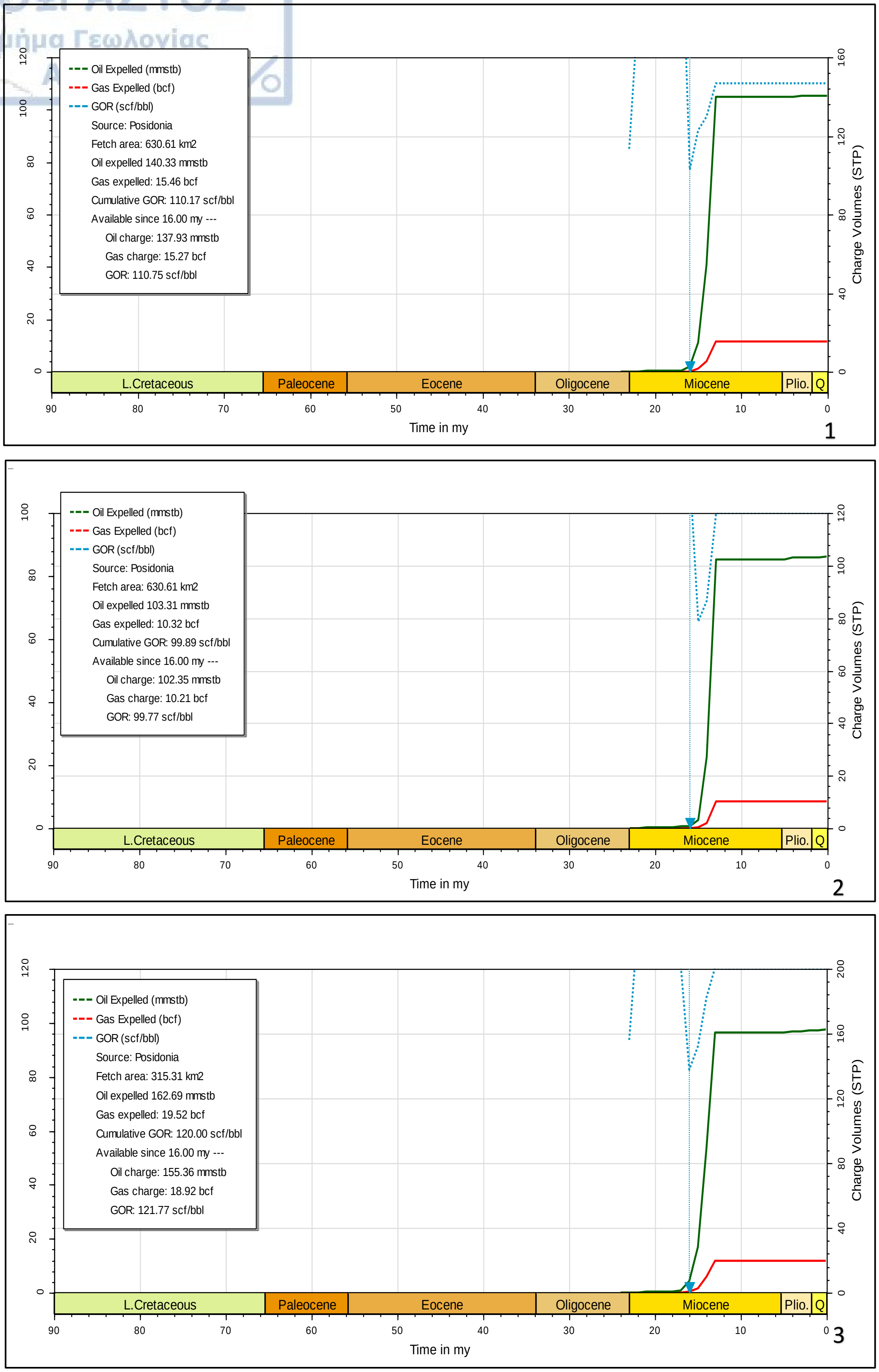

***Figure 32**: Predicted volumes of oil and gas expelled from Posidonia beds for the three thermal regime scenarios 1,2 and 3, respectively.*

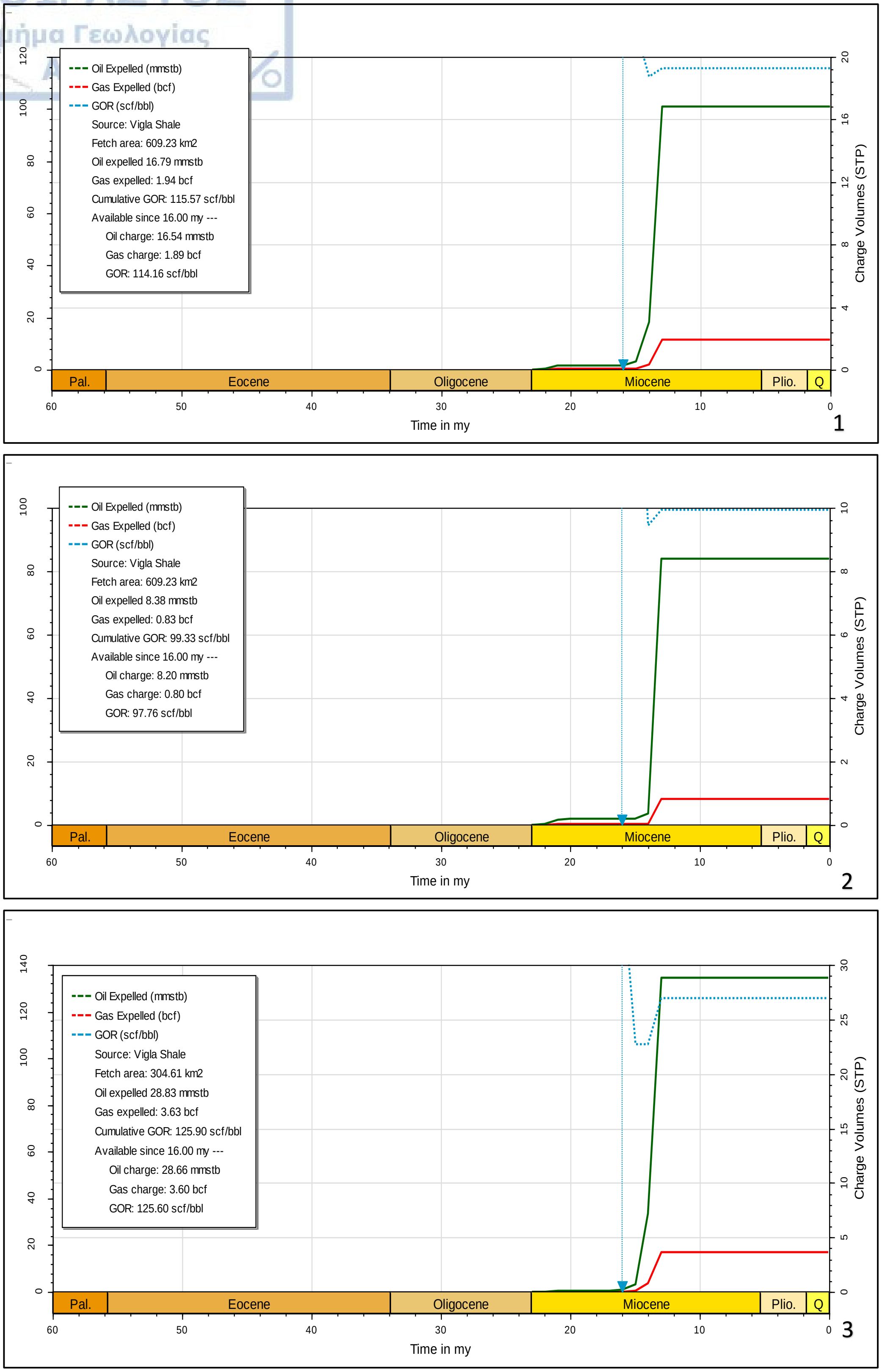

***Figure 33**: Predicted volumes of oil and gas expelled from Vigla shales, for the three thermal regime scenarios 1,2 and 3, respectively.*

Table 13: *Accumulated quantities for the three potential traps.*

Scenarios	Eocene			Mid Oligocene			Miocene		
	Oil (mmbls)	Gas (bcf)	GOR	Oil (mmbls)	Gas (mmbls)	GOR	Oil (mmbls)	Gas (mmbls)	GOR
1	21.8	10.6	508	7.5	4.2	551	0	2.3	-
2	21.8	11.1	487.5	7.5	4.2	551	0	2.9	-
3	21.8	9.4	430	7.5	3.5	468	0	2.9	-

4.3 Rifting Stage

An extra scenario was simulated by adding two rifting events. The applied values are listed in ***Table 1***. The model was created using Scenario III of seal capacity parameters (***Table 2***) and Scenario B of source rock properties (***Table 3***). The purpose of this model is to better understand the impact of the Triassic rifting event in the area of the Ionian Sea, which is well documented by many researchers, to the behavior of the potential source rocks, in terms of thermal maturation.

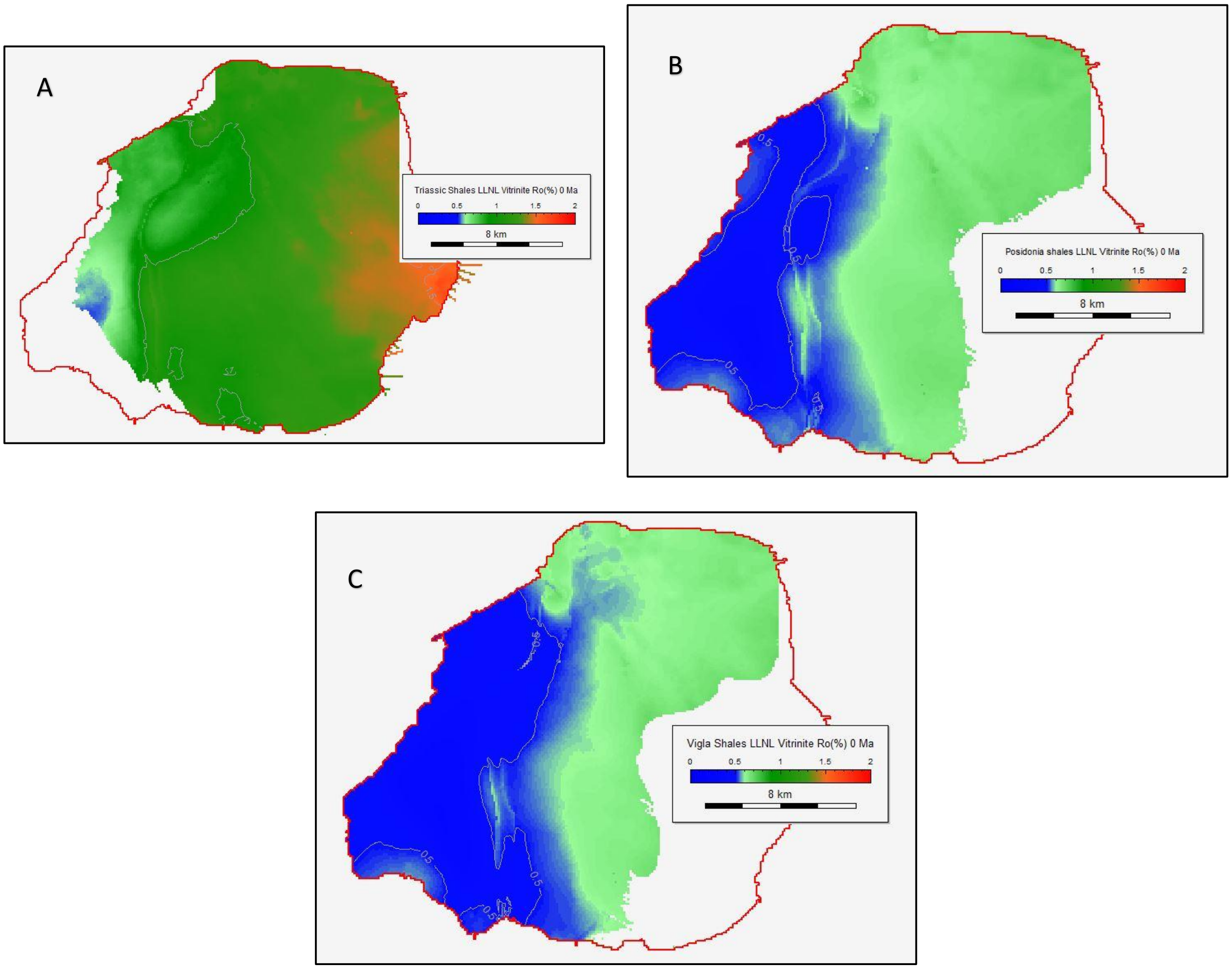

Figure 34*: Vitrinite reflectance equivalent present-day maturity maps for A) Triassic shales, B) Posidonia beds and C) Vigla shales source rocks.*

Comparing the Vitrinite reflectance equivalent present-day maturity maps of ***Figure 34*** with those of ***Figure 11*** (Scenario 2), an increase in maturity is observed for all three source rocks of the area. For Triassic shales, more area is shown to enter the gas window, whereas for Posidonia beds and Vigla shales more area has entered the oil window. Furthermore, with the improvement in maturation, an increased generated petroleum quantity is expected from the source rocks.

Charts of ***Figure 35*** are compared with those of ***Figure 18***. The Triassic shales source rock was affected by two intense rifting events and the result is illustrated by changes in the expelled volumes. ***Figure 35A*** shows the charging history from Triassic's generated quantities. An increase in the initial oil and gas volume is noticed. This is expected due to the maturity history previously quoted. On the contrary, at 16 Ma, the oil volume appears reduced while the gas volume shows an increase. Thus, the increased maturity resulted in higher generated and expelled total volumes, while Scenario 2 reaches higher transformation ratio values at 16 Ma. Also, an earlier starting time for expulsion is noticed. On the other hand, Posidonia beds and Vigla shales, appear with increased expelled quantities for both oil and gas volumes. No change is observed for expulsion timing.

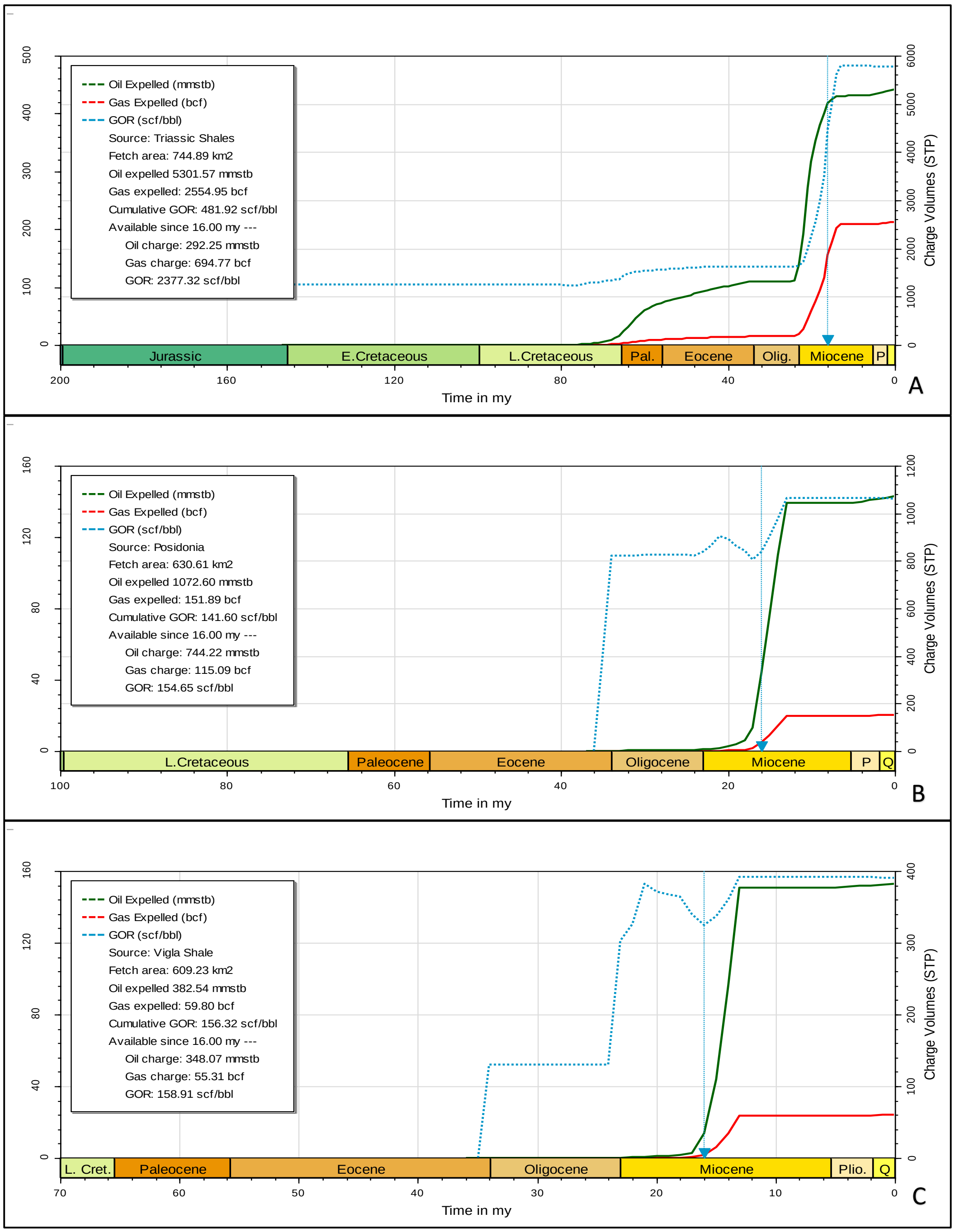

Figure 35: *Predicted volumes of oil and gas expelled from A) Triassic shales, B) Posidonia beds, C) Vigla shales. The red frame and circle highlight the thrusting and high sedimentation rate effect, respectively.*

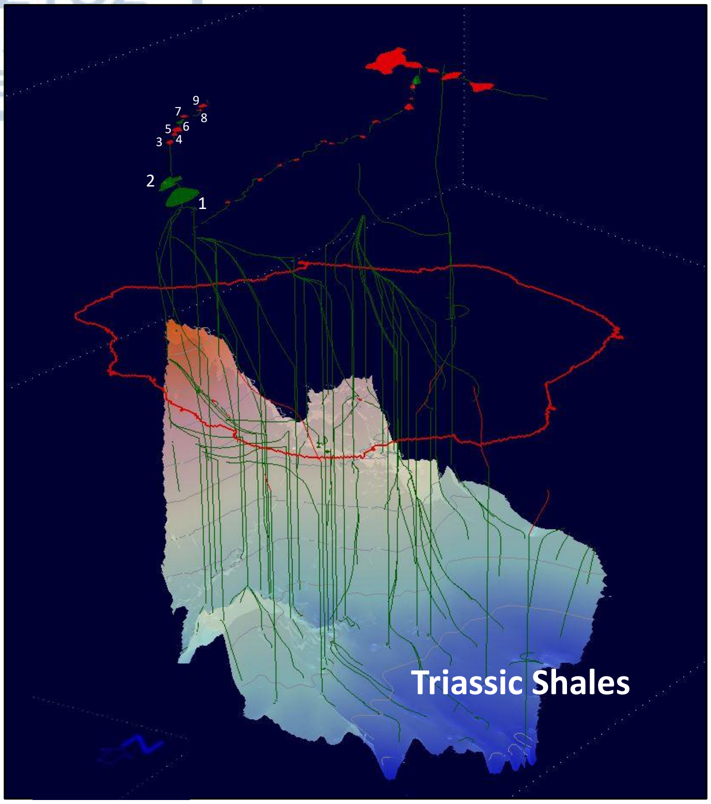

Figure 36: *3D Perspective View of Migration for Triassic shales.*

According to the 3D graphs in ***Figures 36-38***, for Scenario 4 of Table 1, generated volumes from Triassic shales give a multilayer reservoir system with oil accumulations at the Eocene and Oligocene horizons and multiple small accumulations at the Miocene horizons. An important petroleum quantity, in the gas phase, seems to seep towards the surface. This does not issue from any other scenario, indicating the differentiation that this scenario has to the formed structure. Posidonia beds and Vigla shales gave accumulations at the Miocene horizons. For the optimization of these results the source rock horizons were used.

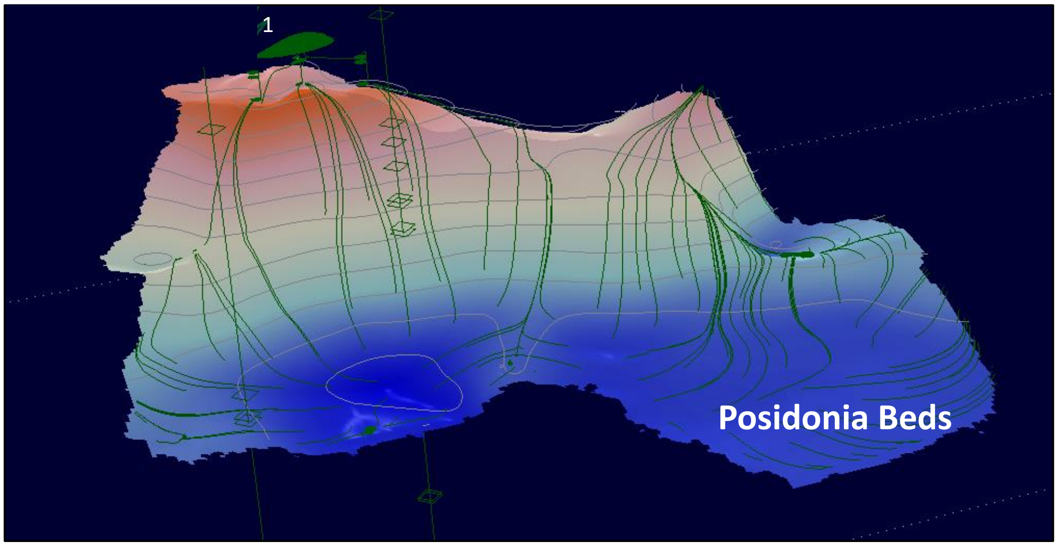

Figure 37*: 3D Perspective View of Migration for Posidonia beds.*

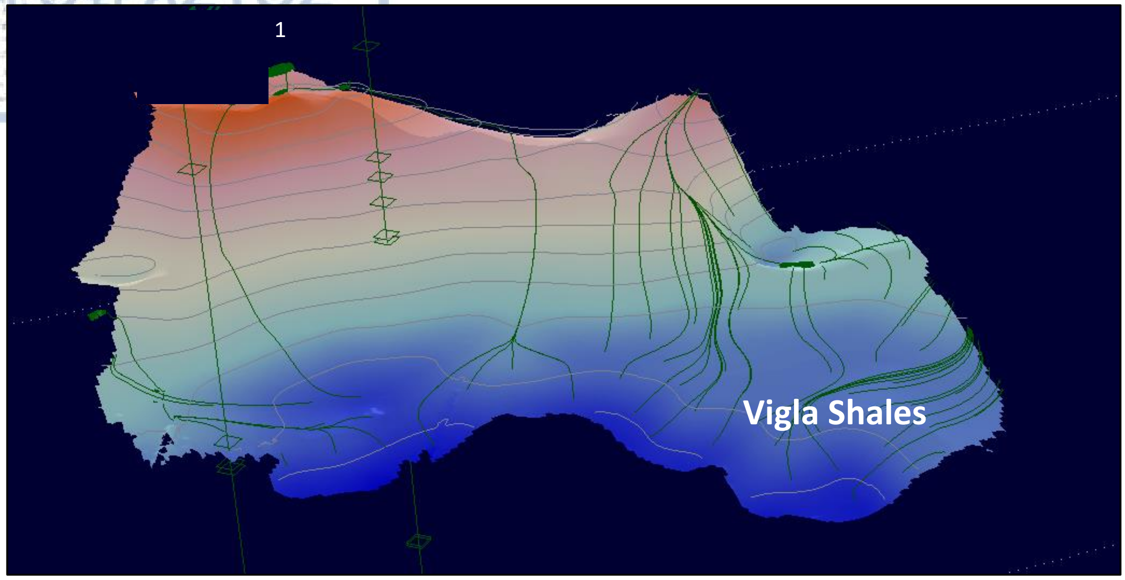

Figure 38*: 3D Perspective View of Migration for Vigla shales.*

Table 14 below lists information about the charging volumes of hydrocarbons deriving from each of the source rocks, both initial and available at 16 Ma.

When comparing ***Tables 8*** and ***14***, an increase in the GOR factor with the addition of the second rifting event is observed. According to GOR (Gas to Oil Ratio), for Posidonia beds and Vigla shales, the oil can be characterized as heavy oil (<300 scf/bbl). There is an exception for Triassic shales where GOR is highly above 300 scf/bbl, specifically 482 scf/bbl, and can be characterized as light oil. All results were found by referring to the same fetch area.

Table 14*: Information on initial and available volumes and GOR for the three potential source rocks.*

Source Rock	Oil (MMstb)		Gas (bcf)		GOR (scf/bbl)	
	Initial	16 Ma	Initial	16 Ma	Initial	16 Ma
Triassic Shales	5301.57	292.25	2554.95	694.77	481.92	2377.32
Posidonia Beds	1072.60	744.22	151.89	115.09	141.60	154.65
Vigla Shales	382.54	348.07	59.80	55.31	156.32	158.91

Another scenario was simulated using a higher value of seal capacity, to ensure larger trapped quantities. The value was increased to 400 m. ***Figures 39*** and ***40***, show increased petroleum quantities with two oil accumulations and various small gas accumulations. The first oil accumulation is at the Eocene level and the second is at the Miocene level. At the second accumulation, a gas cap is detected. It is pointed out that only in this scenario seems that a gas cap is created at the potential reservoir, meaning that an assumption of a reservoir system under the bubble point pressure is formed.

Although a larger area of Triassic shales has entered the gas window, the trapped accumulations are mainly oil. This is one of the examples where the gas generation works as an auxiliary mean to oil quantities, helping them seep towards the reservoir. After a certain point, the gas gets dissolved into the oil.

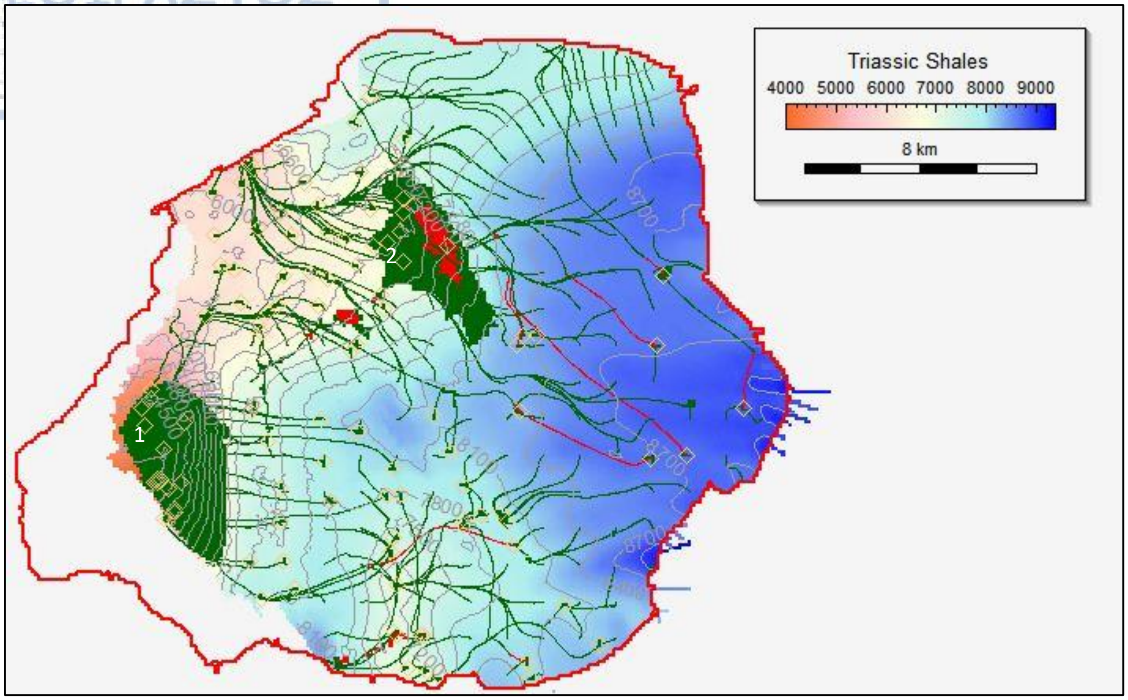

Figure 39*: Migration and accumulation maps for Triassic shales. Seal Capacity is 400 m.*

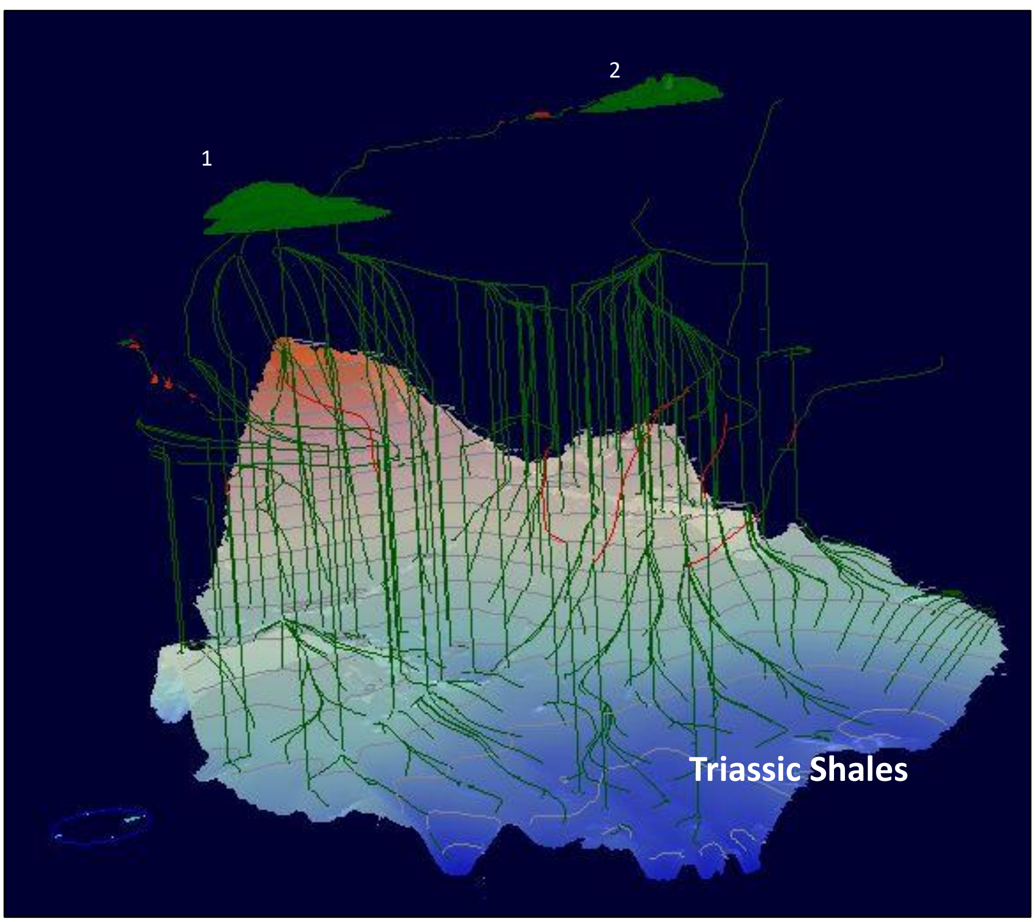

Figure 40*: 3D Perspective View of Migration for Triassic shales Seal Capacity is 400 m.*

4.4 Quality Parameters

It is important to point out that changes in quality parameters do not affect the maturation level of the organic matter. The Vitrinite reflectance equivalent present-day maturity maps for the potential source rocks have been discussed in the thermal regime chapter and would not be quoted again. Furthermore, changes in seal properties of the overlying horizons are assumed to be noticed at the hydrocarbon trapped volumes while the generated quantities remain consistent. For changes in source rock properties, modification at the generated hydrocarbon mass is expected, although no changes in maturation observed.

4.4.1 Seal Properties

Changes were made considering the lithologies, but also the extreme scenarios (two end members) we aimed to create. Information about the applied values for seal capacity are listed in ***Table 2.*** The models were created using Scenario 1 of the thermal regime (***Table 1***) and Scenario B of source rock properties (***Table 3***).

Figure 41 illustrates a 3D perspective view of the migration and possible accumulations. The four created scenarios illustrate a similar reservoir system for every thermal regime scenario. Triassic shales and Posidonia beds, respectively, were applied as the potential source rocks.

On the one hand, using the minimum seal capacity value (Scenario I), no accumulations are noticed. Due to the lack of efficient cap rock, all generated quantities seep out to the surface for both source rocks. On the other hand, the middle scenarios (Scenario II & Scenario III) present a multilayer reservoir system for quantities generated from Triassic shales, and a single reservoir system for those generated from Posidonia beds. This suggests that the petroleum quantities escape from the primary target and get trapped in overlain horizons. Furthermore, in the maximum seal capacity scenario (Scenario IV), a single reservoir system at the primary trap, Eocene level, is observed for both source rocks. In addition, numerous gas accumulations formed at the middle scenarios for the Triassic shales source rock, while no gas cap modeled for the maximum scenario. Thus, the assumption of a reservoir system over the bubble point pressure for Scenario IV is formed.

Tables 15-17 list information about the total available petroleum quantities for each seal capacity scenario, considering different thermal regime scenarios. From the comparison of the different oil and gas volumes, an increase in seal capacity increases in the total petroleum accumulated quantities, for all three potential traps. In more detail, a large increase in trapped volumes at the Eocene level with a simultaneous decrease in the other two traps is observed with the change of seal capacity from 100 to 800 m.

Seal Capacity VS Thermal Regime

Changing the thermal regime using different seal capacity properties infers a conclusion about migration losses for each model. As it already has been referred, Scenario I of seal parameters has the highest losses taking into consideration all thermal regime scenarios, with all generated quantities spill through the surface. Accordingly, Scenarios II and III reveal minimum changes concluding the influence of migration losses but not to a great extent. Finally, Scenario IV, with the maximum seal capacity values, shows intensely changes in the trapped volumes for Scenario 3 of the thermal regime. Thus, a minimum influence from migration losses is assumed for this model.

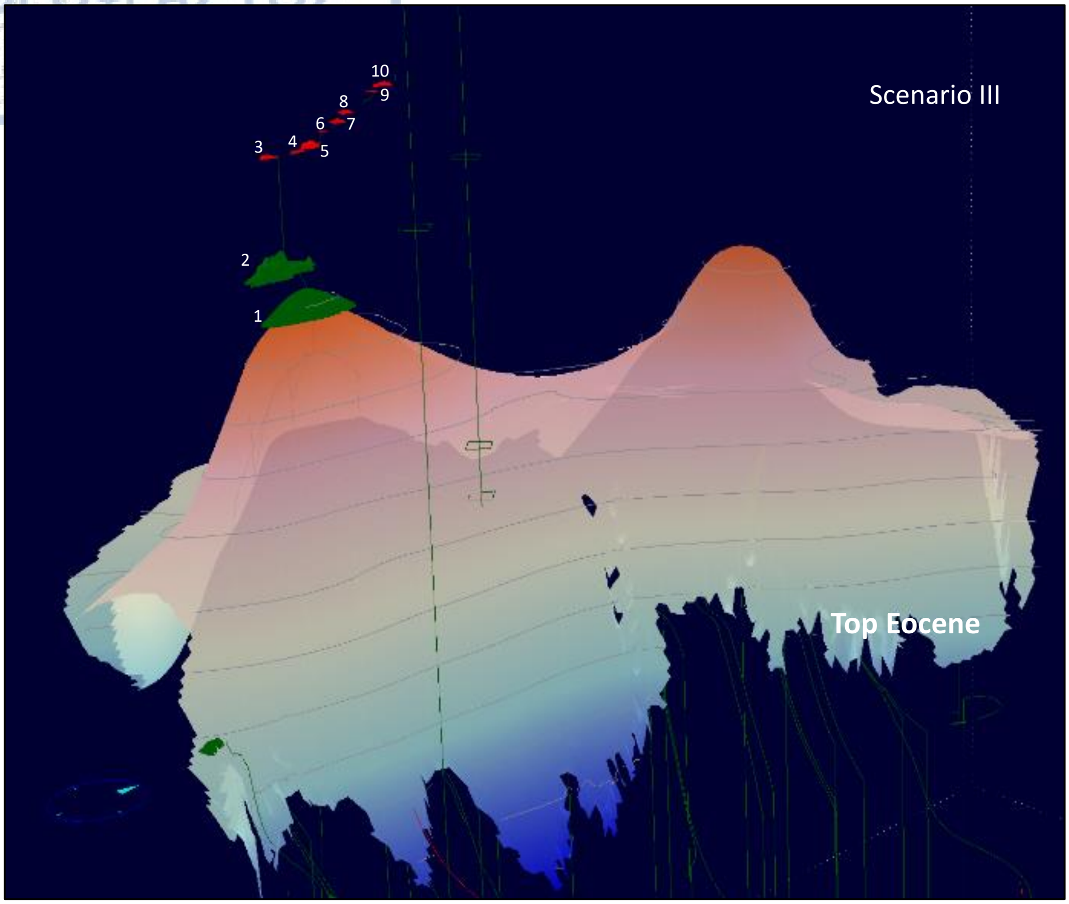

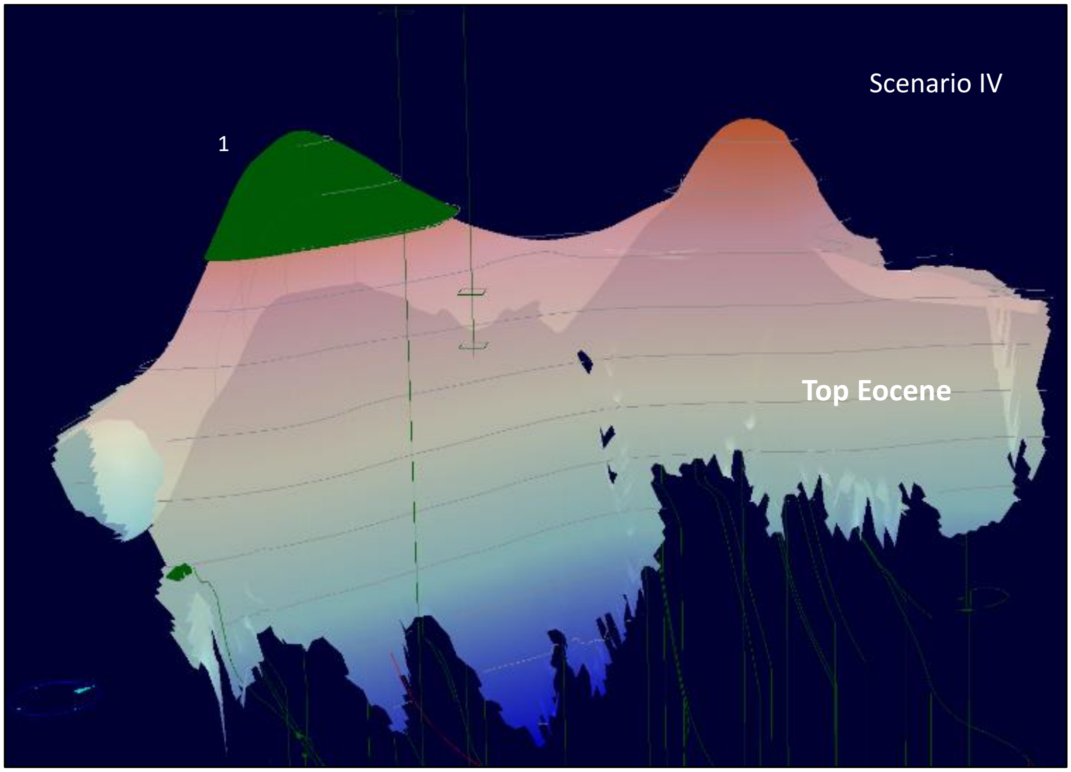

***Figure 41**: 3D Perspective View of Migration for Triassic shales at Scenario III and Scenario IV, respectively.*

Table 15: *Information on possible trapped hydrocarbons for Scenario 1.*

Target	50 m			100 m			800 m		
	Oil (mmbls)	Sol Gas (bcf)	GOR	Oil (mmbls)	Sol Gas (bcf)	GOR	Oil (mmbls)	Sol Gas (bcf)	GOR
Eocene	5.2	2.2	416.1	21.8	10.6	487.5	563.3	140.7	249.8
Mid Oligocene	1.9	0.9	416	7.5	4.2	551	1.1	0.9	819
Miocene	0	3.9	-	0	2.3	-	0	0	-
Total	7.1	7	-	29.3	17.1	-	564.4	141.6	-

Table 16: *Information on possible trapped hydrocarbons for Scenario 2.*

Target	50 m			100 m			800 m		
	Oil (mmbls)	Sol Gas (bcf)	GOR	Oil (mmbls)	Sol Gas (bcf)	GOR	Oil (mmbls)	Sol Gas (bcf)	GOR
Eocene	5.2	2.1	409	21.8	11.1	508	575	137	238
Mid Oligocene	1.9	1	513	7.5	4.2	551	0	0	-
Miocene	0	2.9	-	0	2.9	-	0	0	-
Total	7.1	6	-	29.3	18.2	-	575	137	-

Table 17: *Information on possible trapped hydrocarbons for Scenario 3.*

Target	50 m			100 m			800 m		
	Oil (mmbls)	Sol Gas (bcf)	GOR	Oil (mmbls)	Sol Gas (bcf)	GOR	Oil (mmbls)	Sol Gas (bcf)	GOR
Eocene	5.2	2.1	404	21.8	9.4	430	931	355	381
Mid Oligocene	1.9	0.8	433	7.5	3.5	468	0	0	-
Miocene	0	2.9	-	0	2.9	-	0	0	-
Total	7.1	5.8	-	29.3	15.8	-	931	355	-

Migration Risk Map

Various geological factors have to be certain, so the probability that a prospect will be charged can be determined. Some of these factors that can be defined to a certain point, are the source rock presence, maturity, expelled volumes, and migration losses. Instead, the plumbing system also crucial to the study, comprises of factors that are inevitably uncertain. Those are the carrier beds, structural focusing, top seal capacity, fault seals, and leaks.

Concerning the above, and the migration analysis presented at ***Chapter 4.2.4***, it is critical to identify the migration risk for the primary prospect of the area at the Eocene horizon. The main drivers significant to an equivalent study is migration losses and seal capacity. For the purpose of this dissertation, the focus remains on the properties of the seal.

Figure 42 illustrates the Migration Risk Map for the Eocene horizon. Seven scenarios are represented with increasing seal capacity. The higher levels of the structure are filled in all simulated models, indicating that a certain petroleum quantity gets trapped in this structure. On the other hand, charging for the lower levels appears with a higher risk (maximum 86%). In all scenarios, a sufficient number of flowpaths seems to supply the primary target.

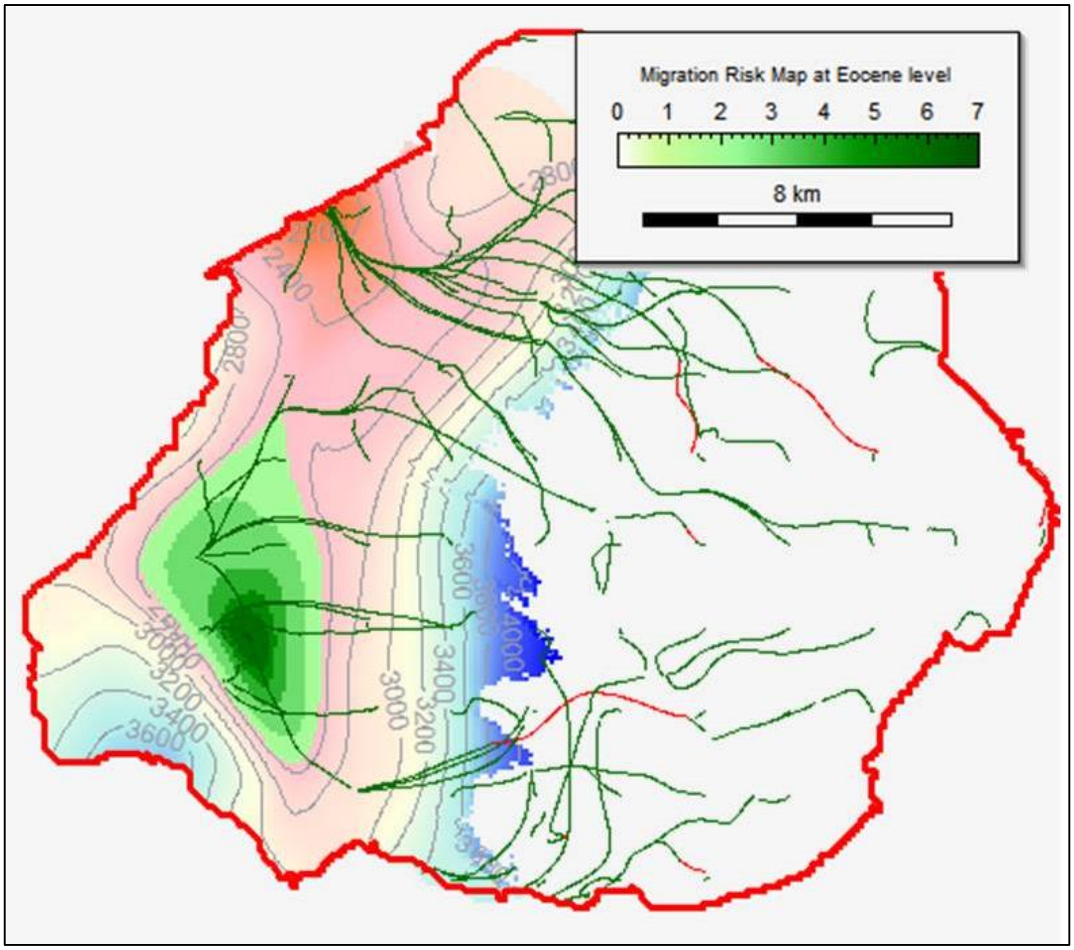

***Figure 42**: Migration Risk Map at Eocene level.*

4.4.2 Source Rock Properties

In order to perform the sensitivity analysis on the source rock properties, two extreme scenarios were created, using minimum and maximum values of TOC, HI, and SR Thickness. The applied values are listed in ***Table 3*** and correspond to Scenario A and Scenario C. Also, for the purpose of the current dissertation, a restricted fetch area was simulated. The models were created using Scenario 1 of thermal regime (***Table 1***) and Scenario IV of seal capacity properties (***Table 2***).

<u>Petroleum Expulsion and Migration History</u>

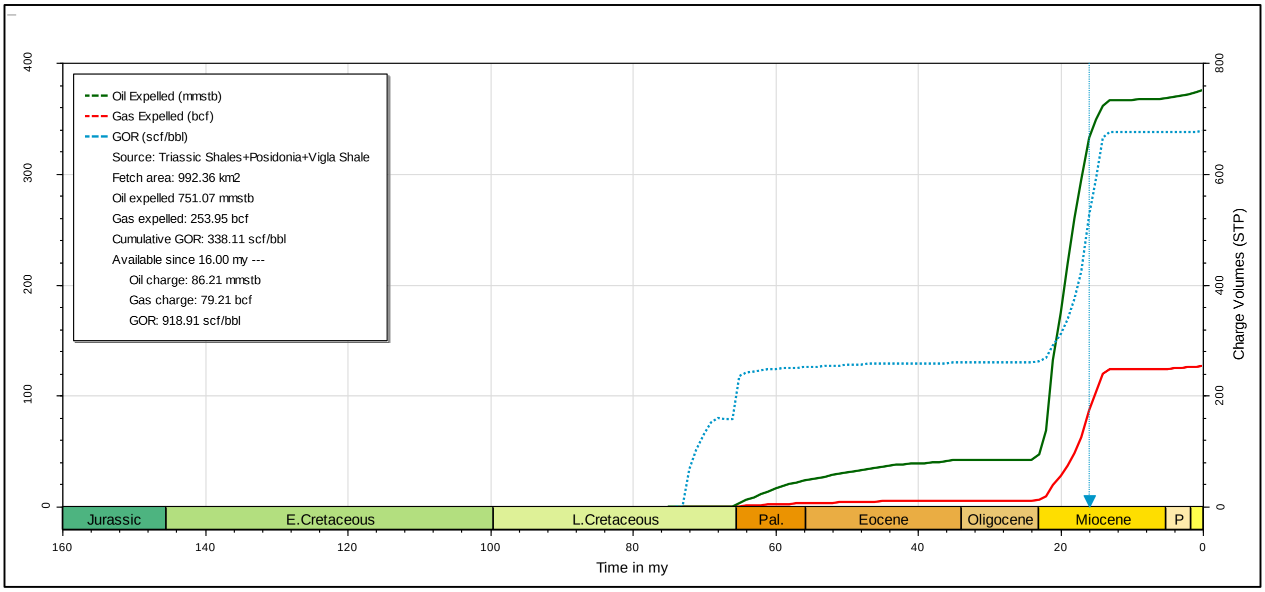

***Figure 43**: Predicted volumes of oil and gas expelled from the three modeled source rocks. The graph represents the Scenario A.*

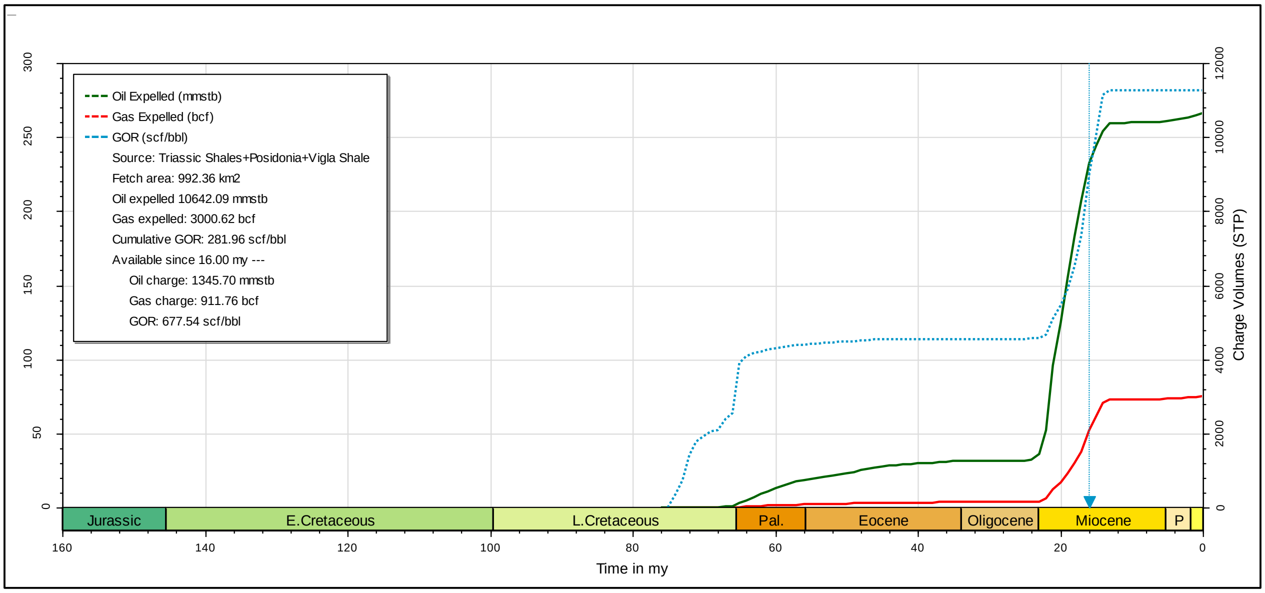

***Figure 44**: Predicted volumes of oil and gas expelled from the three modeled source rocks. The graph represents the Scenario C.*

Figures 43 and 44 show the charging history considering all thee source rocks of the area. Comparing the outcomes, an increase in TOC, HI, and Source Rock Thickness initially affects with an intense increase in the volume of the generated hydrocarbons. Afterward, an increase in hydrocarbon saturation in the source rocks is detected, increasing the expulsion rate. It is important to point out that these scenarios represent the minimum and maximum quantities for the generated hydrocarbons within the fetch area.

Tables 18 and 19 below list information about the charging volumes of hydrocarbons deriving from each of the source rocks. ***Table 18*** refers to initial volumes, while ***Table 19*** refers to volume available at 16 Ma. The created diagrams for each source rock separately are shown in the ***Appendix, Figures P & Q***.

Table 18: *Information of the initial charging volumes and GOR for the three potential source rocks.*

Source Rocks	Parameters					
	Oil (MMstb)		Gas (bcf)		GOR (scf/bbl)	
	Scenario A	Scenario C	Scenario A	Scenario C	Scenario A	Scenario C
Triassic Shales	740	10337.41	525.67	2969.55	341.30	287.26
Posidonia Beds	10.08	271.53	1.18	27.26	117.38	100.40
Vigla Shales	0.67	33.15	0.09	3.86	137.71	114.75
Total	751.07	10642.09	253.95	3000.62	338.11	281.96

Table 19: *Information of the available charging volumes and GOR for the three potential source rocks at 16 Ma.*

Source Rocks	Parameters					
	Oil (MMstb)		Gas (bcf)		GOR (scf/bbl)	
	Scenario A	Scenario C	Scenario A	Scenario C	Scenario A	Scenario C
Triassic Shales	75.63	1047.53	77.96	881.24	1030.81	841.26
Posidonia Beds	9.92	265.40	1.16	26.76	117.35	100.85
Vigla Shales	0.65	32.77	0.09	3.75	137.01	114.56
Total	86.21	1345.70	79.21	911.76	918.91	677.54

No change in generation and expulsion timing observed. In all versions, expulsion for Triassic shales starts at Paleocene (66 Ma) and for Posidonia beds and Vigla shales starts at Miocene (18 and 16 Ma, respectively). The notable in this case is the decrease observed in the GOR factor as the parameters increase. According to GOR, for each source rock, the oil can be characterized as heavy oil (<300 scf/bbl). There is an exception for Triassic shales given the minimum source rock properties, that GOR is slightly above 300 scf/bbl, specifically 341 scf/bbl, and can be characterized as light oil.

According to the 3D graphs at ***Figure 45 and Figure 46***, for Scenario A and C, generated volumes from Triassic shales gives a single reservoir system with accumulation at the Eocene level, whereas Posidonia beds gave accumulation only for Scenario B at the Miocene level. Vigla shales does not contribute to the trapped hydrocarbons for any of the simulated models. For the optimization of these results the source rock horizons were used.

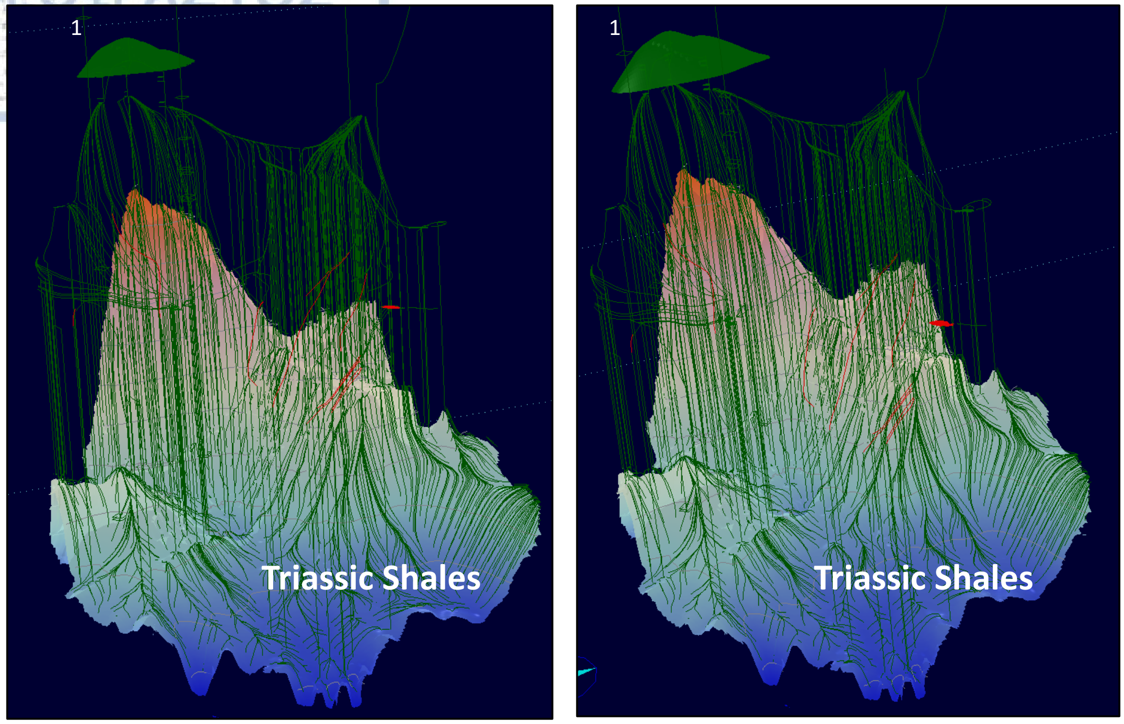

Figure 45: *3D Perspective View of Migration and Trapped Accumulations, based on Triassic shales source rock.*

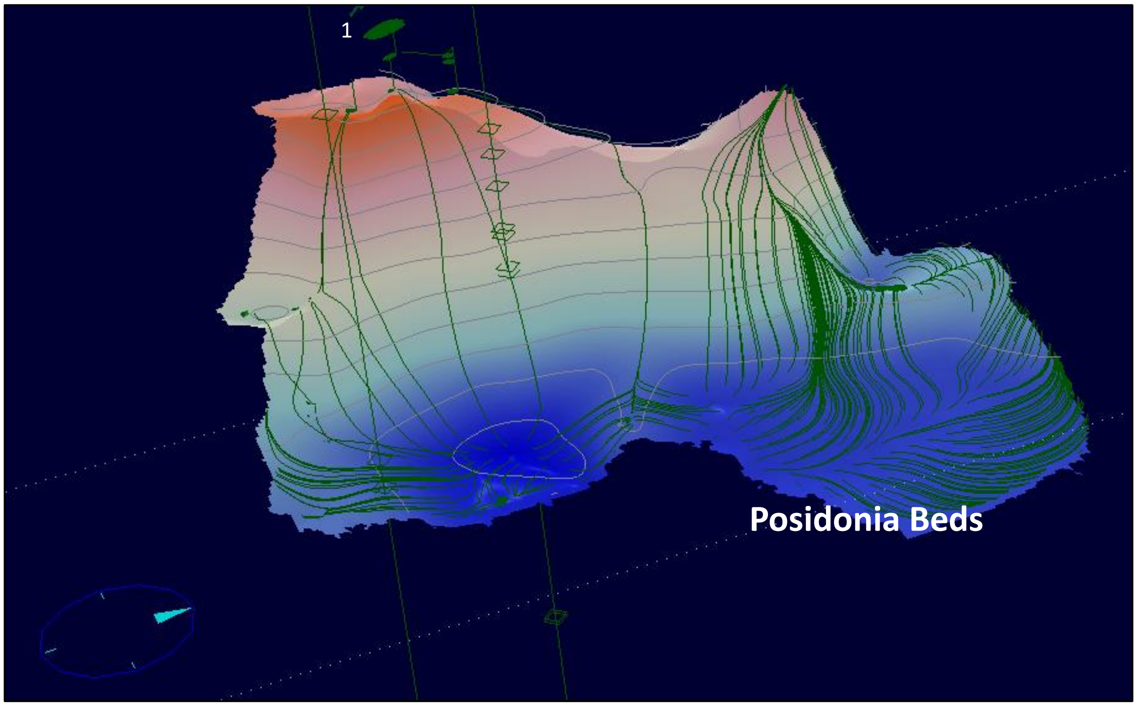

Figure 46: *3D Perspective View of Migration and Trapped Accumulations, based on Posidonia beds source rock.*

5 Conclusions

The western Patraikos Gulf represents an important petroleum province, with significant potential. The petroleum system is represented by:

- Three source rock intervals known as Triassic shales, Posidonia beds and Vigla shales, which are considered as oil prone source rocks.
- The Eocene limestone is considered as the primary reservoir, whereas potential secondary reservoirs (Mid Oligocene, Miocene) are also expected, as modeled.
- The Oligocene flysch is considered as the primary seal formation of the area, although several shaly layers are important cap rocks until the surface.
- The kitchen area is located towards east, where the higher maturity values of the modeled source rocks have been reached.

The basin modeling results indicate that the Triassic shales are the most efficient source rock when compared with Posidonia beds and Vigla shales, in terms of generated and expelled hydrocarbon volumes through time.

The timing of petroleum generation for Triassic shales, Posidonia beds and Vigla shales occurred at 190, 14 and 11 Ma, respectively, whereas generation is still valid as modeled. Oil cracking to gas for the Triassic Shales occurred at 12 Ma.

The timing of the oil and gas generation suggests that all three source rocks are controlled by the thrusting event which occurred at Early Miocene. The thrust affected the temperature and pressure conditions, thus, increasing the maturity and subsequently the generated volumes.

The expulsion of hydrocarbons towards the potential traps was affected by the thrusting emplacement, which gave an intense increase to the charging process. ***Figure 47 and Figure 48*** summarize the generation and expulsion process for the three potential source rocks through time. For the simulation of this model the following parameters were used: Scenario 2 from thermal regime parameters (***Table 1***), Scenario III from seal properties (***Table 2***), and Scenario B from source rock properties (***Table 3***).

Summarizing the results of the sensitivity analysis in ***Table 20***, ***Table 21***, and ***Table 22***, the following conclusions are drawn:

- Scenario 3 (***Table 1***) gives better outcomes for all simulated volumes concerning the thermal regime scenarios. It is observed that the oil quantity remains constant for the three potential traps, while the amount of gas presents slight differentiation. Also, the increase in present day heat flow gives a decrease for the GOR factor.
- The simulation of the Triassic rifting event along with the Jurassic rifting (Scenario 4, ***Table 1***) suggests direct impact on the maturation history, and therefore in the generated hydrocarbon volumes of all three source rocks.
- Scenario IV (***Table 2***), from seal properties sensitivity analysis, resulted in the highest trapped volumes in all three potential targets. The 3D model suggests that the single or multilayer system is seal efficiency dependent. The value of the seal capacity controls either the occurrence of a multilayer reservoir system for the Triassic oil and a single reservoir system for oil attributed to Posidonia beds or the occurrence of a single reservoir system at the primary trap, Eocene level, for both source rocks.

- Scenario C (***Table 3***), from source rock properties sensitivity analysis, delivered higher initial volumes with the quantities being almost doubled, with the increased applied values.
- **Migration risk analysis suggests that a certain petroleum quantity gets trapped in the structure; however, charging for the lower levels appears with 86% maximum risk.**

In all modeled scenarios, migration pathways sufficiently supply the primary target. Migration is primarily vertical due to the dominance of carbonates (mainly limestone). The generated fluids migrate mainly through fracture system. Lateral migration is also observed due to the formation's dips and also the existence of shaly interval within Mesozoic section. The sandy formations at the top of the modeled sections are also favored to lateral migration, as modeled.

Table 23 lists information about the phase of hydrocarbons trapped in the potential reservoir, on a source rock interval basis. Posidonia beds and Vigla shales suggest a single-phase system with oil, while Triassic shales suggest a dual phase system with both oil and gas.

Table 24 lists information about the type of hydrocarbon derived from each source rock on a GOR basis. Triassic shales suggest light oil type of hydrocarbon with an exception of heavy oil in Scenario C, as modeled. Posidonia beds and Vigla shales indicate heavy oil in all simulated scenarios.

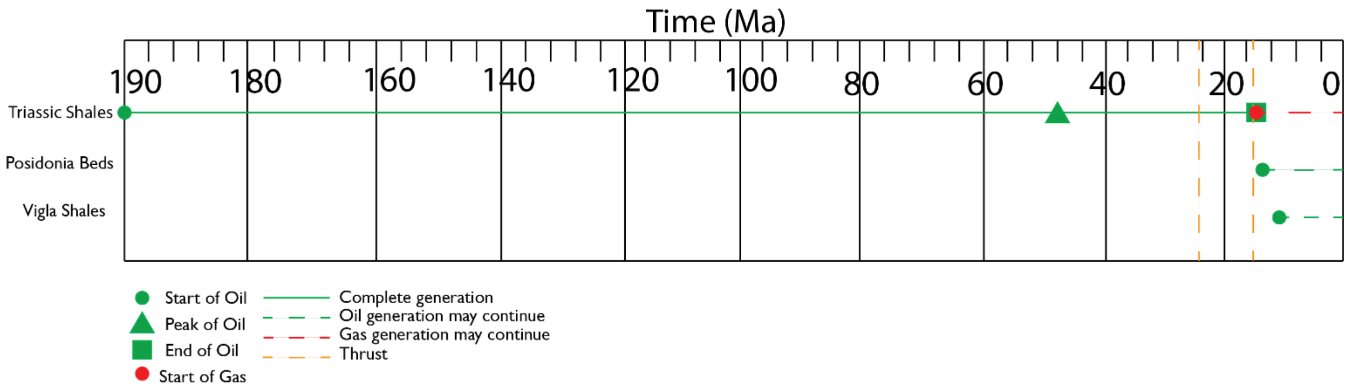

***Figure 47**: Timing of oil and gas generation for the three modeled source rocks. Vertical dashed line at 23 Ma and at 16.6 Ma represents the thrusting period.*

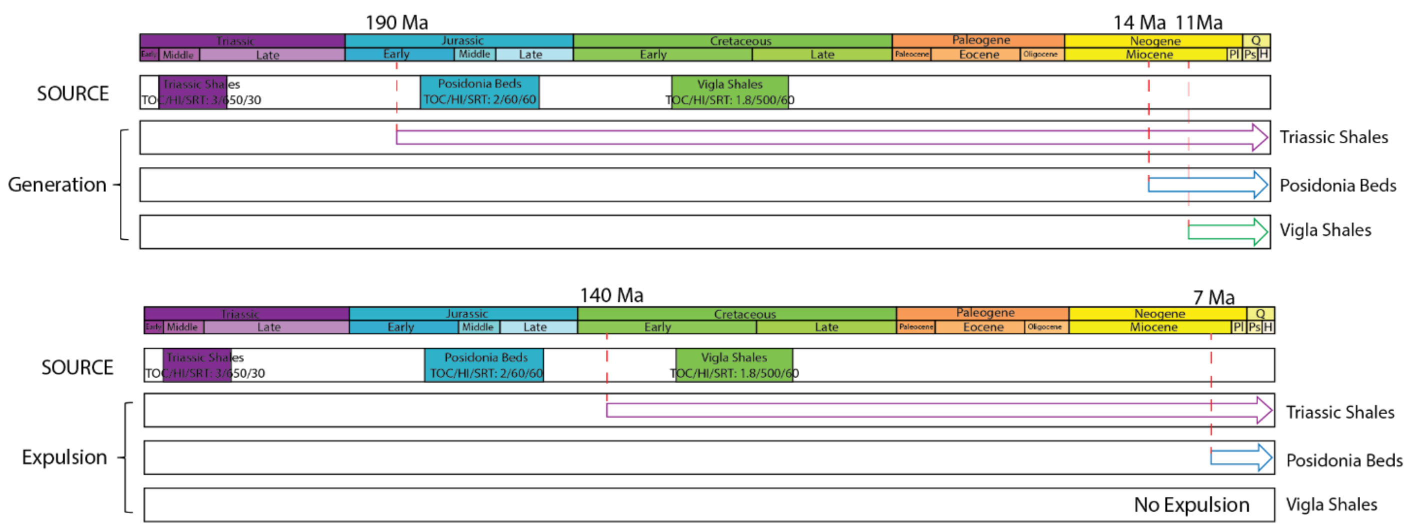

***Figure 48**: Generation and expulsion of the three source rocks through geological time. The geological time scale is in Ma.*

Table 20: *Sensitivity analysis results for thermal regime simulated scenarios, Table 1.*

	Scenario 1 to Scenario 2			**Scenario 2 to Scenario 3**		
	Triassic Shales	**Posidonia Beds**	**Vigla Shales**	**Triassic Shales**	**Posidonia Beds**	**Vigla Shales**
Charging Timing	Later	-	-	-	-	-
Oil Expelled	Increase	Decrease	Decrease	Increase	Increase	Increase
Gas Expelled	Decrease	Decrease	Decrease	Increase	Increase	Increase
Cumulative GOR	Decrease	Decrease	Decrease	Increase	Increase	Increase
Oil Charge	Increase	Decrease	Decrease	Decrease	Increase	Increase
Gas Charge	Decrease	Decrease	Decrease	Increase	Increase	Increase
GOR	Decrease	Decrease	Decrease	Increase	Increase	Increase

Table 21: *Sensitivity analysis results for seal properties simulated scenarios, Table 2.*

	Scenario I to Scenario II	**Scenario II to Scenario III**	**Scenario III to Scenario IV**
Trapped Volumes	Increase	Increase	Increase
GOR	Increase	Increase	Increase

Table 22: *Sensitivity analysis results for source rock properties simulated scenarios, Table 3.*

	Scenario A to Scenario C
Oil Expelled	Increase
Gas Expelled	Increase
Cumulative GOR	Decrease
Oil Charge	Increase
Gas Charge	Increase
GOR	Decrease

Table 23*: Phase of hydrocarbon in reservoir conditions for every simulated Scenario.*

Scenarios	Triassic Shales	Posidonia Beds	Vigla Shales
1	Oil/Gas	Oil	-
2	Oil/Gas	Oil	-
3	Oil/Gas	Oil	-
4	Oil/Gas	Oil	Oil
I	-	-	-
II	Oil/Gas	Oil	-
III	Oil/Gas	Oil	-
IV	Oil	Oil	-
A	Oil	Oil	-
B	Oil/Gas	Oil	-
C	Oil	Oil	-

Table 24*: Type of hydrocarbon, based on GOR factor, for every simulated Scenario.*

Scenarios	Triassic Shales	Posidonia Beds	Vigla Shales
1	Light Oil	Heavy Oil	Heavy Oil
2	Light Oil	Heavy Oil	Heavy Oil
3	Light Oil	Heavy Oil	Heavy Oil
4	Light Oil	Heavy Oil	Heavy Oil
I	Light Oil	Heavy Oil	Heavy Oil
II	Light Oil	Heavy Oil	Heavy Oil
III	Light Oil	Heavy Oil	Heavy Oil
IV	Light Oil	Heavy Oil	Heavy Oil
A	Light Oil	Heavy Oil	Heavy Oil
B	Light Oil	Heavy Oil	Heavy Oil
C	Heavy Oil	Heavy Oil	Heavy Oil

References

Bertotti G., Picotti V., Bernoulli D., Castellarin A., 1993. From rifting to drifting: tectonic evolution of the South-Alpine upper crust from the Triassic to the Early Cretaceous, Sedimentary Geology, 86, 53-76 pp.

Davis M., Kusznir N.,2003. Depth-Dependent Lithospheric Stretching at Rifted Continental Margins, Chapter 4.

Karakitsios. V, 1995. The Influence of Preexisting Structure and Halokinesis on Organic Matter Preservation and Thrust System Evolution in the Ionian Basin, Northwest Greece, AAPG Bulletin, V.79, No.7, 960-980 pp.

Karakitsios V., 2007. Structural Geology o Western Greece's fold-and-thrust belt, Challenge our Myths: Energy Conference & Exhibition, AAPG & AAPG European, 48 pp.

Getsos K., Pomoni-Papaioannou F., Zelilidis A., 2007. A carbonate ramp evolution in the transition from the Apulia platform to the Ionian basin during Early to Late Cretaceous (NW Greece), Bulletin of the Geological Society of Greece, Vol. 40 (1), 53-63 pp.

Mountrakis D., 2010. Geology and geotectonic evolution of Greece, University Studio Press, 373 pp.

Karakitsios V., 2013. Western Greece and Ionian Sea petroleum systems, AAPG Bulletin, V.97, No.9, 1567-1595 pp.

Karakitsios V., Rigakis N., 2007. Evolution and petroleum potential of Western Greece, Journal of Petroleum Geology, Vol.30 (3), 197-218 pp.

Pasquale V., Verdoya M., Chiozzi P., Ranalli G., 1997. Rheology and seismotectonic regime in the northern central Mediterranean, Tectonophysics, 270, 239-257 pp.

Rigakis N., Karakitsios V., Marnelis F., Sotiropoulos Sp., 2013. Geological solutions concluded by Petroleum geochemical data in Western Greece, Bulletin of the Geological Society of Greece, Vol. XLVII 2013

Rigakis N., Karakitsios V., 1998. The source rock horizons of the Ionian Basin (NW Greece), Marine and Petroleum Geology, 15, 593-617 pp.

Karakitsios V., Rigakis N., 2007. Evolution and petroleum potential of western Greece, Journal of Petroleum Geology, Vol.30(3), 197-218 pp.

Rigakis N., 1999. Contribution to stratigraphic research on wells and outcrops of the Alpine formations in Western Greece, in relation to the petroleum generations efficiency of their organic matter, Ph.D. Thesis, University of Athens, 255 pp.

Mavromatidis A., 2009. Review of Hydrocarbon Prospectivity in the Ionian Basin, Western Greece, Energy Sources, Part A, 31:619-632

Sheplev V.S, Reverdatto V.V., 1998. A Contribution to the Further Investigation of McKenzie's Rifting Model, Geophysics, 34(1-2), 63-76 pp.

Aguilera R., 2018. The uncertainty in the Transformation Ratio and its impact on Oil and Gas Exploration-Part I, LinkedIn

Splendore R., Marrotta A.M., 2013. Crust-mantle mechanical structure in the Central Mediterranean region, Tectonophysics, Volume 603, 89-103 pp.

APPENDIX

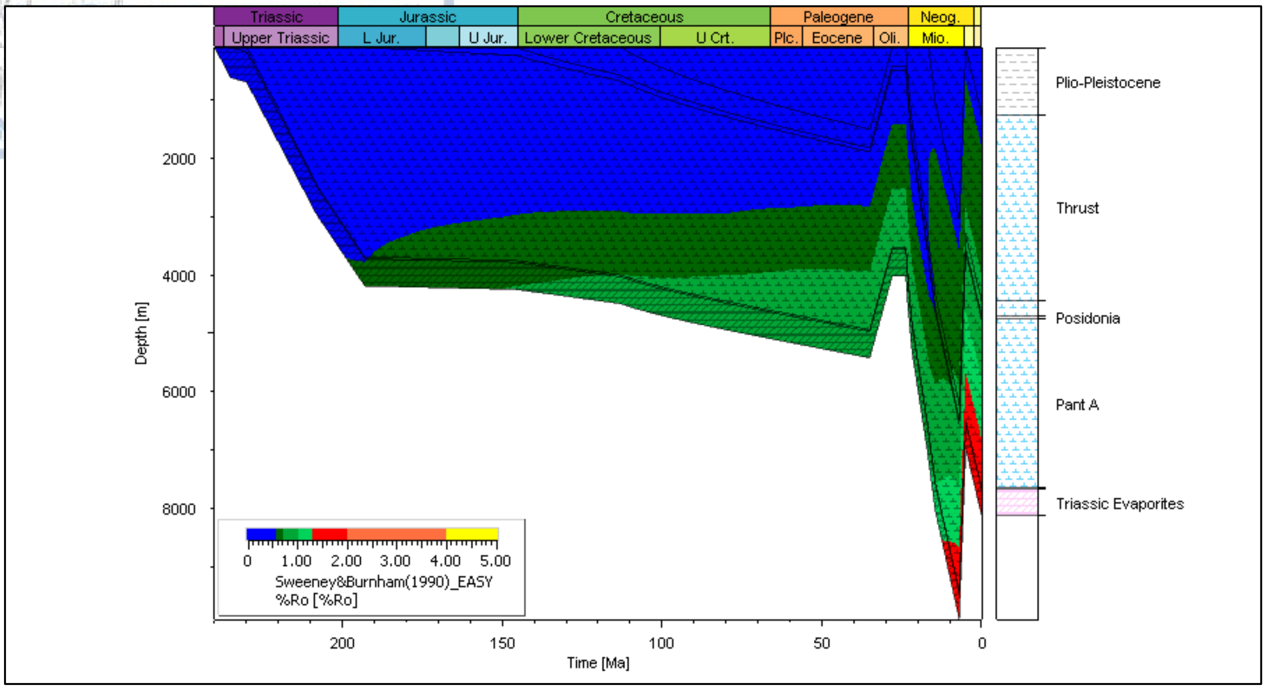

Figure A. *Burial history plot (240 Ma to Present) of the PW-B at Patraikos Gulf. Location shown in Figure 1.*

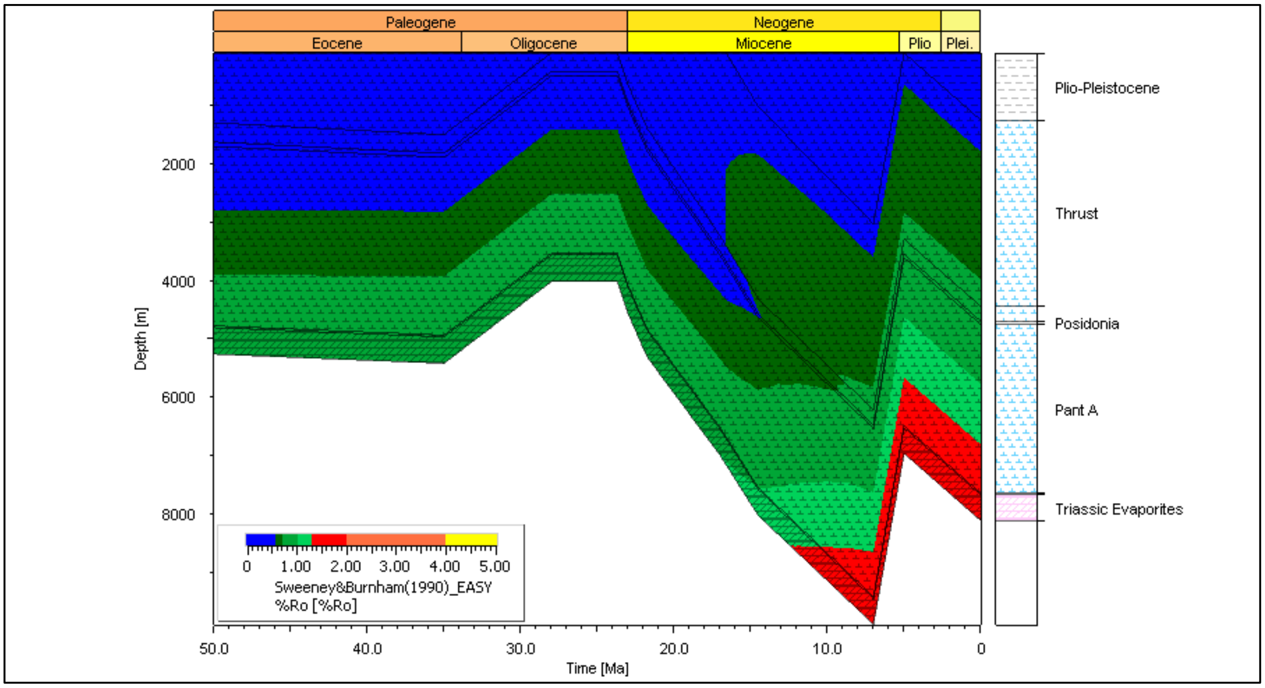

Figure B. *Burial history plot (50 Ma to Present) of the PW-B at Patraikos Gulf. Location shown in Figure 1.*

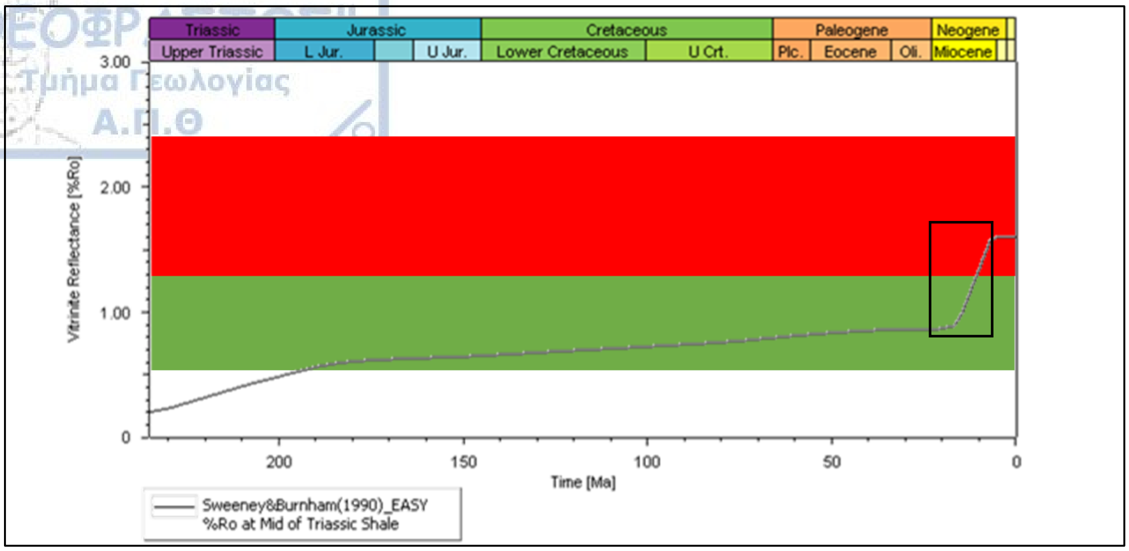

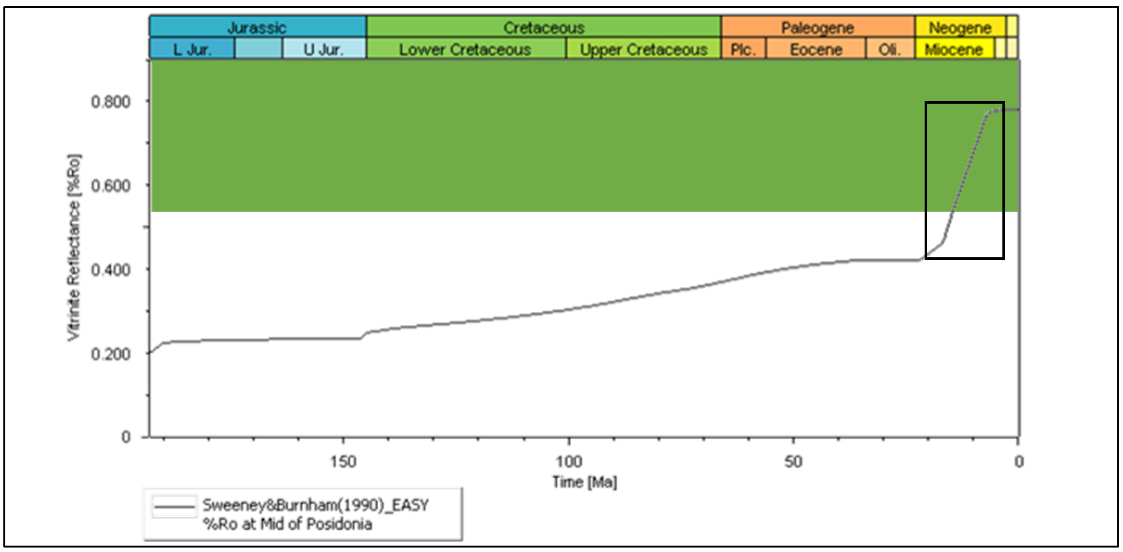

Figure C. *Vitrinite reflectance curve-Time based on Burnham and Sweeney 1990, PW-B. The black frame highlights the thrusting effect.*

Table D. *Timing of oil and gas generation for modeled source rock horizons and the burial history location, for PW-B. Age values are in Ma. Depth values are calculated at depth at which %Ro value is reached (in meters).*

Burial History Location	**Source Rock**			
	Posidonia Beds		**Triassic Shales**	
PW-B	**Age**	**Depth**	**Age**	**Depth**
0.55 %Ro – Start Oil	14	4600	191	3700
1.0 %Ro – Peak Oil	9.5	5900	14.5	7500
1.30 %Ro – Start Gas	-	-	10.5	8500

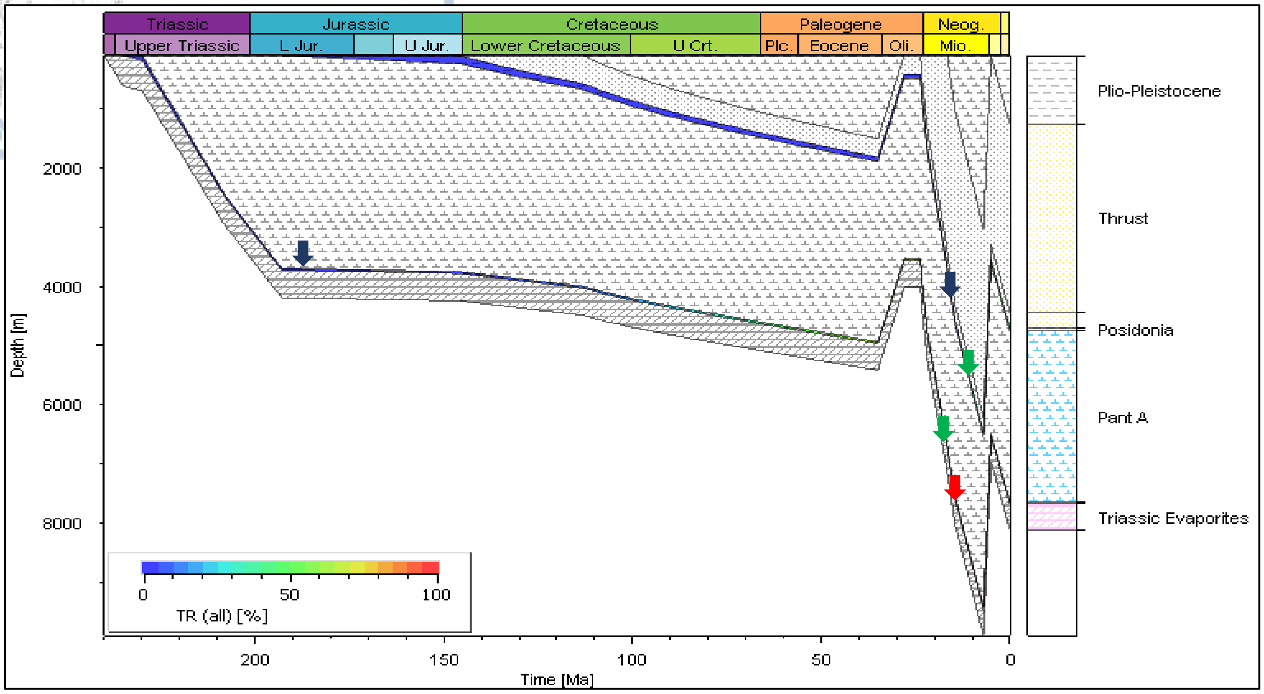

Figure E. *Transformation ratio of organic matter (240 Ma to present) included both modeled source rocks (Triassic shales, Posidonia beds) through geological time, PW-B. Blue, green and red arrows illustrate the start, peak and end of oil generation for all modeled source rock intervals.*

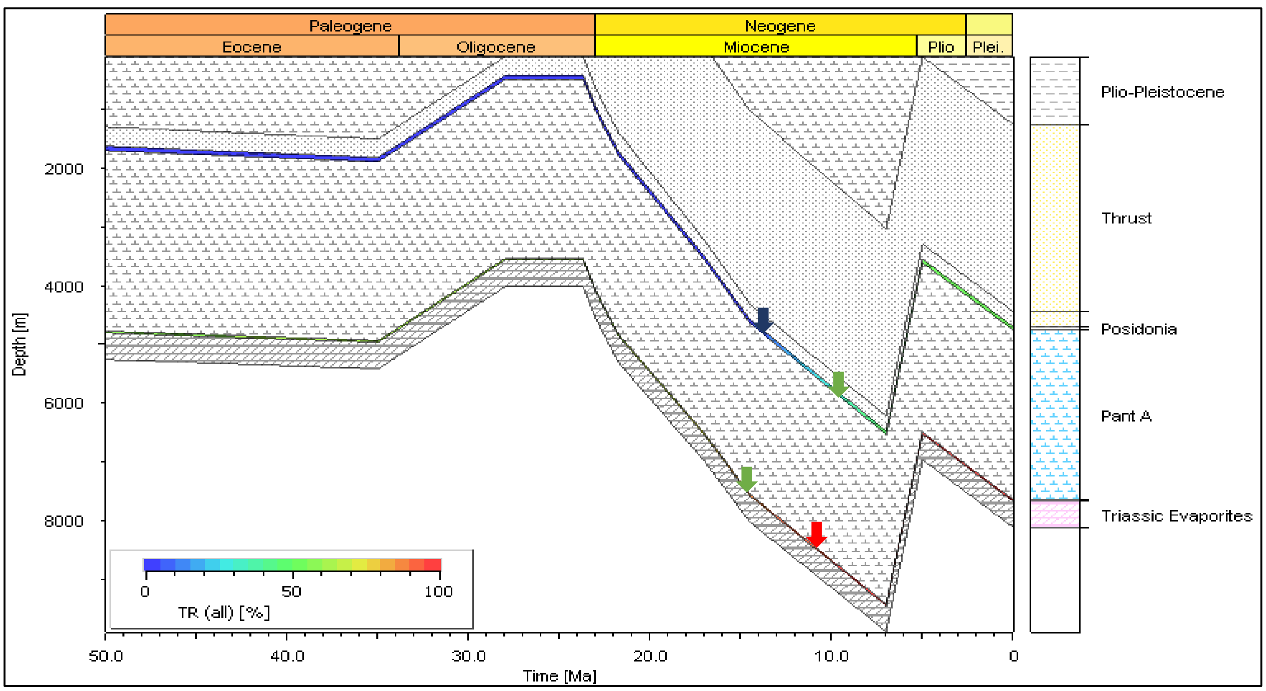

Figure F. *Transformation ratio of organic matter (50 Ma to present) included both modeled source rocks (Triassic shales, Posidonia beds) through geological time, PW-B.*

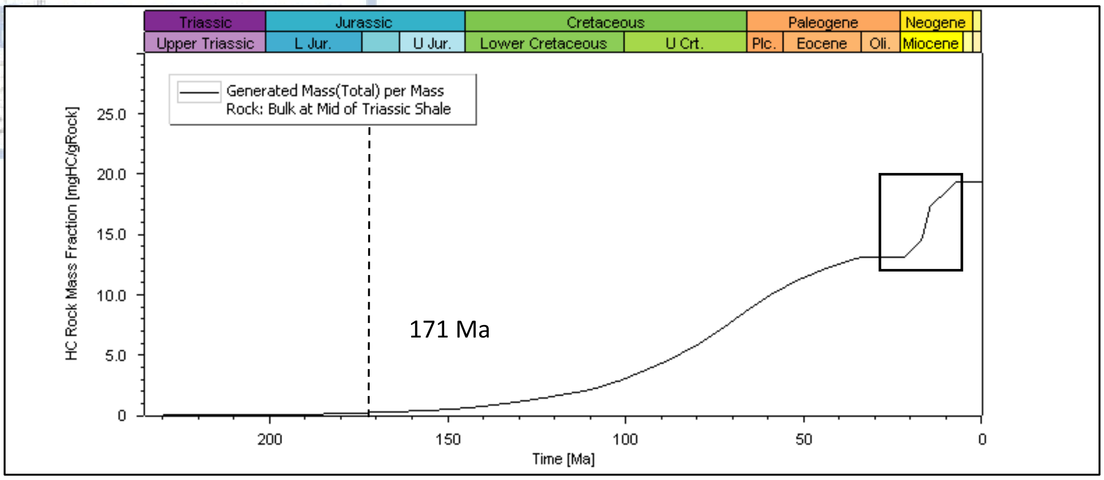

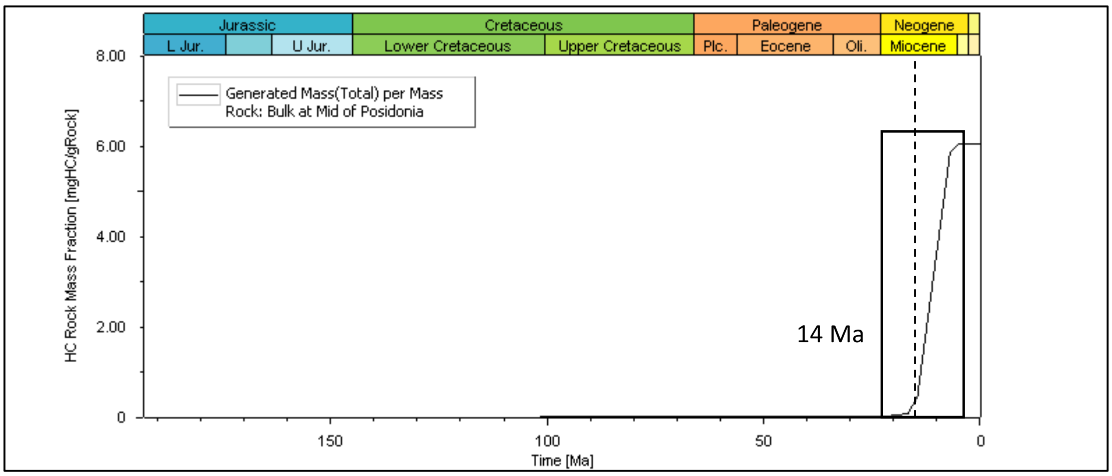

Figure G. *Generation Mass curves through geological time for both modeled source rocks, the Triassic shale and the Posidonia beds, respectively, PW-B. Generation mass values are in mg HC/g Rock and time values are in Ma.*

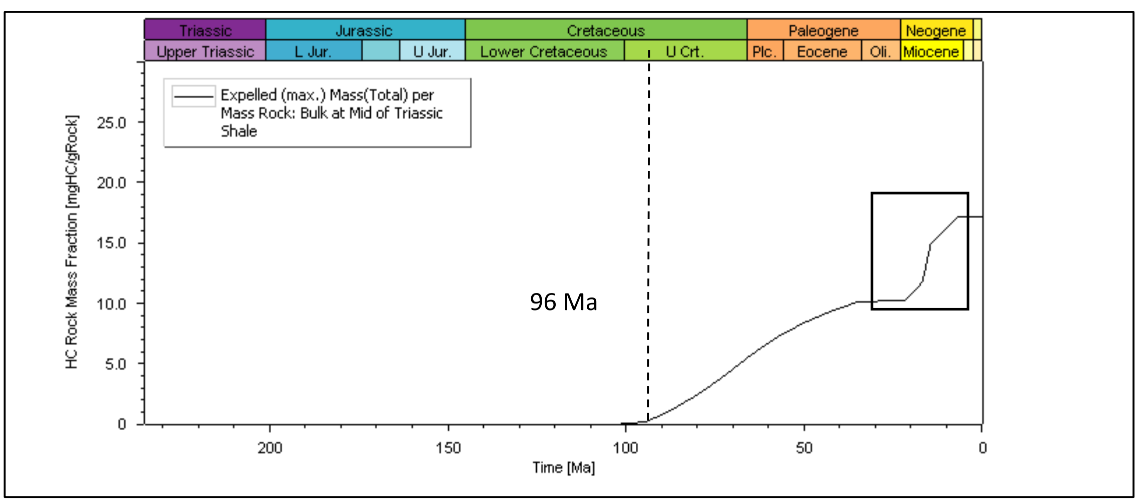

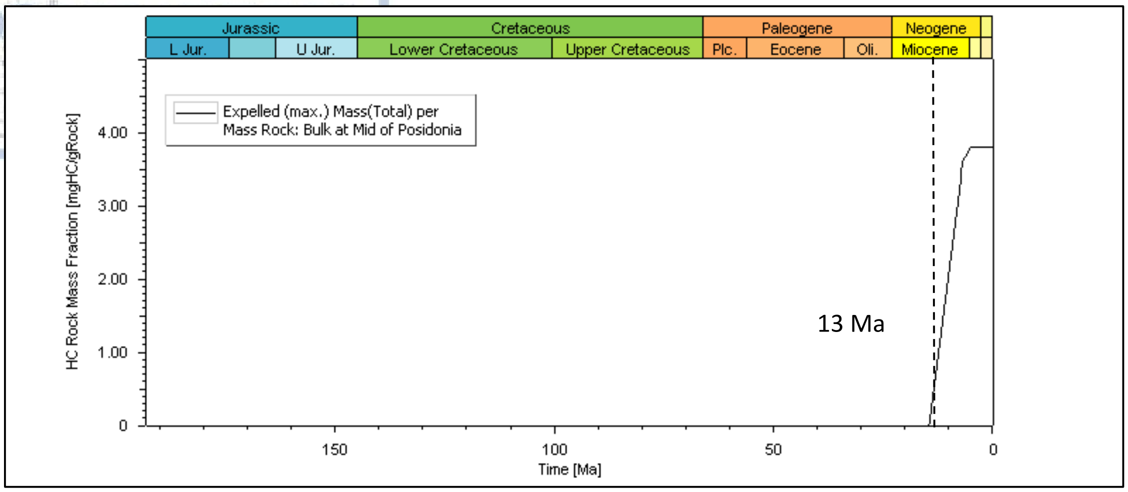

Figure H. *Expulsion Mass curves through geological time for both modeled source rocks, the Triassic shales and the Posidonia beds, respectively, PW-B. Expulsion mass values are in mg HC/g Rock and time values are in Ma.*

Table I. *Generation and Expulsion critical times, generation and expulsion mass values and generation mass value at expulsion starting time, for PW-B. Time values are in Ma. Mass values are in mg HC/ g Rock.*

Source Rock	Generation (Start Ma)	Generation End Value (mg HC/g Rock)	Expulsion (Start Ma)	Generation Value at Expulsion Starting Time (mg HC/g Rock)	Expulsion End Value (mg HC/g Rock)
Triassic Shales	171	19.29	96	3.12	17.11
Posidonia Beds	14	6.06	13	0.45	3.80

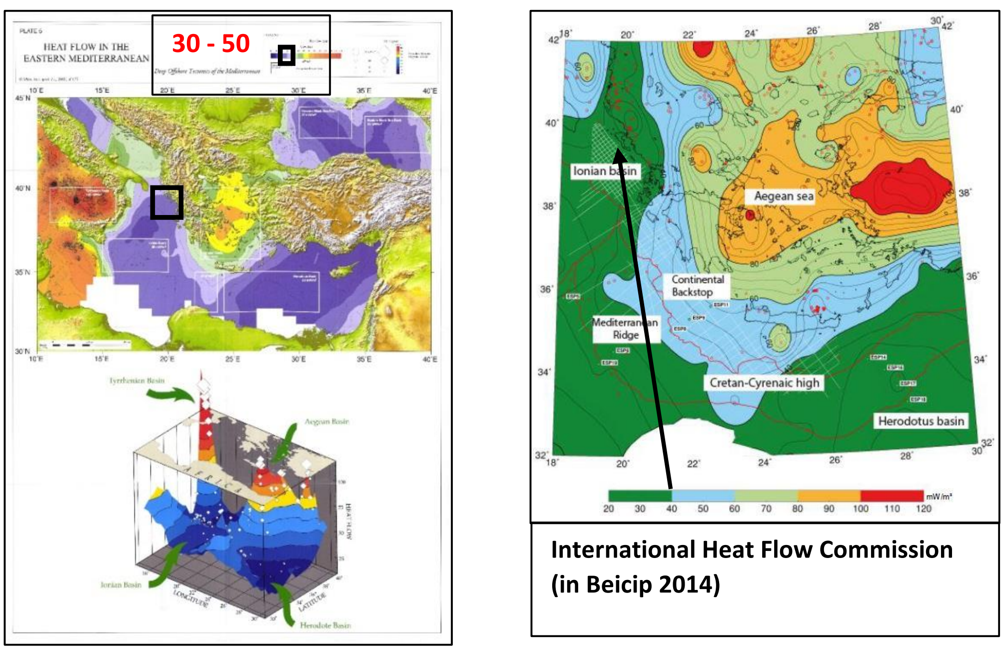

Figure J. *Present Day Heat Flow.*

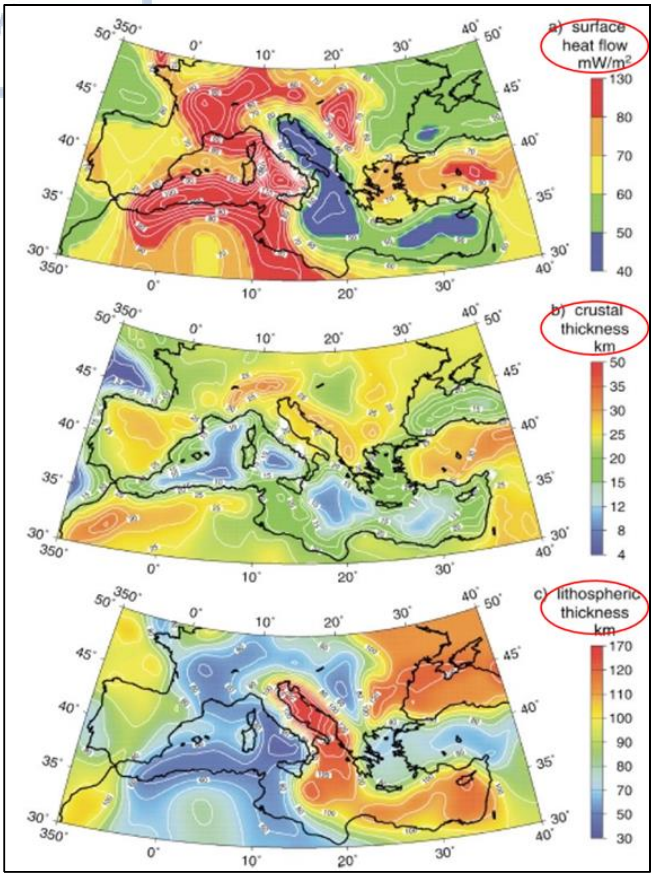

Figure K. *Maps of the a) Surface heat flow, b) Crustal thickness, c) Lithospheric thickness (Source: Cavazza et al.,2004).*

Parameters	Literature
Crust (km)	35-25 (Cavazza et al., 2004).
Lithosphere (km)	120 (Cavazza et al., 2004).
	2.5 (V. Pasquale et al. 1997)
Radioactive Heat Production (mW/m^3)	2.8 (Raffaele Splendore, 2013)
	3 (V.Pasqual et al. 1995)
	2.5 (V. Pasquale et al. 1997)
b-Factor	1.3 (Davis Kusznir 2003)
	1.1 (Bertotti et al. 1993)
Rifting Time (Ma)	247-242, 190-145 (Karakitsios, 2013)
Heat Flow (mW/m^2)	36 *(*International Heat Flow Commission (in Beicip 2014)
	44-49 (Cavazza et al., 2004).

Table L. *Parameters used in the sensitivity analysis.*

Source Rock	Oil (MMstb)		Gas (bcf)		GOR (scf/bbl)	
	Initial	16 Ma	Initial	16 Ma	Initial	16 Ma
Triassic Shales	4665.39	385.41	2255.91	816.65	483.54	2118.94
Posidonia Beds	140.33	137.93	15.46	15.27	110.17	110.75
Vigla Shales	16.79	16.54	1.94	1.89	115.57	114.16

Table M. *Information of initial and available volumes and GOR for the three potential source rocks, Scenario 1.*

Source Rock	Oil (MMstb)		Gas (bcf)		GOR (scf/bbl)	
	Initial	16 Ma	Initial	16 Ma	Initial	16 Ma
Triassic Shales	4808.42	477.29	1850.48	671.79	384.84	1407.51
Posidonia Beds	103.31	102.35	10.32	10.21	99.89	99.77
Vigla Shales	8.38	8.20	0.83	0.80	99.33	97.76

Table N. *Information of initial and available volumes and GOR for the three potential source rocks, Scenario 2.*

Source Rock	Oil (MMstb)		Gas (bcf)		GOR (scf/bbl)	
	Initial	16 Ma	Initial	16 Ma	Initial	16 Ma
Triassic Shales	5086.55	326.29	2359.09	693.92	463.79	2126.70
Posidonia Beds	162.69	155.36	19.52	18.92	120.00	121.77
Vigla Shales	28.83	28.66	3.63	3.60	125.90	125.60

Table O. *Information of initial and available volumes and GOR for the three potential source rocks, Scenario 3.*

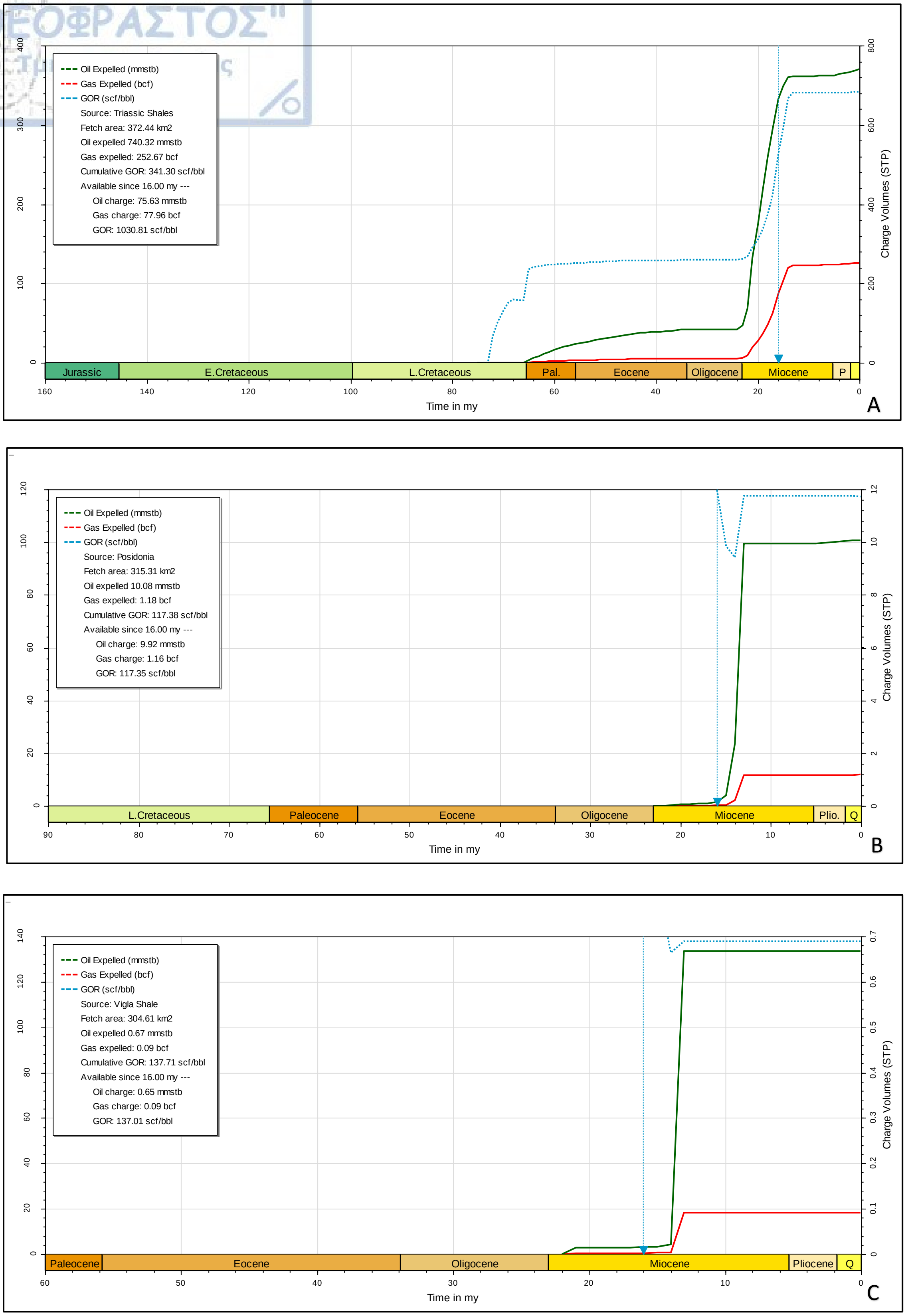

Figure P. *Predicted volumes of oil and gas expelled from a) Triassic shales, b) Posidonia beds, c) Vigla shales. The graphs represent the Scenario A.*

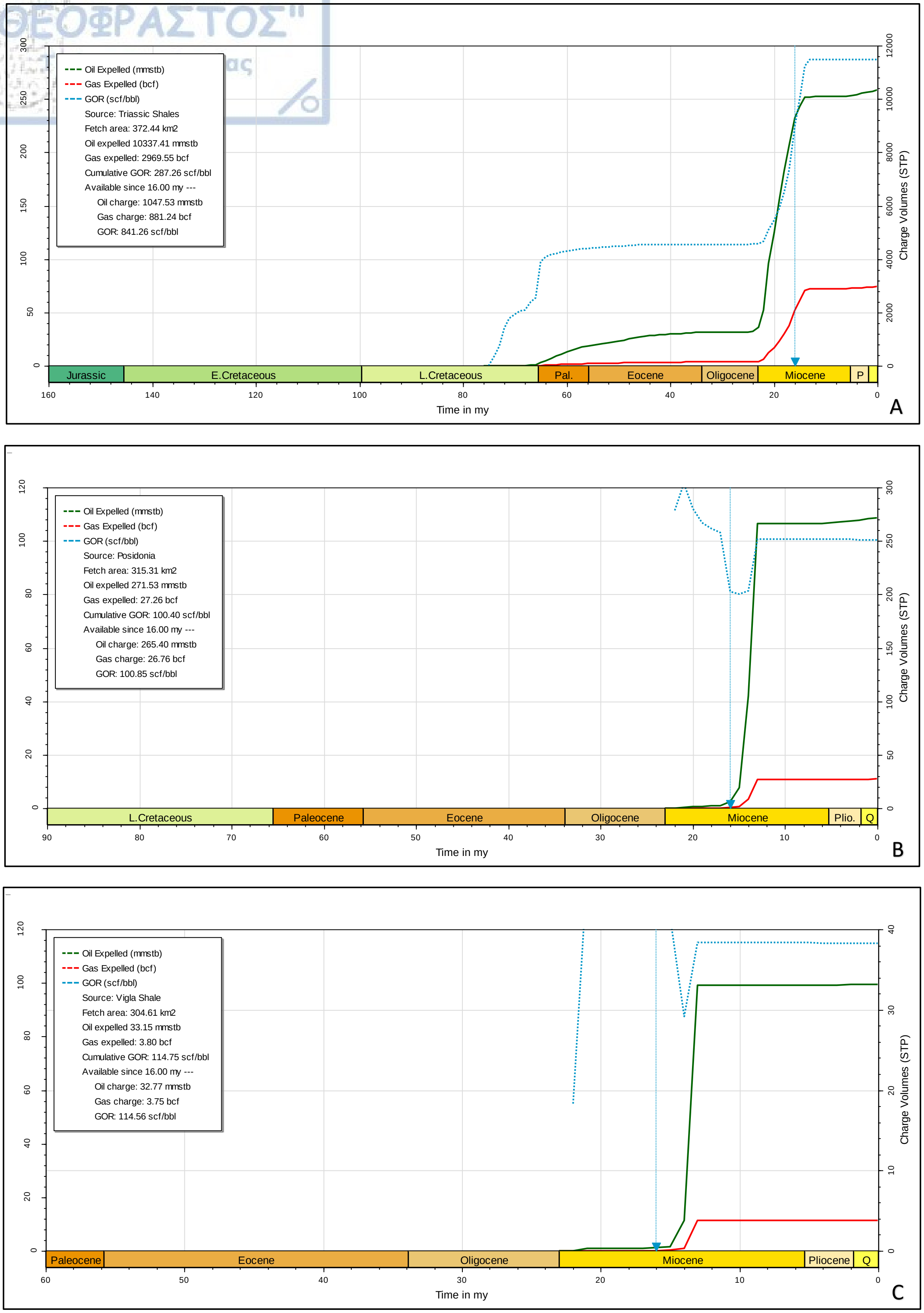

Figure Q. *Predicted volumes of oil and gas expelled from a) Triassic shales, b) Posidonia beds, c) Vigla shales. The graphs represent the Scenario C.*